THE EFFECT OF CONDUCTIVE FILLERS ON THE PROPERTIES OF A PARAFFIN WAX/LLDPE BLEND FOR ENERGY STORAGE

Tiisetso Ephraim Mokoena

Dissertation submitted in fulfilment of the requirements for the Degree

Master of Health Sciences in Environmental Health

in the

Department of Life Sciences

Faculty of Health and Environmental Sciences

at the

Central University of Technology, Free State

Supervisor: Dr M.J. Mochane

Co-supervisor: Dr S.J. Sefadi

BLOEMFONTEIN
August 2021

DECLARATION OF INDEPENDENT WORK

DECLARATION WITH REGARD TO INDEPENDENT WORK

I, **Mokoena Tiisetso Ephraim**, student number , do hereby declare that this research project submitted to the Central University of Technology, Free State for the Master of Health Sciences in Environment, is my own independent work; and complies with the Code of Academic Integrity, as well as other relevant policies, procedures, rules and regulations of the Central University of Technology, Free State; and has not been submitted before to any institution by myself of any other person in fulfilment (or partial fulfilment) of the requirements for the attainment of any qualification.

_____ **22/08/2021**

SIGNATURE OF STUDENT **DATE**

DEDICATIONS

Firstly, I would like to thank Almighty God for the strength, perseverance and dedication he has given me throughout the most challenging years of my postgraduate research. This thesis is a symbol of my dedication to my work and the man I have become as I did not give up when things were tough and challenging to myself for not giving up when things were tough and challenging, and also to my mother (Nonhlanhla Leah Makhubu) for the love, support she gave me and for the struggles she endured with me during this difficult period, for that I will always be grateful and I feel blessed.

ACKNOWLEDGEMENTS

It was a great feeling and reward to be amongst the good researchers who have shown me the path, by shaping me to be a good researcher. They have encouraged and supported me.

I would like to show my appreciation to my main supervisor Dr. M.J Mochane and co-supervisor Dr J.S Sefadi for their great effort and guidance they gave me without any complaints throughout my research writing. Both of you have taught me how to think like a researcher and to be always humble towards other people. I have learnt so much from both of you and for that I will forever be grateful. Ke ya leboha haholo.

In addition, i would also like to thank Nelson Mandela University (NMU) for allowing me to use their laboratory and equipment for my research and as well as UOFS for assisting me with the analysis. To Central University of Technology (CUT) and department of life for allowing me to do my research with them. To National Research Foundation (NRF) and CUT funding for funding me, without those funds this work will not be possible and enjoyable.

Furthermore, I would also like to show my appreciation towards the following people;

- My big brother (Mokoena Motlalepula Patrick) and two little brothers (Mokoena Mokete Lawrance and Mokoena Tladi Jeremane) for always been there for me when I needed them.
- To my child Mpho Kgomo and new little brother Sfiso Makhubu to be in my life. I love both of you my children.
- My father (Mokoena Morie Jonas) for always guiding and advising me about life.
- To my friend, my late girlfriend (Letlatsa Dimakatso Portia) for forever believing in me, and loving me. You never once doubted me, always had high hopes for me. If only you could be here to see that I have made it, but I am sure you still looking after me. Ke ya leboha Laposh hore o be bophelong baka, otla dula ole pelong yaka.
- Mr Lukhanyo and Lebo for helping me with preparation, running techniques and as well as explaining things me.
- To my study partner Ntombizanele Jafta for assisting me when I needed help. It was indeed a long journey with stress and disappointment along the way, but in the end we actually made it.
- Dr S. Magagula for moral support and guidance when I needed it.

ABSTRACT

This study deals with the effect of two conductive fillers (*viz* boron nitride (BN) and single walled carbon nanotubes (SWCNT)) on the properties of the linear low density polyethylene (LLDPE) matrix and LLDPE/paraffin wax blend. The pure LLDPE and paraffin wax/LLDPE blend (30/70) were melt-mixed with 1,2 and 3 wt.% content of BN and SWCNT, respectively. Because it is well-known that both conductive fillers are able to improve the thermal conductivity of the paraffin wax/polymer blends, the aim of this study was to focus on the effect of both conductive fillers on the dispersion of paraffin wax into LLDPE matrix, mechanical properties, crystallization behaviour, and thermal stability of the LLDPE/wax blend. Scanning electron microscopy (SEM) images of the LLDPE/paraffin wax blends depicted a phase separated system, which was further supported by two separate peaks from the differential scanning calorimetry (DSC). The SEM images of 2wt.% BN incorporated into the LLDPE matrix without paraffin wax showed an agglomerated BN nanoparticle within the matrix. It was further shown from the morphology that the addition of BN into the LLDPE/paraffin wax blend had no affinity with the paraffin wax, while the addition of SWCNT showed better dispersion into the LLDPE/paraffin wax/BN blend composites. This better dispersion is attributed to a high affinity between the carbon-based filler and paraffin wax. There was an enhancement in the crystallization temperature and degree of crystallization in the presence of both BN and SWCNT, which is due to the nucleating effect of the two conductive fillers into the LLDPE and LLDPE/wax blend. From the thermal gravimetric analysis (TGA), it is evident that the incorporation of the SWCNT and its synergy with BN enhanced the thermal stability of the LLDPE by forming a heat barrier that could have prevented the entrance of heat into LLDPE matrix. Generally, there was a reduction in tensile strength with the addition of paraffin into the BN/LLDPE and SWCNT/LLDPE composites, which is due to wax crystals crystallizing on the amorphous region of polymer, thereby acting as defect points for the initiation as well as propagation of stress cracking. Furthermore, the incorporation of BN into the LLDPE matrix reduced the impact strength of the composites, with this behaviour being attributed to BN particles acting as crack nucleation sites thereby it is easier for crack to form in the composites and as a result reducing the overall impact strength. The presence of wax into the LLDPE composites was found to reduce the impact strength of the system, which may be ascribed to the low viscosity of paraffin wax which might have acted as flaws with the matrix, acting as a catalyst for initiation as well propagation of stress cracking.

TABLE OF CONTENTS

LIST OF SYMBOLS AND ABBREVIATIONS

ABS	Acrylonitrile butadiene styrene
AIN	Aluminium nitride
AFM	Atomic force microscopy
Ag	Silver
BN	Boron nitride
BNp	Boron nitride particles
BNs	Boron nitride sheets
CB	Carbon black
Cu	Copper
c-BN	Cubic boron nitride
CF	Carbon fiber
CNTs	Carbon nanotubes
DSC	Differential scanning calorimeter
DU-PW	Diurea-paraffin wax
EP	Epoxy
EG	Expanded graphite
FTIR	Fourier Transform Infra-Red
HDPE	High density polyethylene
hv-HDPE	High melt viscosity high density polyethylene
H-PW	High paraffin wax
h-BN	Hexagonal boron nitride
HTPB	Hydroxyl-terminated polybutadiene

LDPE	Low density polyethylene
LLDPE	Linear low density polyethylene
L-PW	Low paraffin wax
LHS	Latent heat storage
MFI	Melt flow index
MWCNT	Multi walled carbon nanotubes
NR	Natural rubber
OBC	Olefin block copolymer
OM	Optical microscopy
OSBN	Silanized hexagonal boron nitride
OSFBN	Silanized flake boron nitride
PBS	Poly (butylene succinate)
PCMs	Phase change materials
PDA	Polydopamine
PE	Polyethylene
PEG	Polyethylene glycol
PLA	Poly (lactic acid)
PHBV	Poly (3-hydroxybutyrate-co-3-hydroxyvalerate)
PHFM	Polypropylene hollow fiber membrane
PTFE	Polytetrafluoroethylene
PP	Polypropylene
PVDF	Poly (vinylidene fluoride)
TEM	Transmission electron microscopy
TGA	Thermogravimetric analysis

TES	Thermal energy storage
TPU	Thermoplastic polyurethane
DMA	Dynamic mechanical analysis
DSC	Differential scanning calorimetry
SEM	Scanning electron microscopy
SGAP	Sub-critical gas-assisted processing
SWCNT	Single walled carbon nanotubes
SHS	Sensible heat storage
SR	Silicon rubber
iPP	Isotactic polypropylene
UHMWPE	Ultra-high molecular weight polypropylene
Wax FT	Hard Fischer Tropsch wax
Wax S	Soft paraffin wax
Wax M3	Soft Fischer Tropsch paraffin wax
xGnP	exfoliated graphite nanoplatelets

T_m	Melting temperature
M_w	Average molecular weight
ΔH_m	Enthalpy of melting
T_c	Crystallization temperature
ΔH_c	Enthalpy of cooling
X_c	Degree of crystallinity

LIST OF TABLES

LIST OF FIGURES

Chapter 1: Introduction

1.1 Background introduction

Energy storage is an extensive topic of interest among engineers and scientist in the industrial world. It plays a vital role in the field of energy conservation because it can reduce the time between the production of energy and the high demand of energy supply. Energy comes in multiple of forms including radiation, chemical and mechanical, electrical potential, kinetic and thermal energy [1]. Thermal energy storage (TES) has gained increasing attention among researchers because it is considered to be the most attractive option as it can store excess energy at peak times and release it at off-peak times [2]. Thermal energy storage can be accomplished either by sensible heat storage (SHS), latent heat storage (LHS) or by a combination of the two. SHS is achieved by adding energy to the material that needs to be stored, thus increasing the temperature of the material without changing its phase. This process, which takes place in the material where the temperature changes, it is cheaper compared than that of LHS. Latent heat is one of the most efficient ways of thermal energy storage and it is largely considered to be a feasible approach for renewable energy in solar thermal systems. The advantages of LHS compared to SHS are high heat release storage densities, small system sizes, and a narrow temperature that changes during charging and discharging processes [3-5]. A LHS material is also referred to as a phase change materials (PCMs). PCMs are substances with a high latent heat of fusion that can store or release thermal energy by melting and solidifying at certain temperatures. Their primary characteristics are the ability to undergo phase transitions (from solid to liquid and vice versa) at relatively low temperatures while they can also absorb large amounts of energy as a latent heat and release this heat back into the surroundings, proportional to their specific enthalpy of melting. They are considered as one of the most promising ways to utilize solar energy [6,7]. **Figure 1.1** illustrates the functions of the PCMs. As the temperature rises, PCMs melts (i.e. phase change occurs from solid to liquid) and they absorb heat energy from the sun. This process shows that when the temperature drops, PCMs solidifies (i.e., phase change occurs from liquid to solid) and release heat energy back into the surroundings [8-10].

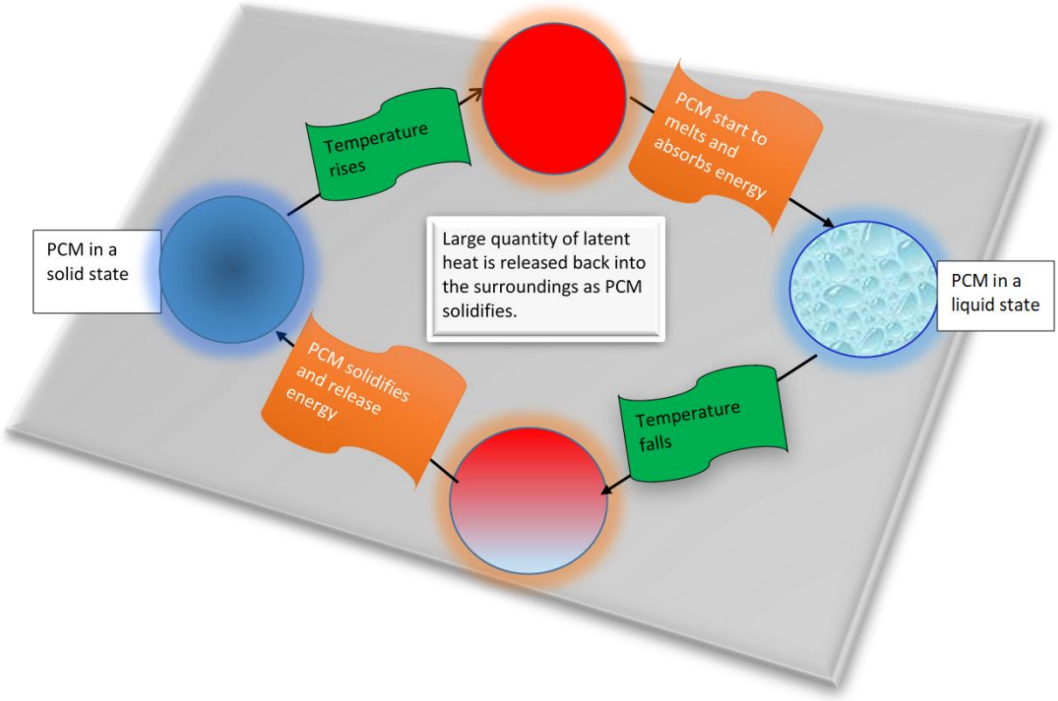

Figure 1.1: Schematic illustration of PCMs.

PCMs are classified into three different categories: inorganic, organic and eutectic PCMs (see **Figure 1.2**). Inorganic PCMs such as hydrated salts, salts, metals, and alloys, usually have high latent heat, high thermal conductivity and small volume change. Due to these properties they have great potential for use in applications such as building materials. However, they have disadvantages as they may be toxic, can easily corrode, may be super-cooling, and phase separation may occur during the phase change process. These drawbacks restrict their practical application [3,11,12,13].

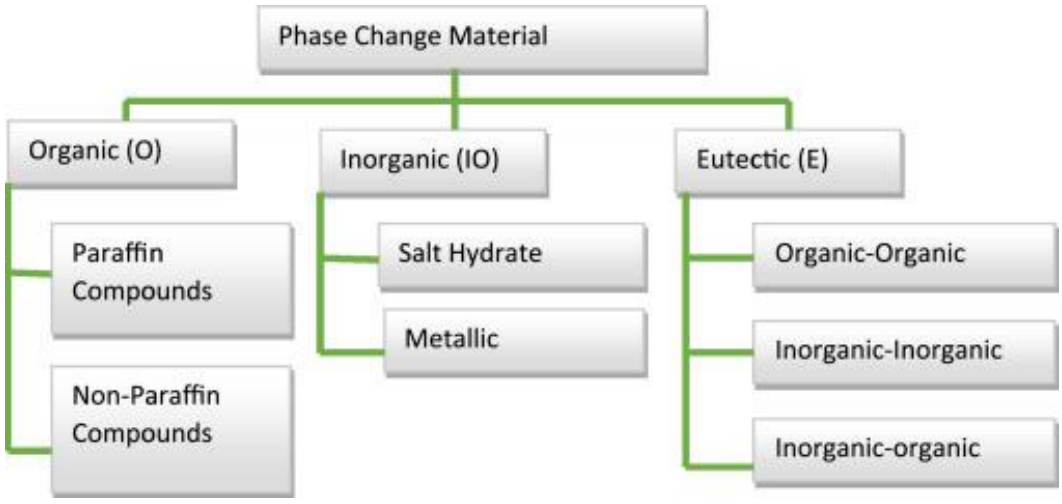

Figure 1.2: Classifications of phase change materials (PCMs).

Organic PCMs can be divided into two categories (**Figure 1.2**), namely paraffin and non-paraffin compounds (e.g., fatty acids and alcohols). They have versatile phase change temperatures, high latent heat, good chemical stability, and are non-toxic with little super-cooling. Eutectic PCMs are comprised of two or more soluble components mixed together, which have the features of simultaneously melt and solidify without materials separation [12,13,14]. The applications of PCMs include solar cooling, use in solar power plants and the space industry, preservation of food, pharmaceutical use, waste heat recovery, domestic hot water retention, building construction materials, and thermal management of electronic devices [15]. The advantages and disadvantages of various PCMs are tabulated in **Table 1.1**.

Table 1.1: Advantages and disadvantages of different kinds of PCMs [13,14,16,17].

Type of PCMs	Advantages	Disadvantages
Organic	• High heat of fusion; • No supercooling; • Availability in a large temperature range; • Chemically stable and recyclable; • Good compatibility with conventional construction materials.	• Low thermal conductivity; • Flammable; • Relative large volume change.
Inorganic	• High heat of fusion; • High thermal conductivity; • Non-flammable; • low volume change; • Available at low cost.	• Supercooling during freezing; • Corrosive to metals; • Toxicity; • Moderate chemical stability.
Eutectics	• Sharp melting point; • High volumetric thermal storage density; • Properties can be tailored to match specific requirements.	• High cost; • Limited data available on their thermos-physical properties.

Organic PCMs, especially paraffin compounds, have been the most widely studied due to their favourable characteristics such as high latent heat of fusion, congruent melting/freezing temperature, negligible super-cooling, low vapour pressure, stability, availability and low price cost. These materials are chemically inert, non-corrosive, and non-toxic. Their properties include a melting point that ranges between 30 ^{o}C and 90 ^{o}C depending on the number of carbons in the wax chains, and melting enthalpy that ranges between 180 and 230 KJ kg^{-1}, which is very high for organic materials. They also have specific heat capacity as their latent heat is about 2.1 $Jg^{-1}K^{-1}$, which indicates that they are excellent energy storage materials [18]. They offer significant advantages over other PCMs. Paraffin waxes are petroleum products, that consist of saturated straight-chain hydrocarbons of a mixture of numerous alkanes. They are characterized by straight or branched carbon chains with a general formula C_nH_{2n+2}, as well as the crystallization of the CH_3 chain that releases a large amount of latent heat. They are white, semi-transparent, tasteless, odour less solids, combustible and have good dielectric properties. Furthermore, they are soluble in benzene, ligroin, warm alcohol, chloroform, and carbon disulphide, but insoluble in water and acids [19,20,21]. The melting point and the latent heat increases with the number of carbon atoms. In Table 1.2, different PCMs and their properties are summarized.

Table 1.2: Indicates the different PCMs and their properties [10,14,22].

Materials	**Melting temperature (^{o}C)**	**Melting enthalpy (KJ kg^{-1})**
Paraffin	30-90	180-230
Polyethylene glycol (PEG)	20-25	146
Salt hydrates	11-120	100-200
Metallic	30-96	25-90
Capric + palmitate	22.1	153

After melting, paraffin waxes have a tendency to leak from the system during phase transition (i.e. from solid to the liquid phase) which is a severe problem associated with them. Furthermore, they exhibit low thermal conductivity (0.1-0.3 W $m.K^{-1}$) during phase conversion/transition which is also a significant drawback that limits their use in thermal exchange applications. These drawbacks directly affect their heat storage capacity and efficiency [6,14,23,24]. A significant way to overcome the drawbacks of paraffin waxes is to blend them with various polymers to suppress the leakage so that they can retain a compact

shape even after they have melted. Blending paraffin waxes with polymers provides an opportunity to utilize PCMs with unique and controlled structures.

Over the past years, the blending of polyolefins, especially polyethylene (PE) and polypropylene (PP), with paraffin waxes has been studied by various researchers [24-26]. PE appears to be the most suitable polymer to blend with paraffin waxes due to its chemical and structural similarities, which leads to the incorporation of a large amount of wax in PE matrix without significant wax leakage due to incompatibility between the components. However, compatibility between PE and PW depends on different factors such as wax type, type of PE and the branching type, degree of crystallinity, and the molecular weight [24,26-28]. PE is a hydrophobic thermoplastic polymer that is formed from ethylene ($CH_2 = CH_2$) and it can be used in many applications due to its unique properties such as high chemical resistance, and good dimensional stability when exposed to moisture. It has the chemical formula $(-CH_2 - CH_2)_n$ which contains the carbon and hydrogen elements where n represents the degree of polymerization. There are many types of polyethylenes such as high-density polyethylene (HDPE), low-density polyethylene (LDPE), linear low-density polyethylene (LLDPE) and ultra-high molecular weight polyethylene (UHMWPE) [29,30].

In this study, linear low-density polyethylene (LLDPE) was used as a matrix to prevent soft-paraffin wax from leaching during phase transition (from solid to liquid) as the PCM was fixed into a compact shape. LLDPE has better mechanical properties such as higher tensile strength, tear strength, flexibility, and good environmental stress crack resistance compared to LDPE and HDPE polymers [19,28,31]. However, the incorporation of wax into LLDPE matrix exhibits a low thermal conductivity, which is also another disadvantage associated with LLDPE/wax blend system. This shortcoming reduces the rate of storage and extraction of heat during the phase transitions, and it limits its use as an energy storage material. To improve the low thermal conductivity of the LLDPE/wax blend, different methods have been employed which involves the dispersion of conductive carbon-based, metallic and ceramic materials with a high thermal conductivity into the LLDPE/wax blend. Carbon-based and ceramic materials have attracted more interest due to their high thermal conductivities [5,32,33].

A conductive filler is a material that is added to a polymer to modify its properties, especially in terms of thermal performances. Conductive fillers are classified into three main types: carbon-based fillers, ceramic fillers, and metallic fillers [3]. Carbon nanotubes (carbon based) and boron nitride (ceramic based) are both preferred as conductive fillers due to their superior properties and ability to enhance thermal conductivity in the blend composites. Carbon

nanotubes (CNTs) are considered as an ideal filler for preparation of conductive polymer composites due to their excellent mechanical, electrical and thermal properties. These excellent properties of CNTs make them a suitable candidate for applications such as sensors, electronic circuits and devices, energy storage and energy conversion devices. Single-walled carbon nanotubes (SWCNT) used behave like conductors or semi-conductors depending on the chirality of the graphite sheets [33,34]. However, the high cost and electrical conductivity of the carbon materials limit their applications, especially in electronic packaging where electrical insulation is required as it compromises its use [35]. Thus, the addition of boron nitride (BN) as a second conductive filler is advantageous because it will retain dielectric properties of the material. BN is a percent insulator; hence it is more applicable in heat dissipation for electronic devices that require both high thermal conductivity and high electrical insulation. Incorporating BN nanofiller into the blends creates high insulating properties and also good thermal conduction that effectively dissipates the heat generated within the material to prevent thermal runaway [36,37,38].

The combination of BN and SWCNT (hybrid material) compliments each other due to their properties as mentioned above. It is thus expected of them to provide excellent properties in the blend composites. Based on this background, the study reports on the preparation and morphology, thermal stability, thermal and mechanical properties of the prepared blend composites.

1.2 Research Aims

This study investigates the preparation of shape-stabilized PCMs composed of paraffin wax, linear low-density polyethylene (LLDPE), and two conductive fillers (viz BN and SWCNT). It was envisaged that this composites would have an excellent latent heat (energy storage) with little or no wax leakage during the phase-transition process. As it is well known that both conductive fillers enhance the thermal conductivity of the system from previous work, the aims were to investigate their effect and their synergy on the properties such as: mechanical, thermal properties and as well as their thermal stability.

1.3 Research Objectives

The objectives of this project were to:

(i) Investigate the effects of single walled carbon nanotubes (SWCNTs) and boron nitride (BN) on the properties of LLDPE and LLDPE/wax blend; and to

(ii) Investigate the effect of the synergy between boron nitride (BN) and single walled carbon nanotubes (SWCNTs) on the properties of LLDPE and LLDPE/wax blend.

1.4 Thesis Organization

The outline of this thesis is as follows:

Chapter 1: Introduction

Chapter 2: Literature Review

Chapter 3: Methodology

Chapter 4: Results and Discussions

Chapter 5: Conclusion

1.5 References

[1] Mochane, M.J., & Luyt, A.S. **2012**. Preparation and properties of polystyrene encapsulated paraffin wax as possible phase change material in a polypropylene matrix. *Thermochimica Acta* 544: 63-70.

http://doi.org/10.1016/j.tca.2012.06.017

[2] Jiang, Z., Ouyang, T., Yang, Y., Chen, L., Fan, X., Chen, Y., Li, W., & Fei, Y. **2018**. Thermal conductivity enhancement of phase change materials with form-stable carbon bonded carbon fiber network. *Materials and Design* 143: 177-184.

http://doi.org/10.1016/j.matdes.2018.01.052

[3] Mngomezulu, M.E. **2009**. Phase change materials based on polyethylene, paraffin wax and wood flour. *MSc Thesis*, University of the Free State, Qwaqwa.

[4] Molefi, J.A. **2008**. Investigation of phase change conducting materials prepared from polyethylenes, paraffin waxes and copper. *PhD Thesis*, University of the Free State, Qwaqwa.

[5] Mochane, M.J., & Luyt, A.S. **2015**. The effect of expanded graphite on the flammability and thermal conductivity properties of phase change material based on PP/wax blends. *Polymer Bulletin*, 72: 2263-2283.

http://doi.org/10.1007/s00289-015-1401-9

[6] Sobolciak, P., Mrlik, M., AlMaadeed, M.A., & Krupa, I. **2015**. Calorimetric and dynamic mechanical behaviour of phase change materials based on paraffin wax supported by expanded graphite. *Thermochimica Acta*, 617: 111-119.

http://doi.org/10.1016/j.tca.2015.08.026

[7] Sobolciak, P., Abdelrazeq, H., Ozerkan, N.G., Ouederni, M., Nogellova, Z., AlMaadeed. M.A., Karki, M., & Krupa, I. **2016**. Heat transfer performance of paraffin wax-based phase change materials applicable in building industry. *Applied Thermal Engineering*, 107: 1313-1323.

http://doi.org/10.1016/j.applthermaleng.2016.07.050

[8] Mochane, M.J. **2011**. Polymer encapsulated paraffin wax to be used as phase change material for energy storage. *MSc Thesis*, University of the Free State, Qwaqwa.

[9] Mengjie, S., Fuxin, N., Ning, M., Yanxin, H., & Shiming, D. **2018**. Review on building energy performance improvement using phase change materials. *Energy and Buildings*, 158: 776-793.

http://doi.org/10.1016/j.enbuild.2017.10.066

[10] Nazir, H., Batool, M., Osorio, F.J.B., Isaza-Ruiz, M., Xu, X., Vignarooban, V., Phelan, P., Inamuddin., & Kannan, A.M. **2019**. Recent development in phase change materials for energy storage: A review. *International Journal of Heat and Mass Transfer*, 129: 491-523.

https://doi.org/10.1016/j.ijheatmasstransfer.2018.09.126

[11] Lin, Y., Jia, Y., Alva, G., & Fang, G. **2018**. Review on thermal conductivity enhancement, thermal properties and applications of phase change materials in thermal energy storage. *Renewable and Sustainable Energy Reviews* 82: 2730-2742.

http://doi.org/10.1016/j.rser.2017.10.002

[12] Liu, Z., & Yang, R. **2017**. Synergistically-enhanced thermal conductivity of shape-stabilized phase change materials by expanded graphite and carbon nanotube. *Applied Science* 7: 574.

http://doi.org/10.3390/app7060574

[13] Vasu, A., Hagos, F.Y., Noor, M.M., Mamat, R., Azmi, W.H., Abdullah, A.A., & Ibrahim, T.K. **2017**. Corrosion effect of phase change materials in solar thermal energy storage application. *Renewable and Sustainable Energy Reviews,* 76: 19-33.

http://doi.org/10.1016/j.rser.2017.03.018

[14] Frigione, M., Lettieri, M., & Sarcinella, A. **2019**. Phase change materials for energy efficiency in buildings and their use in mortars. *Materials,* 12:1260.

http://doi.org/10.3390/ma12081260

[15] Akeiber, H., Nejat, P., Abd. Majid, M.Z., Wahid, M.A., Jomehzadeh, F., Famileh, I.Z., Calautit, J.K., Hughes, B.R., & Zaki, S.A. **2016**. A review on phase change material (PCM) for sustainable passive cooling in building envelopes. *Renewable and Sustainable Energy Reviews* 60: 1470-1497.

http://doi.org/10.1016/j.rser.2016.03.036

[16] Savija, B. **2018**. Smart crack control in concrete through use of phase change materials (PCMs): A review. *Materials* 11: 654.

https://doi.org/10.3390/ma11050654

[17] Zhou, D., Zhao, C.Y., & Tian, Y. **2012**. Review on thermal energy storage with phase change materials (PCMs) in building applications. *Applied Energy* 92: 593-605.

http://doi.org/10.1016/j.apenergy.2011.08.025

[18] Krupa, I., Nogellova, Z., Spitalsky, Z., Janigova, I., Boh B., Sumiga, B., Kleinova, A., Karkri, M., & AlMaadeed, M.A. **2014**. Phase change materials based on high-density

polyethylene filled with microencapsulated paraffin wax. *Energy Conversion and Management*, 87: 400-409.

http://doi.org/10.1016/j.enconman.2014.06.061

[19] Krupa, I., & Luyt, A.S. **2000**. Thermal properties of uncross-linked and cross-linked LLDPE/wax blends. *Polymer Degradation and Stability*, 70: 111-117.

PII: S0141-3910(00)00097-5

[20] Krupa, I., & Luyt, A.S. **2001**. Physical properties of blends of LLDPE an oxidised paraffin wax. *Polymer*, 42: 7285-7289.

PII: S0032-3861(01)00172-0

[21] Krupa, I., Mikova, G., & Luyt, A.S. **2007**. Phase change materials based on low-density polyethylene/paraffin wax blends. *European Polymer Journal*, 43: 4695-4705.

http://doi.org/10.1016/j.europolymj.2007.08.022

[22] Sobolciak P., Abdelrazeq, H., Ouederni, M., Karkri, M., Al-Maadeed, M.A., & Krupa, I. **2015**. The stabilizing effect of expandable graphite on the artificial aging of shape stabilised phase change materials. *Polymer Testing*, 46: 65-71.

http://doi.org/10.1016/j.polymertesting.2015.06.017

[23] Han, L., Jia, X., Li, Z., Yang, Z., Wang, G. & Ning, G. **2018**. Effective encapsulation of paraffin wax in carbon nanotube agglomerates for a new shape-stabilized phase change material with enhanced thermal-storage capacity and stability. *Industrial and Engineering Chemistry Research* 57: 13026-13035.

http://doi.org/10.1021/acs.iecr.8b02159

[24] Sobolciak, P., Karkri, M., Al-Maadeed, M.A. & Krupa, I. **2016**. Thermal characterization of phase change material based on linear low-density polyethylene, paraffin wax and expanded graphite. *Renewable Energy* 88: 372-382.

http://doi.org/10.1016/j.renene.2015.11.056

[25] Popelka, A., Sobolciak, P., Mrlik, M., Nogellova, P., Chodak, I., Ouederni, M., AlMaadeed, M.A., & Krupa, I. **2018**. Foamy phase change materials based on linear-low density polyethylene and paraffin wax blends. *Emergent Materials*, 1: 47-54.

http://doi.org/10.1007/s42247-018-0003-3

[26] Kim, D., Park, I., Seo, J., Han, H., & Jang, W. **2015**. Effects of the paraffin wax (PW) content on the thermal and permeation properties of the LDPE/PW composite films. *Journal of Polymer Research,* 22: 19.

http://doi.org/10.1007/s10965-014-0650-x

[27] Abdelrazeq, H., Sobolciak, P., Al-Maadeed, M.A., Ouederni, M, & Krupa, I. **2019**. Recycled polyethylene/paraffin wax/expanded graphite based heat absorbers for thermal energy storage: An Artificial Aging Study. *Molecules,* 24:1217.

http://doi.org/10.3390/molecules24071217

[28] Molefi, J.A., Luyt, A.S., & Krupa, I. **2010**. Comparison of LDPE, LLDPE and HDPE as matrices for phase change materials based on a soft Fischer-Tropsch paraffin wax. *Thermochimica Acta,* 500: 88-92.

http://doi.org/10.1016/j.tca.2010.01.002

[29] Kurtz, S.M. **2016**. A primer on UHMWPE. *UHMWPE Biomaterials handbook (Third Edition),* PhD.

[30] AlMaadeed, M.A., Labidi, S., Krupa, I., & Ouederni, M. **2015**. Effect of waste wax and chain structure on the mechanical and physical properties of polyethylene. *Arabian Journal of Chemistry,* 8: 388-399.

http://dx.doi.org/10.1016/j.arabjc.2014.01.006

[31] Krupa, I., & Luyt, A.S. **2001**. Thermal and mechanical properties of extruded LLDPE/wax blends. *Polymer Degradation and Stability,* 73: 157-161.

PII: S0141-3910(01)00082-9

[32] Tian, B., Yang, W., He, F., Xie, C., Zhang, K., Fan, J., & Wu, J. **2017**. Paraffin/carbon aerogel phase change materials with high enthalpy and thermal conductivity. *Fullerenes, Nanotubes and Carbon Nanostructures,* 25: 512-518.

http://doi.org/10.1080/1536383X.2017.1347638

[33] Aalaie, J., Rahmatpour, A., & Maghami, S. **2007**. Preparation and characterization of linear low density polyethylene/carbon nanotube nanocomposites. *Journal of Macromolecular Science, Part B: Physics*, 46: 877-889.

http://doi.org/10.1080/00222340701389100

[34] Bagchi, A., & Nomura, S. **2006**. On the effective thermal conductivity of carbon nanotube reinforced polymer composites. *Composites Science and Technology*, 66: 1703-1712.

http://doi.org/10.1016/j.compscitech.2005.11.003

[35] Shen, H., Guo, J., Wang, H., Zhao, N., & Xu, J. **2015**. Bioinspired modification of h-BN for high thermal conductive composite films with aligned structure. *ACS Applied Materials & Interfaces*, 7: 5701-5708.

https://doi.org/10.1021/am507416y

[36] Merlo, A., Mokkapati, V.R.S.S., Pandit, S., & Mijakovic, I. **2018**. Boron nitride nanomaterials: biocompatibility and bio-applications. *Biomaterials Science*, 6: 2298.

https://doi.org/10.1039/c8bm00516h

[37] Yang, S., Huang, Y., Lei, J., Zhu, L., & Li, Z. **2017**. Enhanced thermal conductivity of polyethylene/boron nitride multilayer sheets through annealing. *Composites: Part A*, 107: 135-143.

https://doi.org/10.1016/j.compositesa.2017.12.031

[38] Hidayah, I.N., Mariatti, M., Ismail, H., & Kamarol, M. **2016**. Effect of selective localization on dielectric properties of boron nitride nanofiller filled linear low density polyethylene (LLDPE)/silicone rubber (SR) blends. *Polymer Testing*, 56: 131-139.

https://dx.doi.org/10.1016/j.polymertesting.2016.10.001

Chapter 2: Literature Review

2.1 Definition of paraffin wax and its uses for energy storage

Paraffins are saturated mixtures of N-alkanes with a melting temperature ranging between 0 ^{o}C to 102 ^{o}C, depending on the number of carbons in the chains. They are characterized by straight or branched carbon chains with a general formula C_nH_{2n+2} [1]. **Table 2.1** summarizes different types of paraffin waxes, their melting temperatures, carbon chains, latent heat and as well as their applications.

Table 2.1: Properties of different types of paraffin waxes [2]

Paraffins	**Melting points (^{o}C)**	**Latent heat (J/g)**	**Number of carbon chains**	**Applications**
L-PW wax	18-23	213-237	C16-C17	Cooling buildings
H-PW wax	56-68	253	C16-C17	
Soft paraffin wax	40-60	209-269	C18-C40	Solar water heater system
Hard Fischer-Tropsch wax	77	213-269	C28-C128	
Paraffin wax (grade RT42)	42	200-249	C12-C22	Solar collectors
Paraffin wax (grade RT50)	49	238	C25	Solar water heater system

The melting points and the latent heat of paraffin waxes with their number of carbon chains are shown in **Table 2.1**. Their properties (a combination of high specific heat capacity of latent heat and a high melting enthalpy) render paraffin waxes excellent for energy storage density. Paraffin waxes are chemically stable, do not degrade after repeated use, and are highly compatible with a wide variety of materials [2,3,4]. Paraffin waxes are widely used in candles, wax paper, and sun blocker as well as in cosmetic products such as lipstick, mascara, and moisturizing creams. They are also used for the paper coating, glass cleaning preparations, hot-melt carpet backing, biodegradable mulch, lubricants, stoppers for acid bottles, and electrical insulation [1].

2.2 Preparation and morphology

2.2.1 Polymer/paraffin wax blends

In order to understand the morphology of the polymer/paraffin wax, different techniques such as scanning electron microscopy (SEM), transmission electron microscopy (TEM), optical microscopy (OM), and atomic force microscopy (AFM) are employed. Various factors that affect the morphology of polymer/paraffin wax have been reported in the literature i.e., preparation methods, molecular weight and structure of waxes, wax content in the blends, as well as the shape and type of the polymer have been well documented [2,5,6]. The methods of preparation for polymers/paraffin wax blends include: melt mixing using Brabender Plastograph, solution mixing, twin screw and single extruder batch kneader, injection molding, and hot-press molding. The types of morphology that can be found in the polymer/paraffin wax blends are usually referred to as homogeneous and heterogeneous phases [5,7,8,9]. Chen and Wolcott [10] investigated miscibility of polyethylene/paraffin blends as phase change materials. The PE/paraffin wax blends with different weight ratios were melt compounded using a parallel co-rotating twin screw extruder. The dispersion of paraffin into three types of PE (i.e. HDPE, LDPE and LLDPE) was examined using AFM. It was observed that paraffin wax was well dispersed in the PE matrix, although the blends were not uniform because the shape and size of the paraffin wax domain were visible in the PE matrix. Furthermore, an intermediate phase was formed between HDPE and paraffin wax, and it was concluded that paraffin wax was less miscible with HDPE compared to LLDPE and LDPE. AlMaadeed and co-workers [11] investigated the effect of waste wax on three types of polyethylene. The blends with different weight ratios were prepared using a lab-scale twin screw extruder. The authors found that increasing the contents of the wax enhances the phase separation and miscibility. For HDPE blends with 10% wax content, it was reported that the wax dispersed throughout the system, which resulted in a homogenous phase. Whereas, with wax content of 20%, 30%, and 40%, agglomeration of wax was observed which indicated a poor interfacial adhesion between the wax and HDPE matrix. In case of LLDPE blends with low wax content (10%), the wax was well dispersed into the LLDPE matrix and at higher wax contents (20%, 30%, and 40%), agglomeration of the wax at the surface of LLDPE polymer was also observed. This also indicated a poor interfacial adhesion between the wax and LLDPE matrix. Furthermore, in LDPE blends, the dispersion of the wax was observed at lower contents (10% and 20%) while

at higher wax contents (30% and 40%), agglomeration of wax was observed, which also resulted in a poor interfacial adhesion between wax and LDPE matrix at higher content. Similar findings were observed by AlMaadeed *et al.* [12] who investigated the HDPE/wax composites with wax contents of 30, 40 and 50%. All the blends were prepared using a lab scale Brabender twin screw extruder. It was reported that an increased wax content enhanced wax agglomeration and, as a result, a less uniform distribution within the HDPE matrix was observed. Krupa and co-workers [4] blended two types of paraffin wax (*viz* soft paraffin wax and hard paraffin-wax) with LDPE at 50/50 polymer/wax ratio. The blends were prepared by mixing the samples in a 30ml mixing chamber of a Brabender Plasticorder PLE 311. It was reported that the LDPE/hard-paraffin blends exhibited a homogenous surface, with a slight indication of wax separation, while the LDPE/soft-paraffin wax blends showed a phase separation. The main reason for observing this different behaviour was that soft-paraffin wax has a lower molecular weight and viscosity, which thus made it easier to separate from the LDPE polymer compared to hard-paraffin wax that has a higher molecular weight. Krupa and Luyt [13] investigated the properties of extruded LLDPE/wax blends. All the LLDPE/wax blends were blended using an industrial extruder. The fractured surface of the blends was examined using SEM analysis. It was reported that an increase in wax content caused the LLDPE/wax blends to rapture along different lines. Mu and co-workers [14] investigated two types of paraffin wax (L-PW and H-PW) blended with high melt viscosity HDPE (hv-HDPE). All the blends were prepared using a twin-screw extrusion. It was reported that the waxes were well dispersed and distributed throughout the hv-HDPE matrix. However, voids were observed on the surface of the hv-HDPE/L-PW blend, which could have been a consequence of air trapped during blending process. The blends were treated with xylene to extract the wax component. It was seen that there were many voids observed in the etched surface of the hv-HDPE/H-PW blend, whereas on the etched surface of hv-HDPE/L-PW blend, the holes were less apparent. It is evident that low melting paraffin wax was more successful in forming a compact blend compared to a high melting paraffin wax. Kim *et al.* [15] prepared LDPE/paraffin wax blends by melt compounding and reported that the blend containing 50% of LDPE formed aggregates and there was a phase separation between LDPE and paraffin wax. This was an indication of a weak interfacial adhesion between LDPE and paraffin wax. At a lower content of wax i.e., 5/95 w/w LDPE/paraffin wax and 10/90 w/w LDPE/paraffin wax blends, no phase separation was observed between the polymer and paraffin wax, which indicated that there was a good interfacial interaction between LDPE and paraffin wax.

2.2.2 Polymer/conductive filler composites

It is well known that a strong interfacial interaction between the polymer and conductive filler, is very important as it affects the overall morphology and properties of the resultant composites. In various studies factors that affected the morphology of polymer/conductive fillers composites were the functionalization of the filler and content of the filler(s) [16,17]. Du and Cui [16] investigated the morphology of micro- and nano-BN filled polypropylene (PP) composites. It was observed that the nano-sized BN particles were uniformly dispersed in the PP matrix with various contents of nano-sized BN. The above behaviour was expected as the nanosized material interacts better with a polymer matrix, and as a result, better dispersion was observed. Furthermore, the latter authors reported a better interaction also between the PP/micro-BN composites. The behaviour that was observed for micro-BN was noteworthy as, in most case especially of unmodified microparticles, there tends to be agglomeration of the particles. Guo *et al.* [17] investigated the morphology of pure MWCNTs (denoted as p-MWCNTs), silanized MWCNTs (denoted as s-MWCNTs) and acidified MWCNTs (denoted as a-MWCNTs) that were all blended with poly (vinylidene fluoride) (PVDF) forming PVDF/MWCNTs composites. It was observed that p-MWCNTs were not dispersed well in the PVDF/p-MWCNTs composites as higher content of the filler was utilized in the system, resulting in agglomeration of the conductive filler. This emphasized that there was a poor interfacial interaction between p-MWCNTs and the PVDF matrix. Cracks were also observed in the PVDF/p-MWCNTs-composites with different loading of p-MWCNTs. In case of the acidified-MWCNTs particles in the PVDF composites, there was a reduction of large particles in comparison to PVDF/p-MWCNTs composites, which suggested that the agglomeration of MWCNTs was significantly reduced after acidification. However, cracks were still observed in the PVDF/a-MWCNTs composites which indicated that there was still a need for further improvement between the p-MWCNTs and PVDF matrix. On the other hand, the silanized MWCNTs in the PVDF composites gave better results than both pure and acidified MWCNTs. This was shown by well dispersed s-MWCNTs in the PVDF matrix which indicated a good interfacial interaction between the s-MWCNTs and the PVDF matrix. This good dispersion of s-MWCNT in the matrix allowed the particles to contact with one another, thus forming a filler network structure. Zhang *et al.* [18] investigated the interfacial interaction of the compatibilized and modified BN filler on the morphology of polyethylene/BN composites while Zhou *et al* [19] investigated the impact of a compatibilized and modified BN filler

blended with acrylonitrile butadiene styrene (ABS). Both authors reported that the modification of the BN particles was important because there was an improvement of BN dispersion in the composites which resulted in a good interfacial interaction between the BN filler and polymer matrix. Furthermore, the aggregates of the BN filler in both studies were significantly reduced. The usage of the compatibilizer was also found to increase the dispersion of the BN filler more compared to pristine BN and even modified BN. Based on the results reported by the above studies, one can conclude that the usage of a compatibilizer better improved adhesion between the BN filler and the polymer matrix more when compared with modified BN. Zhang and Zheng [20] investigated morphology of the BN flakes/poly (vinylidene fluoride) (PVDF) composites. The degree of dispersion of the BN flakes in the PVDF matrix was evaluated by SEM analysis. It was reported that the BN flakes were uniformly distributed in the PVDF matrix. Interestingly it was mentioned that the aggregates of the BN flakes were reduced by hot press, causing a homogenous dispersion of the BN flakes into PVDF matrix. It was also found that the BN flakes contacted one another when the material was pressed, which was advantageous in terms of forming a thermally network structure. Fei *et al.* [21] investigated morphology of the fractured surfaces of thermoplastic polyurethane (TPU)/BN composites with 10, 20, 30 40 and 50 % BN loading. It was reported that the BN platelets were well dispersed, and all the BN platelets were embedded in the TPU matrix. However, voids were still observed in the TPU/BN composites, which indicated that there was a pull-out of the BN platelets during fractionation of the samples. Generally, it is known that the filler pull-out is an indication of a poor interaction between BN platelets and TPU matrix. Furthermore, increasing BN content in the TPU/BN composites decreased the distance between the BN platelets, thus allowing them to contact one another to form thermally conductive pathways. Weng *et al*. [22] prepared the boron nitride/epoxy composites with 5 and 20 vol% of hexagonal boron nitride (h-BN) and cubic boron nitride (c-BN). Morphology of the fractured samples was examined by SEM analysis. Voids and defects observed in the BN/EP composites irrespective of the type of boron nitride used. It was reported that the voids in the composites were generated when the BN filler was peeled off or when pull-out occurred during fracturing of the samples. Moreover, increasing h-BN and c-BN contents in the composites, resulted in large agglomeration of the BN particles, which indicated that there was an uneven distribution of the BN particles in the EP matrix. An *et al.* [23] investigated morphology of the boron nitride/lignosulfonate/natural rubber (NR) composites and observed that the BN particles were embedded in the NR matrix. Lignosulfonate was not observed on the SEM micrographs which might have be due to its amorphous structure after carbonization. Furthermore, no voids and gaps were observed in the

composites which indicated that BN filler was well dispersed in the NR matrix with no obvious agglomeration. Zha *et al.* [24] reported on the morphology of the PP/BN composites filled with 1 vol% MWCNTs assisted by ethylene-α-octene block copolymer (OBC). It was observed that the BN sheets were dispersed in the PP matrix, however, there was gaps between the PP matrix and BN sheets which indicated a poor interfacial bonding between them. The incorporation of MWCNTs uniformly dispersed in the PP matrix with the help of OBC whereas, in the absence of OBC, there were large aggregates of MWCNT in the composites. In case of the PP/BN/OBC/MWCNTs composites, the MWCNTs particles were uniformly dispersed between the BN sheets in the composites with the aid of OBC. However, in the absence of OBC, the MWCNTs particles were found to agglomerate in the PP/BN/MWCNTs composites.

2.2.3 Polymer/paraffin wax/conductive filler blend composites

Conductive fillers are normally added into the polymer/wax blends to enhance their conductivity and flammability. As it was the case for polymer/wax blends, the conductive blend composites were also prepared by melt-mixing using Brabender Plastograph, solution mixing, twin screw and single extruder batch kneader, injection molding, and hot-press molding. There are also various factors that can affect the morphology of the polymer/paraffin/conductive blends composites which includes: mixing methods, particle size, surface modification of the filler, particle dispersion, orientation, and filler content [2,25,26]. Mixing different particle sizes and shape with the polymer/paraffin wax blends could decrease the voids between the particles, while reducing the filler content could also increase/improve the filler dispersion in the matrix. Modification of fillers has been shown to be the most effective and advantageous method to improve the interfacial interaction between fillers and the polymer blends and/or blends composites [18,25]. Motloung *et al.* [27] investigated LDPE/medium-soft Fischer-Tropsch paraffin wax (M3 wax) blends filled with two conductive fillers (carbon black and zinc metal). The blends composites were prepared via melt mixing using a Brabender Plastograph. It was reported that carbon black was well dispersed in the LDPE/M3 wax blend whereas zinc particles were randomly dispersed and agglomerated in some areas. It was also observed that there was a weak interaction between carbon black and zinc particles in the composites. However, there was a stronger interaction of zinc particles with the wax compared with the polymer matrix and/or carbon black, showing that the zinc particles primarily dispersed in the wax. Fredi *et al.* [28] investigated epoxy (EP)/paraffin wax (PW) blends filled

with carbon nanotubes (CNTs). All the blends composites were prepared by melt-mixing (80/18/2 w/w/w EP/PW/CNTs, 70/27/3 w/w/w EP/PW/CNTs, and 60/36/4 w/w/w EP/PW/CNTs). For samples with the highest wax content (i.e. 60/36/4 w/w/w EP/PW/CNTs denoted as EP-Par40-CNT), it was reported that the paraffin wax and the epoxy resin assumed a co-continuous structure. However, pores were seen in all the samples which indicated that air had been entrapped during the preparation of the samples. Furthermore, it was observed that the presence of CNT filler in the blends improved the interfacial adhesion between the epoxy and the paraffin wax. AlMaadeed and co-workers [12] investigated the effect of expandable graphite (EG) on the HDPE/wax blends. The composites were fabricated using a lab scale Brabender twin screw extruder. It was reported that the phase separation was more pronounced with the addition of EG particles, even though EG were dispersed in the blend matrix. Furthermore, Mhike *et al.* [29] investigated the effect of two types of graphite (natural graphite and expanded graphite [e-graphite]) on the LDPE/soft-paraffin wax blend composites. All the blends (90/10 w/w [wax/LDPE]/graphite and 90/10 w/w [wax/LDPE]/e-graphite) composites were prepared by twin screw extruder. It was observed that the sample containing e-graphite showed a much better particle dispersion in the LDPE/wax matrix compared to the sample containing the natural graphite. This may be ascribed to a high aspect ratio of expanded graphite when compared with natural graphite. Mochane and Luyt [30] also investigated the effect of expanded graphite (EG) on the properties of phase change material based on PP/wax blends. Melt-mixing using Brabender Plastograph was used to prepare all the samples. It was reported that in the absence of wax, the EG particles agglomerated in the PP matrix, however in the presence of wax there was a better dispersion of the EG in the PP matrix. It was concluded that low molecular weight wax contributed to a better dispersion of EG in the PP matrix. It was then concluded that this behaviour was because the wax penetrated in between the EG layers, thus separating the EG layers which made it easier to disperse well in the PP matrix. Molaba *et al.* [7] investigated the influence of medium soft-paraffin wax on the morphology of the iPP/silver nanocomposites. All the samples were prepared by melt-mixing using Brabender Plastograph. It was reported that the Ag nanoparticles formed aggregates in the iPP/wax blends and that the Ag nanoparticles had a higher affinity with the wax than iPP, which resulted in Ag favouring the molten wax phase during the crystallization of iPP. Furthermore, at higher Ag content the particles were not well dispersed and the extent of agglomeration was increased. In another study Molefi *et al.* [6] investigated the polyethylene/wax blends filled with copper particles. The samples were prepared by melt-mixing using a Brabender Plastograph. It was found that the composites showed a two-phase morphology, which implied that the LDPE and

wax were immiscible with each other. Furthermore, the particles were clearly covered by the wax layer, showing that the Cu particles had a stronger affinity for the wax than LDPE. A similar behaviour was observed by Molaba and co-workers [7].

2.3 Thermal stability

2.3.1 Polymer/paraffin wax blends

Many studies have investigated the thermal stability of polymer/paraffin wax blends [3,11,14,15,31,32,33]. Thermogravimetric analysis (TGA) is the preferred technique used to determine the weight loss and decomposition of the materials when the sample is heated at a constant heating rate [34,35]. Different factors were found to affect the thermal stability of polymer/wax blends, such as the content of the paraffin wax, type of polymer matrix and paraffin wax. Mu *et al.* [14] reported on the thermal stability of high melt viscosity high density polyethylene (hv-HDPE) blended with high paraffin wax (H-PW) and low paraffin wax (L-PW). The investigated composition of the Hv-HDPE/H-PW blends were 50/50, 35/65 and 25/75, whereas for the Hv-HDPE/L-PW blends, the contents/compositions were 60/40, 50/50, and 35/65 wt.%. It is a well-known fact that in the blends consisting of wax and polymer, the content of the polymer is higher than that of the phase change material. One can realize that in the latter study [14], the compositions of the wax in blends were higher than that of the polymer. It was reported that the thermal stability of all the blends decreased with increasing wax content. This was because the waxes (H-PW and L-PW) has shorter chains than the pure hv-HDPE polymer. Furthermore, it was also reported that both blends (hv-HDPE/H-PW and hv-HDPE/L-PW) degraded via two-steps degradation. This indicated that the hv-HDPE polymer and waxes were immiscible. The first degradation step at temperatures around 220 ^{o}C was ascribed to the evaporation of the wax, while the second degradation step at temperature(s) around 450 ^{o}C was due to the degradation of the polymer matrix. Chen and co-workers [31] investigated thermal characteristics of poly (lactic acid) (PLA)/paraffin wax blends prepared by conventional melt compounding and sub-critical gas-assisted processing (SGAP). The investigated composition(s) of PLA/PW blends were reported as 80/20, 65/35 and 50/50 wt%. The onset temperatures of degradation of the conventional compounded PLA/PW blends were reported as 301.6 ^{o}C, 299.3 ^{o}C and 286.2 ^{o}C, respectively which were slightly lower than that of the pure PLA polymer at 327.0 ^{o}C. This behaviour was ascribed to the presence of the short

chains of the paraffin wax and its low thermal stability. Furthermore, the samples processed with SGAP showed higher maximum temperature degradations (378.9 ^{o}C, 380.3 ^{o}C and 379.4 ^{o}C, respectively) when compared with PLA polymer (371.3 ^{o}C). Sotomayor et al. [32] investigated the thermal stability of the pure high density polyethylene (HDPE) and HDPE/paraffin wax (PW) blends. The investigated compositions of HDPE/PW blends were 95/5, 90/10, 80/20, 70/30, 60/40, and 50/50 wt%. It was observed that both pure HDPE and PW degraded in one-step degradation temperatures at 410 ^{o}C and 200 ^{o}C, respectively. HDPE was obviously observed to have the highest thermal stability in comparison to PW. Meanwhile, the HDPE/PW blends degraded in two-step degradation. The first step was detected at the temperatures around 233-237 ^{o}C, which was attributed to the decomposition of the wax. The second degradation step at the temperature range of 309-510 ^{o}C, was due to the degradation of HDPE polymer. The thermal stability of all the blends (95/5, 90/10, 80/20, 70/30, 60/40, and 50/50 wt%) were found to be less than that of the pure HDPE, which indicated that there was a reduction in thermal stability of the HDPE by incorporating wax. It seemed as if the wax volatiles that were released earlier catalysed the degradation of the polymer matrix, and as a result, the thermal stability decreased with the addition of wax. Gao and co-workers [33] studied thermal stability of paraffin-based hydroxyl-terminated polybutadiene (HTPB) binder containing a three-dimension (3D) diurea-paraffin wax (DU-PW). The investigated composition of DU-PW/HTPB composites were 20/80, 40/60, and 60/40 wt.%, respectively. It was reported that there was one weight loss stage detected for paraffin wax (PW) and diurea (DU)-PW. PW had the lowest thermal stability when compared with DU-PW, PW/HTPB and DU-PW/HTPB composites. The incorporation of DU into PW increased the thermal stability of the PW, which due to the PW chains entrapped into DU, as a result, it delayed the evaporation of wax. Furthermore, the HTPB polymer degraded in two-steps degradation which corresponded to depolymerization and decomposition of HTPB. PW/HTPB blend also degraded in two-steps degradation process. The first stage was correlated to the evaporation of PW and partial decomposition of HTPB polymer. The second stage correlated with the decomposition of HTPB polymer. The addition of PW and DU-PW into HTPB reduced the thermal stability of the HTPB polymer, but no explanation was given as to why PW and DU-PW reduced the thermal stability of the HTPB. One can conclude based on the previous literatures that the decrease in thermal stability may be ascribed to the low molecular weight and less thermally stable waxes which are capable of acting as catalyst for the degradation of polymer matrices. Furthermore, it was observed that the DU-PW/HTPB samples showed higher thermal stability when compared with the PW-HTPB, which was attributed to a better

interaction between the PW and HTPB in the presence of DU. Kim et al. [15] observed that pure components (SF-0 (paraffin wax) and SF-100 (LDPE)) decomposed completely with a one-step degradation, while the two blends (SF-5 and SF-10) degraded in two distinguishable steps. The examined compositions were 100 (SF-0) and 100 (SF-100) for pure materials and 95/5 (SF-5) as well as 90/10 (SF-10) for the PW/LLDPE blends. It was also observed that the thermal stability of all the composites was lower than that of the LDPE polymer. Furthermore, pure wax (SF-0) showed one weight loss step which is correlated with the decomposition temperature of wax evaporated at 242.0 ^{0}C. The SF-5 (5/95 w/w paraffin wax/LDPE blend) sample degraded in two steps. The first degradation step occurred temperatures around 229.7 ^{o}C which was correlated to the evaporation of the wax. The second degradation step occurred at temperatures around 415.6 ^{o}C which was attributed to the decomposition of LDPE polymer. Similar behaviour was observed with the SF-10 (10/90 w/w paraffin wax/LDPE blend) whereby the corresponding temperatures of evaporated wax and decomposition of LDPE were recorded at 238.1 ^{o}C and 411.5 ^{o}C, respectively.

2.3.2 Polymer/conductive filler composites

Various conductive fillers such as boron nitride (BN), carbon nanotubes (CNTs), carbon black (CB), expandable graphite (EG), graphene, copper (Cu), aluminium nitride (AIN) and silver (Ag) are incorporated into polymer matrices not only to improve the thermal conductivity but also to enhance the thermal stability [22,36-45]. However, it was worth noticing that factors such as the content of the filler, filler type and size of the particles can affect the thermal stability of the polymer/conductive filler composites. Oner *et al.* [37] investigated the thermal stability of poly (3-hydoxybutyrate-co-3-hydroxyvalerate) (PHBV)/BN nanocomposites with 0.5, 1, 2, and 3 wt% BN content. Two types of BN were used, namely (i) silanized hexagonal type BN denoted as OSBN and (ii) silanized flake type BN denoted as OSFBN. It was reported that pure PHBV and BN/PHBV composites degraded in one-step degradation in the temperatures around 230-300 ^{o}C. The addition of two types of boron nitride (BN), unmodified and modified, enhanced the thermal stability of the PHBV matrix. The thermal stability of the modified BN/PHBV composites showed higher thermal stability than the unmodified BN composites. For an example, the PHBV/1OSBN and PHBV/1OSFBN (*i.e.* both at 1 wt% BN) composites degraded at 252.70 ^{o}C and 251.10 ^{o}C, respectively, while the unmodified BN composites showed slight degradation values i.e. PHBV/1BN at 250.30 ^{o}C and PHBV/1FBN

at 247.09 °C. The authors provided no reason for this observation, but one may assume that in the modified system, the polymer chains restricted segmental movement which was denoted by enhanced thermal stability. It can thus be concluded that the incorporation of modified and unmodified BN into PHBV was successful in terms of improving the thermal stability of the neat PHBV. Weng *et al.* [22] investigated the thermal stability and thermal conductivity of boron nitride/epoxy composites. Two types of boron nitride (hexagonal-BN and cubic-BN) were employed for fabrication of the composites. It was reported that the weight loss values of EP resin at $T_{5\%}$, $T_{10\%}$, and $T_{50\%}$ were 325.12 °C, 371.07 °C, and 429.14 °C, respectively. The incorporation of BN into EP resin improved the thermal stability of the composites. The weight loss of h-BN (20 vol%)/EP composites at $T_{5\%}$, $T_{10\%}$, and $T_{50\%}$ values were 352.93 °C, 387.78 °C, and 441.02 °C, respectively, whereas the weight loss of c-BN (20 vol%)/EP composites at $T_{5\%}$, $T_{10\%}$, and $T_{50\%}$, the values were 366.38 °C, 391.94 °C, and 438.04 °C, respectively. Furthermore, the decomposition temperature of the c-BN composites at $T_{5\%}$, and $T_{10\%}$ (20 vol% loading of boron nitride) was much higher than the h-BN composites at the same filler loading. This behaviour was due to diamond-like structure of the c-BN, which acted as a much better heat barrier than the hexagonal structure of the h-BN. However, at $T_{50\%}$ the decomposed temperature of the h-BN composites was much higher than that of the c-BN composites, which was due to layered structure of h-BN that had large interface with the EP matrix. Ren *et al.* [38] investigated the thermal stability of ultra-high-molecular-weight polyethylene (UHMWPE)/boron nitride (BN) and UHMWPE/(BN+multi walled carbon nanotubes (MWCNTs) composites with 30 and 50 wt.% of BN as well as 1 wt.% of MWCNTs. In this study, two types of BN i.e. hexagonal BN particles denoted as BNp and BN sheets denoted as BNs, were utilized for the fabrication of the composites. It was reported that the initial decomposition temperature and decomposition peak temperature of pure UHMWPE were 445.2 °C and 467.3 °C, respectively. However, the incorporation of BN and BN+MWCNTs hybrid fillers had a little effect on the thermal stability of the UHMWPE composites because there was a slight increase in decomposition temperature of the composites. The decomposition peak temperature of the UHMWPE/BNs and UHMWPE/BNp composites were 468.6 °C and 467.0 °C, respectively. on the other hand, decomposition peak temperature of the UHMWPE/(BNs+MWCNT) and UHMWPE/(BNp+MWCNT) composites were 469.2 °C and 470.1 °C, respectively. This effect on the UHMWPE matrix was attributed to the presence of BN and hybrid fillers which were found to restrict the movement of the polymer chain which, in turn, improved the decomposition temperature. However, it has been shown that, in some cases the incorporation of conductive fillers into polymers reduced the thermal stability of the

materials [39,41]. Lule and Kim [41] investigated the thermal stability of poly (butylene succinate) (PBS)/aluminium nitride (AIN) nanocomposites. It was observed from the TGA curves that the introduction of the raw AIN and modified AIN into PBS matrix reduced the thermal stability of the pure PBS polymer because the composites degraded slightly at lower temperatures compared to that of the pure PBS polymer. However, the literature does not provide a clear reason as to why the incorporation of AIN filler into PBS matrix reduced the thermal stability. Furthermore, the char residue of the composites was found to be high in comparison to that of the pure PBS polymer. Yu *et al.* [39] reported that pure BN was a highly stable material with no significant weight loss compared to pure EP and the composites. Three significant weight loss steps were detected for the BN/epoxy (EP) composites. The first step was observed at around 145-270 ^{o}C which was ascribed to the pyrolysis of the low molecular weight substance. The second degradation step occurred around 270-420 ^{o}C, which was attributed to the decomposition of the EP resin. The third degradation step was observed at around 420-620 ^{o}C which was due to the combustion of the residual carbon of the epoxy resin. The TGA curves showed that the BN composites reduced thermal stability of the EP resin, but the char yield of the composites was higher than that of EP resin.

2.3.3 Polymer/paraffin wax/conductive filler blend composites

Conductive fillers are added into the polymer/wax blends to increase thermal stability of the polymer/wax blends. Several studies have been reported on the thermal stability of polymer/paraffin wax/conductive filler composites [6,12,29,30,46]. Mochane and Luyt [30] investigated the effect of expanded graphite (EG) on the thermal stability of the polypropylene (PP)/wax blends. The EG content added to PP/wax blends (60/40 w/w) were 3, 6, and 9 weight to weight. The TGA curves showed that the EG is highly thermally stable and has the highest thermal stability compared to the decomposition temperatures of PP and wax. It was observed that all the samples containing wax degraded in two-steps degradation. The first degradation step occurred between 250 ^{o}C to 300 ^{o}C was associated with the degradation of the wax, whereas the second degradation step took place between 250 ^{o}C to 450 ^{o}C and was ascribed to the degradation of the PP. The thermal stability of the PP/wax blends were improved with the incorporation of EG and increasing EG content. It was concluded that EG served as the barrier, which prevented further degradation of the PP matrix while it also trapped the volatile decomposition products that can only escape at higher temperatures. AlMaadeed *et al.* [12]

reported that a two-steps degradation was observed for the HDPE/wax blends. The first step occurred at 220 ^{o}C which was attributed to the degradation of the wax, while the second step was at 400 ^{o}C temperature which was correlated with the HDPE polymer. The incorporation of EG (5, 10, 15 wt%) into HDPE/wax blends enhanced the thermal stability of the composites. This behaviour was ascribed to a decrease in chain mobility which delayed the degradation of the composites. Luo *et al.* [47] investigated the thermal stability of the flexible paraffin/multi-walled carbon nanotubes (MWCNTs)/polypropylene hollow fiber membrane (PHFM) composites. The composites were fabricated using 0.47, 0.71, and 0.93 wt% of MWCNTs. It was reported that the paraffin decomposed in one-step at a temperature of 238.45 ^{o}C while PHFM and the composites decomposed in two-steps degradation. The first degradation step for pure PHFM was recorded in the temperatures between 411.56–435.84 ^{o}C and the second step occurred in the region of 436.41–528.29 ^{o}C. As for the composites, the first degradation step was observed in the temperatures between 243.37-247.82 ^{o}C and the second step in the temperatures between 395.57–412.02 ^{o}C. The first step was ascribed to the degradation of the paraffin whereas the second step was correlated with the degradation of the polypropylene hollow fiber membrane (PHFM) polymer. The thermal stability of the composites was reduced in the presence of MWCNTs as compared to that of the pure PHFM polymer, which indicated that MWCNTs did not enhanced the thermal stability of PHFM. Zhang *et al.* [48] reported on the thermal stability of the expandable graphite (EG)-paraffin wax (PW)-silicon rubber (SR) composites. It was shown that pure PW degraded in one-step, at temperatures in the range of 145-390 ^{o}C, whereas the pristine SR also degraded in one step between 370 to 650 ^{o}C. This was due to the degradation of the C-C, C-H, Si-C side chain and Si-O-Si main chain. It was also observed that SR had higher thermal stability when compared with PW, which indicated that SR has the potential as a host or matrix for PW. In case of the EG-PW-SR composites, two-steps degradation was detected. The first step was ascribed to the degradation of the PW and the second step was correlated to the degradation of the SR. Furthermore, the presence of EG in the EG-PW-SR composites, delayed the decomposition of PW. This was evident by a higher onset of degradation temperatures compared with pure PW. There was high char yield obtained due to good thermal stability of the SR and capillary force which was provided by the porous structure of EG. Molefi *et al.* [6] investigated the thermal stability of different types of polyethylene (low-density polyethylene [LDPE], linear low-density polyethylene [LLDPE] and high-density polyethylene [HDPE]) mixed with paraffin wax and copper (Cu). All the PE/paraffin wax blends were mixed at 60/40 wt%. It was reported that the composites degraded in two-steps. The addition and increase of Cu particles (1, 3, 5 and 10 wt%), enhanced the

thermal stability of the composites which was clearly higher than of the PE/wax blends. This was ascribed to the reduction of the free radical chain mobility by Cu particles which reduced the degradation process. Interestingly, the authors also observed that, with the HDPE/wax/Cu composites, the effect of Cu was less pronounced because of the higher crystallinity of HDPE that gave rise to higher thermal stability compared to the LDPE and LLDPE composites, respectively. Cao ad co-workers [46] investigated thermal performance of PW/EG/carbon fiber (CF)/HDPE composites. It was reported that the two pure components (HDPE and PW), both degraded in one-step, whereas the composites degraded in two-steps. The first degradation step occurred at temperatures around 190 ^{o}C to 330 ^{o}C, which may be ascribed to the evaporation of wax, while the second step occurred at temperatures between 450-480 ^{o}C, which was attributed to the degradation of HDPE in the composites.

2.4 Thermal properties

2.4.1 Polymer/paraffin wax blends

Many studies have reported on the thermal properties of polymer/paraffin wax blends [2,4,7,11,49,50]. Thermal properties of polymer/paraffin wax blends were investigated by utilizing the differential scanning calorimetry (DSC). Parameters such as melting temperature, melting enthalpy and crystallization temperatures were reported for polymer/paraffin wax blends. It has been reported that the addition of paraffin wax into polymer matrices (especially the polyolefins and polyethylene's) decreased the melting temperature of pure polymer in polymer/wax blends. Generally, when phase change materials are added into polymers, two endothermic events are detected which indicates that neither the wax nor the polymers are miscible. Krupa and co-workers [4] investigated the effect of two types of wax (Wax S and Wax FT) on the thermal properties of polyethylene. Wax S denotes soft paraffin wax, while Wax FT denotes hard Fischer Tropsch wax. In the latter study [4] the compositions of the wax added into the polymer matrix were 30, 40, 50 and 60%. It was reported that, for LDPE/Wax S blends, the melting temperature of the polyethylene matrix decreased with an increase of Wax S content into the blends, while the melting enthalpy of all the blends increased with increasing Wax S content due to higher crystallinity of the wax. Similar observations were reported for LDPE/Wax FT blends. The decrease in melting temperatures was less significant in the Wax FT compared to Wax S. This may be ascribed to a better interaction between LDPE

and Wax S, hence the reduction in melting temperatures. AlMaadeed *et al.* [12] reported that the incorporation of paraffin wax in the HDPE/paraffin wax blends reduced the melting temperature of the matrix from 133 ^{o}C to 126 ^{o}C, 124 ^{o}C and 123 ^{o}C with wax content of 30, 40 and 50%, respectively. It is well known that the decrease in melting temperature is an indication of the reduction in lamellar thickness. It was further reported that the melting enthalpy of HDPE decreased with increasing in wax content i.e. 169 to 133.4, 119 and 110 j/g with wax content(s) of 30, 40 and 50%, respectively. Molefi and co-workers [49] investigated the thermal properties of LDPE, LLDPE and HDPE matrices blended with soft-paraffin wax (M3 wax). It was reported that pure M3 wax showed two melting peaks (i.e. the major and a shoulder peak). The shoulder melting peak was observed at about 33 ^{o}C and a major peak was reported at around 58 ^{o}C. The theory behind the minor and major peaks are associated with the solid-solid phase transition and melting of the crystallites, respectively. It was observed that the LDPE/wax blends showed two defined endothermic peaks. The first endothermic peak was detected between 30-70 ^{o}C (which consisted of shoulder peak at 33 ^{o}C and two overlapping peaks between 45-70 ^{o}C). As explained earlier, the peak 33 ^{o}C was due to the solid-solid phase transition and two overlapping peaks between 45-70 ^{o}C are attributed to the melting of the crystallites. The second endothermic peak was associated with the melting peak of the LDPE crystallites. Similar observations were reported for the LLDPE/wax and HDPE/wax blends, however, there was no development of overlapping peak in these blends, as was the case for LDPE/wax blends. Furthermore, the melting enthalpies of the HDPE/wax blends were found to be higher than that of LDPE/wax and LLDPE/wax blends, respectively. The behaviour was ascribed to the higher crystallinity of HDPE in comparison to both LDPE and LLDPE polymers. Zhou *et al.* [51] investigated thermal properties of paraffin/HDPE phase change blends. Pure paraffin wax was reported to have two endothermic peaks. The peak shoulder at about 54-56 ^{o}C was ascribed to the solid-solid transition and the main peak between 68-70 ^{o}C was attributed to the melting temperatures of the crystallites. Two clearly distinguished endothermic peaks were detected on the HDPE/paraffin wax blends. The first melting peak that occurred around 68-70 ^{o}C was due to the melting of paraffin wax, while the second melting peak between 120-140 ^{o}C which was ascribed to the melting of HDPE crystallites. It can be concluded from these observations that the blend of HDPE/paraffin wax are immiscible, hence the two defined endothermic peaks were detected. Similar observations were reported by Akishino *et al.* [52] who investigated the thermal behaviour of the blends consisting of polyethylene wax and paraffin. The pure paraffin showed two clearly endothermic peaks, whereby the peak shoulder was observed at 45 ^{o}C and the main endothermic peak occurred at

65 °C. However, the polyethylene wax showed three endothermic peaks at different temperatures. The main peak (first highest peak) was observed around 50 °C, which was attributed to solid-solid transition of paraffin. The shoulder peak (second highest peak) was detected around 58-60 °C which was due to the melting fraction of the wax with low molecular weight. The third peak which was observed between 90-100 °C, can be correlated to melting of the small fraction of the linear low-density polyethylene. Furthermore, it was reported that temperatures at which the third peak occurred decreased with decreasing polyethylene content in the blend. Chen and Walcott [10] investigated miscibility of the paraffin wax/polyethylene blends and reported that, when the paraffin wax content was decreased, the magnitude of the peaks shifted towards lower temperatures in this order: HDPE/paraffin < LDPE/paraffin < LLDPE/paraffin. This behaviour indicated that the effect of LLDPE on the paraffin crystallization was much greater than either HDPE and LDPE, due to a shift in crystallization peaks.

2.4.2 Polymer/conductive filler composites

Many studies investigated the thermal properties of the polymer/conductive filler composites [43,51,54,55,56,57] and there is agreement that DSC analysis is the best method for analysing the melting and crystallization temperatures of the polymer/conductive filler composites. Jin-hua *et al.* [51] reported that the melting and crystallization temperatures of the LLDPE/MWCNTs nanocomposites slightly increased with increasing MWCNTs content. This suggests that MWCNTs do not prevent the crystallization of the LLDPE polymer but rather acts as a nucleation reagent for LLDPE matrix. Shi *et al.* [54] reported two melting peaks for pure LLDPE, whereby the first sharp peak (primary peak) was detected around 120 °C which was attributed to the crystals of thick lamellae, whereas the second broad peak (secondary peak) that was observed between 80-115 °C which was ascribed to the appearance of small imperfect crystals with thin lamellae. The addition of and increasing content of MWCNTs shifted the melting temperatures of the composites towards higher temperatures. This may be attributed to the nucleation effect of the MWCNTs into the polymer matrix, which might have occurred as a result of a shift in the melting temperature of the polymer in the composite. The crystallization temperature of the LLDPE/MWCNTs composites increased with increasing MWCNTs content. Furthermore, the melting enthalpy (114.9 J/g) of the LLDPE/MWCNTs composites was higher than that of LLDPE (107.5 J/g). In addition, the crystallinity of the

LLDPE/MWCNTs composite (39.6%) containing 3 wt.% MWCNTs was higher than that of the neat LLDPE (36.7%). This behaviour was attributed to the heterogeneous nucleation effect of MWCNTs. Russo *et al.* [55] investigated the effect of pristine MMWCTs and hybrid fillers on thermal properties of polypropylene (PP). It was reported that the addition of MWCNTs into PP matrix had less effect on the melting temperature of the PP/MWCNT composites i.e. 167 ^{o}C for composites and 166 ^{o}C for pure PP. However, the addition of hybrid fillers i.e. MWCNT+BN into PP matrix, had a slight effect on the melting temperature of PP matrix in the hybrid composites as the temperature increased to 169 ^{o}C when compared with pure PP. In relation to crystallinity, it was found that PP/MWCNTs composites had no significant effect on the crystallinity of the PP matrix. However, in case of the hybrid PP/MWCNT/BN composites there was a reduction in crystallinity from 41% for pure PP to 39% for the PP/MWCNT/BN composites. Wu *et al.* [56] prepared the BN@ultra-high molecular weight polyethylene (UHMWPE) composites with 2.1, 4.4, 9.4, 15.1, 21.6, 29.3, and 38.3 vol% of BN. It was reported that the melting temperature of the BN@UHMWPE composites slightly decreased with increasing BN loading when compared with pure UHMWPE, which may be ascribed to imperfect lamellar crystallites in the composites compared to the well-formed lamellae in the pure UHMWPE. Furthermore, there was a reduction in the enthalpy of melting when the BN content increased. For an example, the incorporation of 38.3 vol% of BN into the UHMWPE matrix, decreased the melting enthalpy of the composites (50.4 J/g) when compared with pure UHMWPE (146.7 J/g). There was no reason provided for such an observation. Furthermore, the degree of crystallinity of the BN@UHMWPE composites was decreased with increasing BN content. However, at 4.4 vol% BN content the degree of crystallinity increased to 54%, which was higher than that of pure UHMWPE (50%). The behaviour indicated that increasing the filler content, can affect the crystallinity and crystal growth. Based on the above observation it may be argued that appropriate filler content acts as a nucleation site which then facilitates the nucleation process. Pan *et al.* [57] investigated the influence of hexagonal BN (hBN) on the melting and crystallization temperatures of PTFE composites. PTFE/hBN composites were prepared with 5, 10, 20 and 30 vol% hBN content. It was observed that the addition and increasing BN content did not influence the melting temperature of the PTFE/hBN composites because at the highest hBN content (30 vol%) the melting temperature was 330.0 ^{o}C which was almost the same as pure PTFE (330.1 ^{o}C). There was an increase in degree of crystallinity with the addition of 30 vol% of BN into PTFE matrix when compared with pure PTFE. Furthermore, it was also observed that the crystallization temperatures shifted slightly towards higher temperatures with increasing hBN filler. This observation may be ascribed to

the nucleation effect of the filler as a result enhancing the crystallization temperatures. Furthermore, the observation indicated that there was heterogeneous nucleation caused by the hBN filler. Lomate *et al.* [43] reported on thermal properties of LDPE/copper (Cu) composites with 0.5, 1, 1.5, 2, 2.5, and 3 wt% Cu content. The melting temperature of the pure LDPE was detected at 124.34 ^{o}C, meanwhile there was no drastic change in melting temperature of the LDPE-Cu composites. At 0.5, 1, 1.5 and 2 wt.% of the Cu content, the melting temperature of the LDPE/Cu composites was 124.59, 124.87, 125.10 and 125.31 ^{o}C, respectively. However, with the addition of 2.5 and 3 wt% Cu contents, a slight increase in melting temperature of the LDPE/Cu composites was observed which were recorded as 126.46 and 127.31 ^{o}C. This indicated that copper nanoparticles restricted the he movement of polymer chain and as a result shifting the melting temperature to higher values. Feng *et al.* [58] investigated the effect of hybrid fillers (BN and MWCNTs) on the thermal properties of the HDPE polymer. All the composites were prepared with 10, 20, 30 wt% BN and 3 wt% MWCNTs and the compatibilizer (HDPE-g-MAH) added into the system. It was reported that BN filler alone had a little effect on the melting temperature of the HDPE matrix. However, the crystallization temperature of the HDPE/BN composites increased with increasing BN content. The addition of 30 wt.% BN into the polymer matrix increased the crystallization temperature from 119.92 ^{o}C (neat polymer) to 124.71 ^{o}C for the composites. This behaviour showed that BN nanoparticles had no effect on the HDPE crystal structure. The crystallinity of the hybrid composites increased to 75.80% with 10 wt.% BN filler in the composites which was higher than that of pure HDPE, which was 73.41%. Che *et al.* [59] investigated the thermal properties of the HDPE/BN/CNT hybrid composites. The composites were prepared by melt blending and moulded by hot pressing and hot rolling with 5, 25wt% BN and 3wt% CNT content which were kept constant in the hybrid composites. It was reported that the melting temperature of pristine HDPE moulded by hot pressing (denoted as HDPE-P) was 126.7 ^{o}C whereas the melting temperature of the pure HDPE moulded by hot rolling (denoted as HDPE-R) was 131.7 ^{o}C. It was also observed that the variation of the melting temperature with the addition and increasing content of hybrid fillers in the composites was very small for both process. The melting temperature of the HDPE/25BN/3CNT-P hybrid composites was 126.6 ^{o}C and that of HDPE/25BN/3CNT-R hybrid composites was recorded as 129.6 ^{o}C. This indicated that the network structure of both fillers was not effective in influencing the melting temperature of the composites.

2.4.3 Polymer/paraffin wax/conductive filler blend composites

Several studies have reported on the effect of conductive fillers to improve the thermal properties of the polymer/paraffin wax blends [6,7,12,27,29,30]. It has been reported that the addition of conductive fillers on the polymer/wax blends reduced the leakage of the paraffin wax and/or phase change materials in the blends. However, in some cases the addition of the conductive fillers had a slight effect on the melting and crystallization temperatures. Molaba *et al.* [7] investigated the influence of medium-soft paraffin wax on the thermal properties of the isotactic-polypropylene (iPP)/silver (Ag) nanocomposites. The authors reported that both the quenched and slowly cooled iPP/wax/Ag nanocomposites containing 10 wt.%, had two separate melting peaks associated with the melting temperature of wax and iPP crystals, respectively. Moreover, an increase in Ag (*viz* 2,3,4 and 5 wt% content) showed no significant changes in the melting temperatures and normalised enthalpies for both quenched and slowly cooled samples. However, the melting enthalpies of the quenched samples were found to be lower compared to that of slowly cooled samples. The reason for such an observation was attributed to the fact that slowly cooled samples had enough time to form crystals when compared with the quenched samples. Molefi *et al.* [6] investigated the effect of copper (Cu) on the polyethylene (PE)/wax blends. Three types of polyethylene investigated were LDPE, LLDPE and HDPE. It was observed that the presence of Cu particles slightly changed the thermal properties of all the polyethylene (PE)/wax blends. It was reported that wax had high affinity for Cu particles and crystallized on the surface of Cu. The melting enthalpy of the HDPE/wax/Cu composites at 1% of the Cu particles was found to be much higher than that of the LDPE/wax/Cu and LLDPE/wax/Cu composites at the same copper content. It was also observed that an increase in Cu content (3, 5 and 10%) reduced the melting enthalpy of the HDPE/wax/Cu, LDPE/wax/Cu and LLDPE/wax/Cu composites as compared to 1% of Cu content. Abdelrazeq *et al.* [60] investigated the thermal properties of HDPE/PW blend and HDPE/PW/EG composites, before aging, after 30 days and after 100 days of aging. The incorporation of 50% PW shifted towards higher temperatures. This was evidence by minor peak of PW before aging occurring 22 ^{o}C and after 100 days of aging the peak shifted to 24.6 ^{o}C. This peak was attributed to the solid-solid phase transition. The major peak of PW before aging occurred at 44.7 ^{o}C and after 100 days of aging the peak shifted to 46.5 ^{o}C. The melting enthalpy of the HDPE/PW blend was significantly decreased (from 61.8 J/g to 38 J/g) with sample containing 50% of wax. However, the presence of EG (5,10, and 15%) in the

HDPE/PW/EG composites containing 50% of PW, decreased the enthalpy melting of all three contents due to the stabilizing effect of EG. It can be concluded that higher amount of EG (15%) had a positive effect on the blend leakage. This was evidenced by low %drop in the enthalpy melting 17.2% for HDPE/PW/15%, when compared with 44.7% of HDPE/PW (60/40). One can conclude that there was a lower leakage of paraffin in the composites containing higher EG content (15%) than in the HDPE/PW blend without the presence of EG. Zhang et al. [48] investigated the thermal properties of expandable graphite (EG)/paraffin wax (PW)/silicon rubber (SR) composites. Two phase change peaks (minor and major peak) were observed on both heating and cooling curves of the materials. The minor peak was observed at the temperatures between 30-35 ^{o}C, which was associated with the solid-solid phase change of PW and the major peak in the temperature range between 48-55 ^{o}C which was due to the solid-liquid phase change of PW as explained earlier in this document. The enthalpy of melting and crystallization of the EG/PW/SR composites was greatly decreased when the EG content increases in the composites. Furthermore, the theoretical value of enthalpy was found to be higher than the measured enthalpy. This was an indication that there was a loss of PW during the preparation of the polymer/paraffin/conductive filler composites. Xu and co-workers [61] investigated the thermal properties of graphene/hexadecane/HDPE composites. The composites with 60, 70 and 80% hexadecane containing 1.5% graphene exhibited latent heat melting ranges 108.9, 138.3, and 159.1 J/g, respectively, which was much lower than that of pure hexadecane (227 J/g). The results showed that when the hexadecane content increased from 60 to 80%, there was no significant improvement in the heat storage capacity due to leakage of hexadecane, hence a reduction in the latent heat values.

2.5 Mechanical properties

2.5.1 Polymer/paraffin wax blends

Tensile test is a technique that is used to characterize the mechanical strength of polymeric materials and their composites. The sample are typically pulled to its breaking point in order to determine their tensile strength. Properties such as Young's modulus, elongation at yield, elongation at break, stress at yield and stress at break are normally reported in order to conclude about the mechanical properties of a particular material(s). Many authors have indicated that the wax content has strong influence on the mechanical properties of the polymer

[12,28,32,49,50,62]. There are different factors that were reported to affect the mechanical properties of the polymer/wax blends such as the type of wax, preparation method of the blends, content of the wax, and the type of polymer matrix chosen. Molefi and co-workers [49] investigated the comparison of LDPE, LLDPE and HDPE blended with soft Fischer-Tropsch paraffin wax. It was reported that the stress at break decreased with increasing M3 wax (soft Fischer-Tropsch paraffin wax) content in all the investigated PE/M3 wax blends. This behaviour was ascribed to poor tensile properties and low molecular weight of the paraffin wax, thus increasing its wax content in the blends is expected to decrease the tensile strength of the blends. It was also reported an increase in wax content, decreased the elongation at break for all PE/M3 wax blends. This may be attributed to the immiscibility of the two components in blends i.e. paraffin wax and polymer matrix. It is well-known that phase separated materials loses their drawability which strongly reduces the elongation at break. Furthermore, the Young's modulus was observed to increase when the wax content in the LDPE and LLDPE blends was increased, which was an indication that the modulus of the wax was higher than that of both polymers. This behaviour can be associated with high degree of crystallinity of the wax component when compared with both LLDPE and LDPE polymers. On the other hand, the Young's modulus of HDPE was reported to decrease with increasing wax content, which was very interesting as one would have expected a higher young's modulus for such a system. Sotomayor *et al.* [32] investigated the mechanical properties of the pure HDPE and HDPE/soft-paraffin wax blends. The yield stress of pure HDPE and HDPE/paraffin wax blends was investigated at the composition ratio of polymer: paraffin wax of 100/0, 80/20, and 70/30 vol%. The yield stress of the HDPE polymer matrix in blends decreased with the addition of 20 vol% paraffin wax content. The observation can be explained by lower drawability due to less force needed to pull the material in comparison to neat HDPE polymer. However, the yield stress disappeared completely when the wax content was increased up to 30 vol%, which showed that the material became brittle and lost its drawability. It was also observed that the stress at break and elongation at break of all the HDPE/paraffin wax blends (i.e. 95/5, 90/10. 80/20, 70/30, 60/40 and 50/50 vol%) decreased with increasing paraffin wax content. Furthermore, the Young's modulus of the HDPE/wax blends decreased with increasing paraffin wax content because the modulus of paraffin wax was lower than that of the HDPE polymer, thus a reduction in Young's modulus. Similar behaviour was observed by Mngomezulu *et al.* [50] who investigated the HDPE/soft Fischer-Tropsch-paraffin wax blends. It was reported that the stress at break, elongation at break and Young's modulus was decreased with increasing soft-paraffin wax content, as it is observed in most of the polymer/wax blends systems. Al. Maadeed

et al. [12] investigated the mechanical properties of HDPE/wax blends. It was reported that the Young's modulus of HDPE was decreased with the incorporation of 30 wt.% wax content from 730 MPa to 360 MPa. This behaviour was due to low molecular weight and low modulus of wax in the HDPE/wax blend. Furthermore, the tensile strength of the HDPE/wax blend was also reduced with increasing wax content, which showed that there was weak interfacial bonding between HDPE and wax. Elnahas *et al*. [62] investigated the mechanical properties of the LDPE/wax blends at 100/0, 98/2, 96/4, 94/6, 92/8, 90/10, 85/15 (w/w) compositions. It was reported that the tensile strength of the LDPE decreased with the presence and increasing of paraffin wax content. The reason for this behaviour was attributed to low tensile strength of the paraffin was, thus increasing its content in the blend will have negative impact on the tensile strength of the blend. As documented elsewhere in this document, increasing paraffin wax content in the blend also decreased the elongation at break. Furthermore, the Young's modulus was found to decrease with increasing in content of the paraffin wax in the blends. This was due lower modulus of wax when compared with the modulus of the polymer matrix. Chen *et al.* [31] investigated the mechanical properties of PLA/PW blends prepared by conventional melt compounding and sub-critical gas-assisted processing (SGAP). Interestingly, the elongation at break for conventional melt compounding method for fabrication of the blends showed higher elongation at break for the blend *(viz* 15.38%) consisting of 50 wt.% of paraffin wax when compared with neat PLA matrix (i.e. 3.53%). However, there was a reduction in the tensile strength of the PLA/PW blends from 58.94 MPa to 41.04 MPa at the same wax content. Furthermore, the Young's modulus slightly increased with the incorporation of 20 wt% PW content. The same behaviour was also reported by blends prepared by SGAP.

2.5.2 Polymer/conductive filler composites

It is well known from the literatures that in most cases, increasing the content of conductive filler in the composites enhances the mechanical properties of the material. There are different factors that affect the mechanical properties of polymer/conductive filler(s) composites including dispersion of the conductive, particle size of the filler, type of the conductive, modification of the conductive filler, synergistic effect of the fillers and type of the polymer. Many authors have reported on the effect of conductive fillers on mechanical properties of the polymer composites [43,53,54,58,63,64,65,66]. Zhang *et al.* [63] for instance, investigated the mechanical properties of boron nitride/polyvinylidene fluoride fibers composites and

compared them with those of polyvinylidene fluoride fibers fabricated by electrospinning. Boron nitride was modified with dopamine hydrochloride, with the dopamine molecules oxidized to polydopamine (PDA) covering the surface of the boron nitride. It was reported that the tensile strength and Young's modulus of the PDVF increased with incorporation of modified BN denoted as m-BN. The tensile strength and Young's modulus of the m-BN/PDVF composites achieved the highest values at 30 wt% m-BN content which was 24.06 MPa and 1.08 GPa, respectively, which were higher than that of PDVF polymer (9.60 MPa of tensile strength and elastic modulus of 0.87 GPa). The improvement of mechanical strength was due to higher amount of m-BN which improved the interaction between PDVF matrix and m-BN. However, at 40 wt.% content of m-BN there was a slight decrease in the tensile strength and Young's modulus of the m-BN/PDVF composites i.e. 20.77 MPa and 0.96 GPa, respectively. At higher contents of the BN content, there was a slight decrease in mechanical properties of the composites due to the formation of aggregates which leads to a decrease in mechanical. Furthermore, the elongation at break also increased with increasing m-BN content in the m-BN/PDVF composites which reached 0.96% at 30 wt% content of m-BN. Jin-hua *et al.* [53] reported on the mechanical properties of LLDPE/MWCNTs composites. It was detected that the tensile strength increased with increasing in MWCNTs content up to 1.0 wt%. However, there was a reduction in tensile strength with the addition MWCNTs at content(s) higher than 1.0 wt.%, which may be attributed to the formation agglomerates in the composites. The Young's modulus increased with increasing MWCNTs content in the LLDPE/MWCNTs composites. However, it was indicated that at higher MWCNTs content there was a change from deformation to ductile, from ductile to more brittle material. The Elongation of at break was reported to be reducing with the addition of the filler content up to 1 wt.%. Lomate *et al.* [43] investigated the influence of copper (Cu) nanoparticles on mechanical properties of the LDPE/Cu nanocomposites. The tensile strength of the LDPE/Cu composites increased with increasing Cu content. The tensile strength of the composites significantly improved at 2.5 wt.% Cu (*viz* 16.5 MPa) content when compared with pure LDPE (i.e. 6.91 MPa). However, at 3 wt.% Cu content, there was a formation agglomerates which slightly reduced the tensile strength of LDPE/Cu composites to 16 MPa when compared 2.5 wt.% Cu because the interaction between polymer matrix and the Cu nanoparticles was poor at this content. However, one can emphasize the both content(s) (2.5 wt.% and 3 wt.%) of Cu showed higher tensile strength than pure polymer matrix. Feng *et al.* [58] investigated the effect of 3D hybrid fillers (BN and MWCNTs) and single filler BN mixed with the HDPE polymer. It was reported that the Young's modulus of the HDPE/BN30C3 composites (with BN 30 denoting 30 wt.%

of boron nitride and C3 standing for multiwalled carbon nanotubes) was higher i.e. 247% than that of the matrix. This was due to an improvement in crystallinity of the composites in the presence of the multiwalled carbon nanotubes. It was also reported that the elongation at break of the composites was rapidly decreased with the addition of hybrid fillers (BN/MWCNTs) and BN alone. This reduction in elongation at break was caused by high content of fillers and the weak interface between the fillers and polymer matrix.

2.5.3 Polymer/paraffin wax/conductive filler composites

A number of studies have been reported on the mechanical properties of the polymer/paraffin wax/conductive filler composites [2,12,60,67,68]. In this system, few factors such as the type of wax, dispersion of both wax and conductive fillers as well as the type of polymer matrix were found to affect the mechanical properties. AlMaadeed and co-workers [12] reported that the incorporation of EG in the HDPE/RT4 (paraffin wax denoted as TR4) composites had no effect on the tensile strength of the composites since the authors observed no change in tensile strength at 40 wt% RT4 with all the EG contents (5, 10 and 15 wt%). The Young's modulus increased with increasing EG contents in the HDPE/40% RT4 composites and achieved the highest value of 650 MPa at 15 wt.% EG. This behaviour was ascribed to an insignificant agglomeration of EG in the composites and as well as good interfacial interactions between the EG and the blend. Kim *et al.* [67] investigated the mechanical properties of the LLDPE-paraffin/exfoliated graphite nanoplatelets (xGnP) nanocomposites. It was reported that the tensile strength and modulus of the composites increased with increasing xGnP-paraffin content. The tensile strength increased by 22% higher than that of LLDPE with 30 wt% of xGnP-paraffin. However, the addition of 30 wt.% of paraffin wax did not influence the tensile strength of the composites. Furthermore, the elongation at break of the composites decreased when the xGnP-paraffin content was increased. This can be explained by arguing that the addition fillers can restrict the polymer chains which then enhances the brittleness of the material and, as a result, the elongation at break was decreased. Abdelrazeq et al. [60] reported on the mechanical properties of the recycled polyethylene/paraffin wax/expanded graphite composites. It was reported that the addition and increasing in EG content in the HDPE/PW blends increased the Young's modulus. This behaviour was expected since the Young's modulus of the EG filler is much higher than that of the HDPE and PW. The stress at break of the HDPE/PW/EG composites increased with increasing in EG content up to 5.88 MPa at 15

wt.% of EG when compared with 5 wt.% (i.e. 4.53 MPa) and 10 wt.% (5.82 MPa) of EG. However, the neat matrix and the HDPE/PW blends showed higher stress at break values that the graphite blend composites. There was no specific reason provide for such an observation. Furthermore, the elongation at break was decreased with increasing EG content in the HDPE/PW blends. The lowest value of elongation at break was detected at 15 wt.% of EG content which was 4.63%.

2.6 References

[1] Akeiber, H.J., Wahid, M.A., Mahdi, T., Jassim, N.N., & Obeid, M.M. **2016**. Production application of paraffin waxes refining process in Iraq and used as phase change materials. *International Journal of Advanced Research*, 4: 96-100.

ISSN NO 2320-5407

[2] Mochane, M.J., Mokhena, T.C., Motaung, T.E., & Linganiso, L.Z. **2020**. Shape-stabilized phase change materials of polyolefin/wax blends and their composites. *Journal of Thermal Analysis and Calorimetry*, 139: 2951-2963.

https://doi.org/10.1007/s10973-019-08734-3

[3] Popelka, A., Sobolciak, P., Mrlik, M., Nogellova, P., Chodak, I., Ouederni, M., AlMaadeed, M.A., & Krupa, I. **2018**. Foamy phase change materials based on linear-low density polyethylene and paraffin wax blends. *Emergent Materials*, 1: 47-54.

https://doi.org/10.1007/s42247-018-0003-3

[4] Krupa, I., Mikova, G., & Luyt, A.S. **2007**. Phase change materials based on low-density polyethylene/paraffin wax blends. *European Polymer Journal*, 43: 4695-4705.

https://doi.org/10.1016/j.eurpolymj.2007.08.022

[5] Huang, X., Alva, G., Jia, Y., & Fang, G. **2017**. Morphological characterization and applications of phase change materials in thermal energy storage: A review. *Renewable and Sustainable Energy Reviews*, 72: 128-145.

https://doi.org/10.1016/j.rser.2017.01.048

[6] Molefi, J.A., Luyt, A.S., & Krupa, I. **2010**. Investigation of thermally conducting phase-change materials based on polyethylene/wax blends filled with copper particles. *Journal of Applied Polymer Science,* 116: 1766-1774.

https://doi.org/10.1002/app.31653

[7] Molaba, M.P., Dudic, D., & Luyt, A.S. **2015**. Influence of the presence of medium soft-paraffin wax on the morphology and properties of iPP/silver nanocomposites. *eXPRESS Polymer Letters*, 9: 901-915.

https://doi.org/10.3144/expresspolymlett.2015.82

[8] Mpanza, H.S., & Luyt, A.S. **2006**. Influence of different waxes on the physical properties of linear low-density polyethylene. *S. Afr. Journal of Chemistry*, 59: 48-54.

https://doi.org/

[9] Sarath, C.C., Sharks, R.A., & Thomas, S. **2014**. Chapter 1: Polymer Blends. *Nanostructured Polymer Blends,* Page 1-14.

https://doi.org/10.1016/B978-1-4557-3159-6.00001-8

[10] Chen, F., & Wolcott, M.P. **2013**. Miscibility studies of paraffin/polyethylene blends as form-stable phase change materials. *European Polymer Journal*, 52: 44-52.

https://doi.org/10.1016/j.eurpolymj.2013.09.027

[11] AlMaadeed, M.A., Labidi, S., Krupa, I., & Ouederni, M. **2015**. Effect of waste wax and chain structure on the mechanical and physical properties of polyethylene. *Arabian Journal of Chemistry*, 8: 388-399.

https://doi.org/10.1016/j.arabjc.2014.01.006

[12] AlMaadeed, M.A., Labidi, S., Krupa, I., & Karki, M. **2015**. Effect of expanded graphite on the phase change materials of high density polyethylene/wax blends. *Thermochimica Acta*, 600: 35-44.

https://doi.org/10.1016/j.tca.2014.11.023

[13] Krupa, I., & Luyt, A.S. **2001**. Thermal and mechanical properties of extrude LLDPE/wax blends. *Polymer Degradation and Stability*, 73: 157-161.

PII: S0141-3910(01)00082-9

[14] Mu, M., Basheer, P.A.M., Sha, W., Bai, Y., & McNally, T. **2016**. Shape stabilised phase change materials based on a high melt viscosity HDPE and paraffin waxes. *Applied Energy*, 162: 68-82.

https://doi.org/10.1016/j.apenergy.2015.10.030

[15] Kim, S., Moon, H., & Kim, J. **2015**. Thermal characterizations of the paraffin wax/low density polyethylene blends as a solid fuel. *Thermochimica Acta*, 613: 9-16.

https://doi.org/10.1016/j.tca.2015.05.016

[16] Du, B.X., & Cui, B**. 2016**. Effects of thermal conductivity on dielectric breakdown of micro, nano sized BN filled polypropylene composites. *IEEE Transactions on dielectrics and electrical Insulation*, 23: 2116-2125.
https://doi.org/10.1109/TDEI.2016.005845

[17] Guo, H., Wang, Q., Liu, J., Du, C., & Li, B. **2019**. Improved interfacial properties for largely enhanced thermal conductivity of poly (vinylidene fluoride)-based nanocomposites via functionalized multi-walled carbon nanotubes. *Applied Surface Science*, 487: 379-388.
https://doi.org/10.1016/j.apsusc.2019.05.070

[18] Zhang, X., Wu, H., & Guo, S. **2015**. Effect of interfacial interaction on morphology and properties of polyethylene/boron nitride thermally conductive composites. *Polymer-Plastics Technology and Engineering*, 54: 1097-1105.
https://doi.org/10.1080/03602559.2014.974280

[19] Zhou, T., Smith, M.K., Berenguer, J.P., Quill, T.J., Cola, B.A., Kalaitzidou, K., & Bougher, T.L. **2019**. The impact of polymer matrix blends on thermal and mechanical properties of boron nitride composites. *Journal of Applied Polymer Science*, 137: 48661.
https://doi.org/10.1002/app.48661

[20] Zhang, X., & Zheng, J. **2019**. Polymer composites with enhanced mechanical and thermal properties by orientating boron nitride flakes. *IOP Conference Series: Materials Science and Engineering*, 493: 012137.
https://doi.org/10.1088/1757-899X/493/1/012137

[21] Fei, T., Li, Y., Liu, B., & Xia, C. **2019**. Flexible polyurethane/boron nitride composites with enhanced thermal conductivity. *High Performance Polymers*, 32: 324-333.
https://doi.org/10.1177/0954008319862044

[22] Weng, L., Wang H., Zhang, X., Liu, L., & Zhang, H. **2018**. Preparation and properties of boron nitride/epoxy composites with high thermal conductivity and electrical insulation. *Journal of Materials Science: Materials in Electronics*, 29: 14267-14276. https://doi.org/10.1007/s10854-018-9560-8

[23] An, D., Cheng, S., Jiang, C., Duan, X., Yang, B., Zhang, Z., Li, J., Liu, Y., & Wong, C. **2020**. A novel environmentally friendly boron nitride/lignosulfonate/natural rubber composite with improved thermal conductivity. *Journal of Materials Chemistry C,* https://doi.org/10.1039/c9tc05699h

[24] Zha, X., Yang, J., Pu, J., Feng, C., Bai, L., Bao, R., Liu, Z., Yang, M., & Yang, W. **2019**. Enhanced thermal conductivity and balanced mechanical performance of PP/BN composites with I vol% finely dispersed MWCNTs assisted by OBC. *Advanced Materials Interfaces*, 1900081: 1-7. https://doi.org/10.1002/admi.201900081

[25] Xiao, M., & Du, B.X. **2016**. Review of high thermal conductivity polymer dielectric for electrical insulation. *High Volt*, 1: 34-42

https://doi.org/10.1049/hve.2016.0008

[26] Mokoena, T.E., Mochane, M.J., & Mokhena, T.C. **2020**. Interfacial characteristics of nitride-polymer composites. *Handbook of Polymer and Ceramic Nanotechnology*, pp 1-16.

https://doi.org/10.1007/978-3-030-10614-0_7-1

[27] Motloung, B.T., Dudic, D., Mofokeng, J.P., & Luyt, A.S. **2017**. Properties and thermos-switch behaviour of LDPE mixed with carbon black, zinc metal and paraffin wax. *Journal of Polymer Research*, 24: 43.

https://doi.org/10.1007/s10965-017-1205-8

[28] Fredi, G., Dorigato, A., Fambri, L., & Pegoretti, A. **2017**. Wax confinement with carbon nanotubes for phase changing epoxy blends. *Polymers*, 9: 405.

https://doi.org/10.3390/polym9090405

[29] Mhike, W., Focke, W.W., Mofokeng, J.P., & Luyt, A.S. **2012**. Thermally conductive phase-change materials for energy storage based on low-density polyethylene, soft Fischer-Tropsch wax and graphite. *Thermochimica Acta*, 527: 75-82.

https://doi.org/10.1016/j.tca.2011.10.008

[30] Mochane, M.J., & Luyt, A.S. **2015**. The effect of expanded graphite on the flammability and thermal conductivity properties of phase change material based on PP/wax blends. *Polymer Bulleting*, 72: 2263-2283.

https://doi.org/10.1007/s00289-015-1401-9

[31] Chen, Y., Huang, A., Ellingham, T., Chung, C., & Turng, L. **2018**. Mechanical properties and thermal characteristics of poly (lactic acid) and paraffin wax blends prepared by conventional melt compounding and sub-critical gas-assisted processing (SGAP). *European Polymer Journal*, 98: 262-272.

https://doi.org/10.1016/j.eurpolymj.2017.11.026

[32] Sotomayor, M.E., Krupa, I., Varez, A., & Levenfeld, B. **2014**. Thermal and mechanical characterization of injection moulded high density polyethylene/paraffin wax blends as phase change materials. *Renewable Energy*, 68: 140-145.

https://doi.org/10.1014/j.renene.2014.01.036

[33] Gao, X., Zhao, T., Luo, G., Zheng, B., Huang, H., Han, X., Ma, R., & Chai, Y. **2018**. Thermal and mechanical reinforcement of a novel paraffin-based hydroxyl-terminated polybutadiene (HTPB) binder containing a three-dimension (3D) diurea-paraffin wax (DU-PW) for prevention of PW leakage. *RSC Advances*, 8, 1047-1054.

https://doi.org/10.1039/c7ra10574f

[34] Tomic, N.Z. **2020**. Chapter 17. Thermal studies of compatibilized polymer blends. *Compatibilization of Polymer Blends*, page 489-510.

https://doi.org/10.1016/B978-0-12-816006-0.00017-7

[35] Parameshwaran, R., Sari, A., Jalaiah, N., & Karunakaran, R. **2018**. Chapter 13. Applications of thermal analysis to the study of phase-change materials. *Handbook of Thermal Analysis and Calorimetry*, page: 519-572.

https://doi.org/10.1016/B978-0-444-64062-8.00005-X

[36] Raeisi, Z., Moheb, A., Arani, M.N., & Sadeghi, M. **2021**. Non-covalently-functionalized CNTs incorporating poly(vinyl alcohol) mixed matrix membranes for

pervaporation separation of water-isopropanol mixtures. *Chemical Engineering Research and Design*, 167: 157-168. https://doi.org/10.1016/j.cherd.2021.01.004

[37] Oner, M., Kizil, G., Keskin, G., Pochat-Bohatier, C., & Bechelany, M. **2018**. The effect of boron nitride on the thermal and mechanical properties of poly (3-hydoxybutyrate-co-3-hydroxyvalerate). *Nanomaterials*, 8: 940. https://doi.org/10.3390/nano8110940

[38] Ren, P., Si, X., Sun, Z., Ren, F., Pei, L., & Hou, S. **2016**. Synergistic effect of BN and MWCNT hybrid fillers on the thermal conductivity and thermal stability of ultra-high-molecular-weight polyethylene composites with a segregated structure. *Journal of Polymer Research*, 23: 21. https://doi.org/10.1007/s10965-015-0908-y

[39] Yu, C., Zhang, J., Li, Z., Tian, W., Wang, L., Luo, J., Li, Q., Fan, X., & Yao, Y. **2017**. Enhanced through-plane thermal conductivity of boron nitride/epoxy composites. *Composites Part A*, 98: 25-31. https://doi.org/10.1016/j.compositesa.2017.03.012

[40] Moradi, S., Calventus, Y., Roman, F., & Hutchinson, J.M. **2019**. Achieving high thermal conductivity in epoxy composites: Effect of boron nitride particle size and matrix-filler interface. *Polymers*, 11: 1156. https://doi.org/10.3390/polym11071156

[41] Lule, Z., & Kim, J. **2019**. Surface modification of aluminium nitride to fabricate thermally conductive poly (butylene succinate) nanocomposites. *Polymers*, 11: 148. https://doi.org/10.3390/polym11010148

[42] Yin, X., Weng, P., Yang, S., Han, L., Tan, Y., Pan, F., Chen, D., Wang, L., Qin, J., & Wang, H. **2017**. Suspended carbon black fluids reinforcing and toughening of poly(vinyl alcohol) composites. *Materials & Design*, 130: 37-47. https://doi.org/10.1016/j.matdes.2017.05.049

[43] Lomate, G.B., Dandi, B., & Mishra, S. **2018**. Development of antimicrobial LDPE/cu nanocomposite food packaging film for extended shelf life of peda. *Food Packaging and Shelf life*, 16: 211-219. https://doi.org/10.1016/j.fpsl.2018.04.001

[44] Asante, J., Modiba, F., Mwakikunga, B. **2016**. Thermal managements on polymeric epoxy-expandable graphite material. *International journal of Polymer Science*, 2016: Pages 1-12.

https://doi.org/10.1155/2016/1792502

[45] Savini, G., & Orefice, R.L. **2020**. Comparative study of HDPE composites reinforced with microtalc and nanotalcs: high performance filler for improving ductility at low concentration levels. *Journal of Materials Research and Technology*, 9: 16387-16398. https://doi.org/10.1016/j.jmrt.2020.11.090

[46] Cao, M., Huang, J., & Liu, Z. **2020**. The enhanced performance of phase-change materials via 3D printing with prickly aluminium honeycomb for thermal management of ternary lithium batteries. *Advances in Materials Science and Engineering*, 2020: Page 1-11.

https://doi.org/10.1155/2020/8167386

[47] Luo, D., Wei, F., Shao, H., Xiang, L., Yang, J., Cui, Z., Qin, S., & Yu, J. **2018**. Shape stabilization, thermal energy storage behaviour and thermal conductivity enhancement of flexible paraffin/MWCNTs/PP hollow fiber membrane composites phase change materials. *Journal of Material Science*, 53: 15500-15513.

https://doi.org/10.1007/s10853-018-2722-5

[48] Zhang, Y., Li, W., Huang, J., Cao, M., & Du, G. **2020**. Expanded graphite/paraffin/silicone rubber as high density temperature form-stabilized phase change materials for thermal energy storage ad thermal interface materials. *Materials*, 13: 894.

https://doi.org/10.3390/ma13040894

[49] Molefi, J.A., Luyt, A.S., & Krupa, I. **2010**. Comparison of LDPE, LLDPE, and HDPE as matrices for phase change materials based on a soft Fischer-Tropsch paraffin wax. *Thermochimica Acta*, 500: 88-92.

https://doi.org/10.1016/j.tca.2010.01.002

[50] Mngomezulu, M.E., Luyt, A.S., & Krupa, I. **2010**. Structure and properties of phase change materials based on HDPE, soft Fischer-Tropsch paraffin wax, and Wood flour. *Journal of Applied Polymer Science*, 118: 1541-1551.

https://doi.org/10.1002/app.32521

[51] Zhou, R., Ming, Z., He, J., Ding, Y., & Jiang, J. **2020**. Effect of magnesium hydroxide and aluminium hydroxide o the thermal stability, latent heat and flammability properties of paraffin/HDPE phase change blends. *Polymers*, 12: 180.

https://doi.org/10.3390/polym12010180

[52] Akishino, J.K., Cerqueira, D.P., Silva. G.C., Swinka-Filho, V., & Munaro, M. **2016**. Morphological and thermal evaluation of blends of polyethylene wax and paraffin. *Thermochimica Acta*, 626: 9-12.

https://doi.org/10.1016/j.tca.2016.01.002

[53] Jin-hua, T., Guo-qin, L., Huang, C., & Lin-jian, S. **2012**. Mechanical properties and thermal behaviour of LLDPE/MWCNTs nanocomposites. *Materials Research*, 15: 1050-1056.

https://doi.org/10.1590/S1516-14392012005000122

[54] Shi, S., Wang, L., Xin, C., Zhao, K., Li, C., & Zheng, G. **2017**. Special morphology and its role in mechanical enhancement of linear low-density polyethylene/multiwalled carbon nanotubes composites. *Journal of Applied Polymer Science*, 134: 45525.

https://doi.org/10.1002/app.45525

[55] Russo, P., Patti, A., Petrarca, C., & Acierno, S. **2018**. Thermal conductivity and dielectric properties of polypropylene-based hybrid compounds containing multiwalled carbon nanotubes. *Journal of Applied Polymer Science*, 135: 46470.

https://doi.org/10.1002/app.46470

[56] Wu, X., Liu, W., Ren, L., & Zhang, C. **2020**. Highly thermally conductive boron nitride@UHMWPE composites with segregated structure. *e-Polymers*, 20: 510-518.

https://doi.org/10.1515/epoly-2020-0053

[57] Pan, C., Zhang, J., Kou, K., Zhang, Y., & Wu, G. **2018**. Investigation of the through=plane thermal conductivity of polymer composites with in-plane oriented hexagonal boron nitride. *International Journal of Heat and Mass Transfer*, 120: 1-8

https://doi.org/10.1016/j.ijheatmasstransfer.2017.12.015

[58] Feng, M., Pan, Y., Zhang, M., Gao, Q., Liu, C., Shen, C., & Liu, X. **2021**. Largely improved thermal conductivity of HDPE composites by building a 3D hybrid fillers network. *Composites Science and Technology*, 206: 108666.

https://doi.org/10.1016/j.compscitech.2021.108666

[59] Che, J., Jing, M., Liu, D., Wang, K., & Fu, Q. **2018**. Largely enhanced thermal conductivity of HDPE/boron nitride/carbon nanotube ternary composites via filler network-network synergy and orientation. *Composites Part A*, 112: 32-39.

https://doi.org/10.1016/j.compositesa.2018.05.016

[60] Abdelrazeq, H., Sobolciak, P., Al-Maadeed, M.A., Ouederni, M., Krupa, I**. 2019**. Recycled polyethylene/paraffin wax/expanded graphite based heat absorbers for thermal energy storage: An artificial aging study. *Molecules*, 24: 1217.
https://doi.org/10.3390/molecules24071217

[61] Xu, L., Zhang, J., Liu, C., Li, N., Chen, L., Zhang, S., &Wang, Z. **2020**. Fast thermal response of shape-stabilized thermal storage materials: The case of interconnected netlike graphene/hexadecane/HDPE composites. *ACS Omega*, 5: 12415-12420.
https://doi.org/10.1021/acsomega.0c01183

[62] Elnahas, H.H., Abdou, S.M., El-Zahed, H., & Abdeldaym, A. **2018**. Structural, morphological and mechanical properties of gamma irradiated low density polyethylene/paraffin wax blends. *Radiation Physics and Chemistry*, 151: 217-224.

https://doi.org/10.1016/j.radphyschem.2018.06.030

[63] Zhang, D., Zha, J., Li, W., Li, C., Wang, S., Wen, Y., & Dang, Z. **2018**. Enhanced thermal conductivity and mechanical property of through boron nitride hot string in polyvinylidene fluoride fibers by electrospinning. *Composites Science and Technology*, 156: 1-7.

https://doi.org/10.1016/j.composcitech.2017.12.008

[64] Cheewawuttipong, W., Fuoka, D., Tanoue, S., Uematsu, H., & Iemoto, Y. **2013**. Thermal and mechanical properties of polypropylene/boron nitride composites. *Energy Procedia*, 34: 808-817.

https://doi.org/10.1016/j.egypro.2013.06.817

[65] Li, X., Jia, W., Dong, B., Yuan, H., Su, F., Wang, Z., Wang, Y., Liu, C., Shen, C., & Shao, C. **2019**. Structure and mechanical properties of multi-walled carbon nanotubes-filled isotactic polypropylene composites treated by pressurization at different rates. *Polymers*, 11: 1294.

https://doi.org/10.3390/polym11081294

[66] Mertens, A.J., & Senthilvelan, S. **2016**. Mechanical and tribological properties of carbon nanotube reinforced polypropylene composites. *Journal of materials: Design and Applications*, 0: 1-12.

https://doi.org/10.1177/1464420716642620

[67] Kim, S., Seo, J., & Drzal, L.T. **2010**. Improvement of pf electric conductivity of LLDPE based nanocomposite by paraffin coating on exfoliated graphite nanoplatelets. *Composites Part A*, 41: 581-587.

https://doi.org/10.1016/j.compsoitesa.2009.05.002

[68] Sobolciak, P., Mrlik, M., AlMaadeed, M.A., & Krupa, I. **2015**. Calorimetric and dynamic mechanical behaviour of phase chance materials based on paraffin wax supported by expanded graphite. Thermochimica Acta, 617: 111-119.

https://doi.org/10.1016/j.tca.2015.08.026

Chapter 3: Methodology

3.1 Materials

3.1.1 Linear low-density polyethylene (LLDPE)

LLDPE used in this study, was supplied in pellet form by Sasol Polymers, South Africa. It has an average molecular weight of 191 600 g/mol, a melting temperature range of 122-128 ^{o}C, a density of 0.924 g/cm^{3}.

3.1.2 Paraffin wax (PW)

Paraffin wax was supplied in powder form by Fluka Chemie AG, Buchs, Switzerland. It is consisting of approximately 99% of straight short chain hydrocarbons and it has an average molecular weight of 440 g/mol, a melting temperature range of 50-60 ^{o}C, a density of 0.93 g/cm^{3} and it is primarily used in the manufacturing of candles.

3.1.3 Boron nitride (BN)

Boron nitride used was supplied in powder form by Sigma Aldrich, South Africa. BN was used as a conductive filler and as a reinforcement filler into the LLDPE and/or LLDPE/wax blends. It has a density of 1.9 g/cm^{3}, purity of 99.5% and a length size of 10 micron.

3.1.4 Single-walled carbon nanotubes (SWCNTs)

Single-walled carbon nanotubes (SWCNTs) was supplied by OCSiAl, Luxembourg. SWCNTs were used as one of two fillers, to create synergy with boron nitride. It has a density of 1.35 g/cm^{3}, purity of 75% and metal impurities that is $\leq$ 15%. It has a diameter that is below 2 and a length of >1 micron.

3.2 Methods

3.2.1 Sample preparation

Carbon nanotubes, boron nitride and LLDPE were dried in an oven at 50 ºC overnight before melt-mixing. All the materials were mixed using Rheomix Haake PolyLab QC 600. The samples were mixed at 140 ℃ with a rotational speed of 30 rpm for 10 minutes for all the samples. The fabrication of the blends was done through physical premixing and the mixed components were fed into the heating mixer. For the blend composites, boron nitride and/or carbon nanotubes were incorporated into the mixer 5 minutes after adding the LLDPE or premixed LLDPE/wax. **Figure 3.1** illustrate the Rheomix Haake PolyLab 600 machine employed for fabrication of the investigated samples in this study. The weight percentages for pure LLDPE, LDPE/wax blend and blend composites prepared are shown in **Table 3.1**.

Figure 3.1: Rheomix Haake PolyLab 600 machine

Table 3.1: Summary of the investigated samples

LLDPE (wt.%)	**PW (wt.%)**	**LLDPE/PW (wt.%)**
100	-	70/30
LLDPE/BN (wt.%)	**LLDPE/SWCNT (wt.%)**	**LLDPE/(BN+SWCNT) (wt.%)**

99/1 98/2 97/3	99/1 98/2 97/3	- 98/2 -
LLDPE/PW/BN (wt.%)	**LLDPE/PW/SWCNT (wt.%)**	**LLDPE/PW/ (BN+SWCNT) (wt.%)**
69.3/29.7/1 68.6/29.4/2 67.9/29.1/3	69.3/29.7/1 68.6/29.4/2 67.9/29.1/3	- 68.6/29.4/2 -

3.3 Characterization and sample analysis

3.3.1 Scanning Electron Microscopy (SEM)

SEM was used to study surface morphology of the fractured surface of LLPE/wax blend and LDPE/wax/conductive filler blend composites. This technique utilizes a fine beam of electrons that is scanned over the surface of the material at high speed. The instrument is fitted with a detector that collects the electrons emitted from each point on the surface and the image can be formed by collecting these secondary electrons from each point of the specimen. Furthermore, proper sample preparation is necessary prior characterization which includes plasma etching, conductive coatings by means of evaporation or sputtering; and chemical etching methods [1,2,3]. SEM images were achieved using a Shimadzu ZU SSX-550 Superscan scanning electron microscope. The samples were dipped into liquid nitrogen for about 1-2 minutes and fractured using tweezers into an appropriate size to fit the specimen chamber. One of each fractured piece were gold coated by sputtering to produce conductive coatings onto the samples. SEM analyses were done at 15 kV and at magnifications of 1, 10 and 100 μm. Furthermore, the samples were also immersed in a chloroform solvent for 28 hours at room temperature to extract the paraffin wax from the blend and blend composites. The SEM analysis of the extracted samples was done following the same procedure as for the non-extracted samples.

3.3.2 Melt flow index (MFI)

The samples were analysed according to ISO 1133 at 190°C. The instrument was given 30 minutes to equilibrate after which, approximately 5 g of the sample was charged into the heated barrel. The piston was inserted into the barrel and the respective weight placed on top of the piston to make the total weight of piston and weight 2.16 kg. A support collar was inserted to prevent the piston from moving into the barrel prematurely and give the sample enough time to melt. After 5 minutes, the support collar was removed allowing the piston to move down by gravity and eject the sample. An automatic cutter was used and set to cut every 30 seconds. The amount of the investigated sample flowed through the die over a period of 5 min under 2.16 kg weight were determined. **Figure 3.2** is a photograph of the MFI instrument that was used while **Figure 3.3** shows a schematic representation of the MFI.

Figure 3.2: MFI instrument that was employed in this study for analysing the viscosity of the blends and blend composites

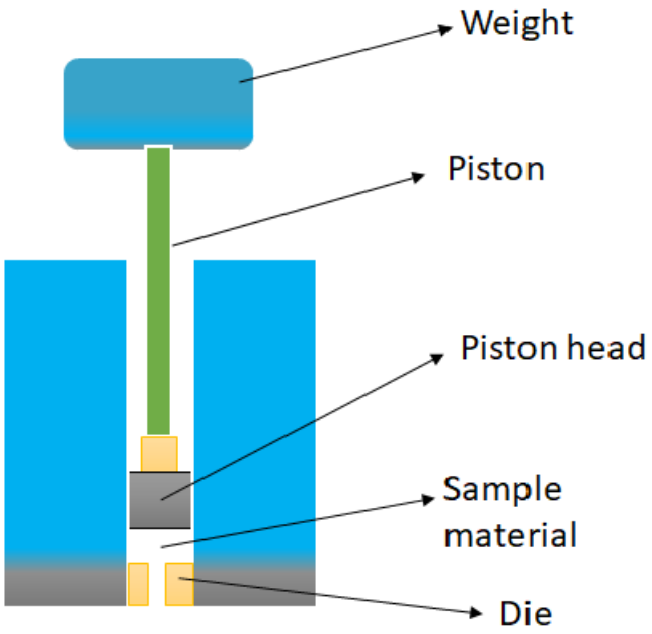

Figure 3.3: Schematic representation of the melt flow index

3.3.3 Thermogravimetric analysis (TGA)

TGA is a technique whereby the mass of the sample is monitored against time or temperature under controlled nitrogen conditions. Data in TGA curve is recorded as mass % or mass as a function of time or temperature [4,5]. It is mainly used to characterize the thermal stability and decomposition of the materials under controlled conditions. There are various factors that may influence the characteristics of the recorded TGA curve, such as sample mass, sample volume, physical form of a sample, shape and nature of the sample holder, and the scanning rate. The samples were analysed on the Discovery TGA S/N: TGA-0336. The samples had a mass ranging between 20-25 mg. They were heated from 30 ^{o}C to 600 ^{o}C at a heating rate of 20 ^{o}C/min under nitrogen flow. **Figure 3.4** shows the TGA instrument that was employed to analyse the thermal stability of the samples.

Figure 3.4: TGA instrument that was employed for analysing the thermal stability of the samples

3.3.4 Differential Scanning Calorimetry (DSC)

DSC is a technique that is used to study the thermal transitions of a material during heating or cooling. Thermal transition is known as the process whereby a material changes its melting temperature, crystallization temperature, and glass transition when heated or cooled at a certain controlled rate [4,6]. DSC equipment consists of two compartments: the control side which contains an empty aluminium pan and the sample side which contains the sample (2-10 mg) in an aluminium pan (see **Figure 3.5**). There are two classes of DSC: (i) power-compensation DSC, whereby the sample and inert reference are heated or cooled independently with identical heaters and thermocouples. (ii) Heat-flux DSC, whereby the sample and inert reference are heated or cooled simultaneously with a single heater. Zinc and indium are the calibration standards with known onset temperatures and enthalpy melting utilized for calibration of the DSC technique. DSC is used to measure glass transition temperature (T_g), melting temperature (T_m), crystallization temperature (T_c) and melting enthalpies (ΔH) [4,6]. Analyses in the current study were conducted using Discovery DSC S/N: DSC1-0376. The instrument was computer controlled and the calculations of the peaks were done using Pyris software. The samples of

mass between 2-10 mg were analysed from 25-160 ^{o}C at heating rate of 20 ^{o}C/min under nitrogen atmosphere. The sample were heated, cooled, and reheated under the above conditions. The melting peak temperature (T_m), enthalpy of melting peak (ΔH_m), crystallization peak temperature (T_c), and enthalpy of crystallization (ΔH_c) were determined from the second heat. **Figure 3.6** shows the top and front view of DSC instrument that was used to analyse the thermal properties of the samples.

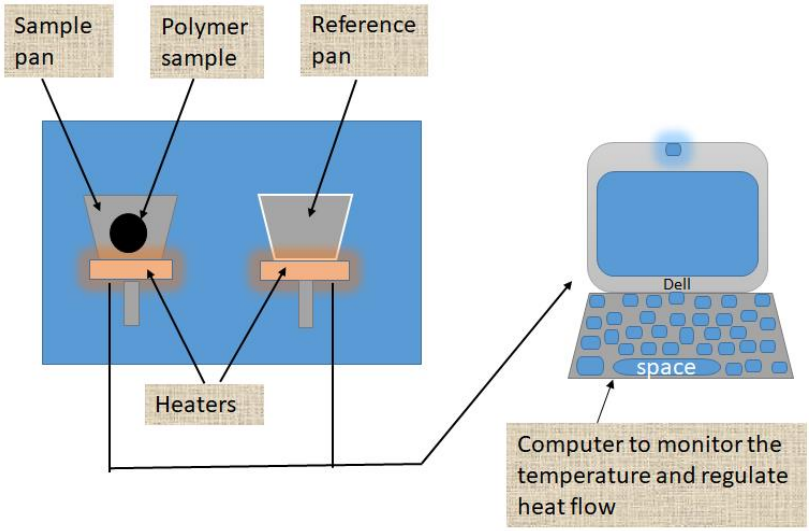

Figure 3.5: Schematic illustration of the DSC technique

Figure 3.6: Top and front view of DSC instrument employed for analysing thermal properties.

3.3.5 Injection Moulding

Injection moulding is the technique whereby the material is subjected into a heat barrel to be mixed. The mixture is forced to go through the sprue into the mould cavity where it is cooled and hardens to the configuration of the mould cavity [7]. **Figure 3.7** shows the injection moulding machine.

Figure 3.7: Injection moulding machine that was used for investigated samples

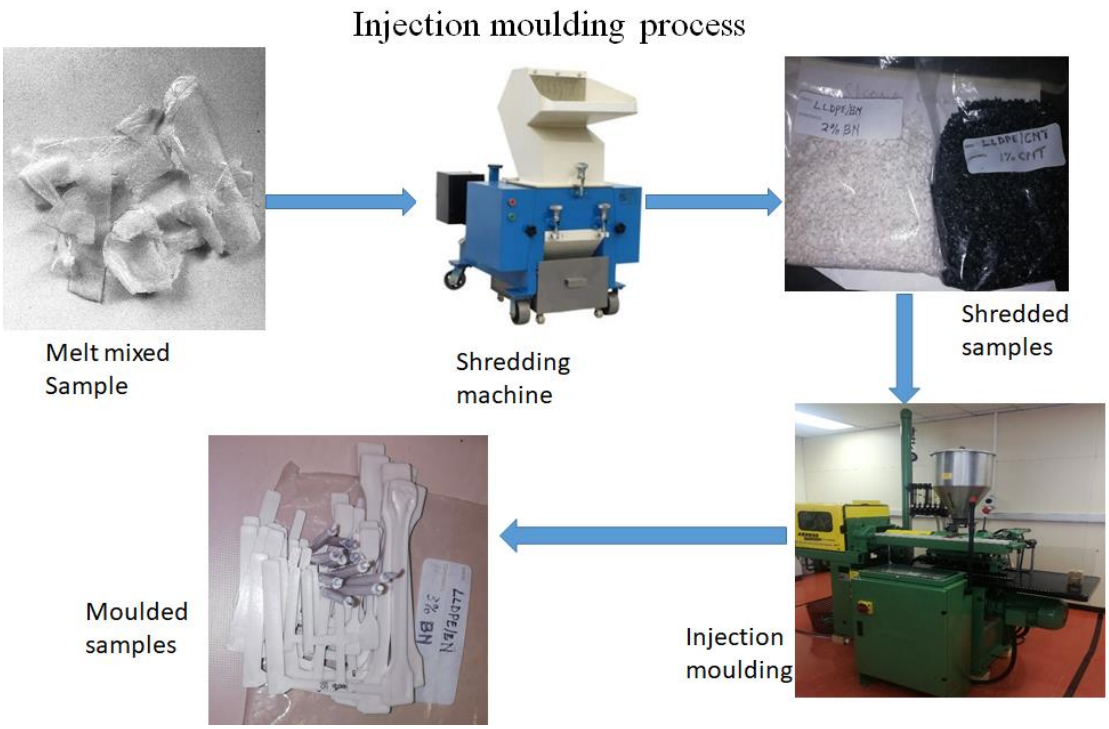

Figure 3.8: Injection moulding process

3.3.6 Tensile testing

Tensile testing is a technique that is used to determine the tensile strength, stress at break, Young's modulus, and as well as elongation at yield. The tensile test is done by firmly tightening the sample with a known dimension between the two grips. In a tensile test, the sample is pulled on both ends in order to measure the force that pulls the sample apart and also measure the elongation of the sample. The product of the tensile test is recorded as a load versus elongation curve, which it is converted into a stress versus strain curve [7,8]. The tensile analysis was done using the Hounsfield H10KT (Tinius Olsen Ltd) tensile tester (see **Figure 3.9**). The dumbshell-shaped samples of the blends and composites (see **diagram 1**) were prepared at 180 ^{o}C with an injection pressure of 400 bar and a mould temperature of 60 ^{o}C using ThermoHaake Minijet II injection moulding machine (ASTM D-638). The settings for tensile tester were as follows: (i) load range 250.0 N, (ii) extension range of 500.0 mm, (iii) gauge length of 25.0 mm, (iv) stretching speed 10.0 mm.min^{-1}, and (v) Approached speed of 0.02 mm.min^{-1}.

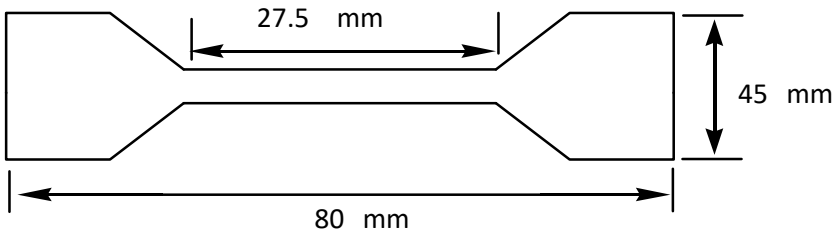

Diagram 1: Schematic diagram of the dumbshell-shaped sample for tensile testing.

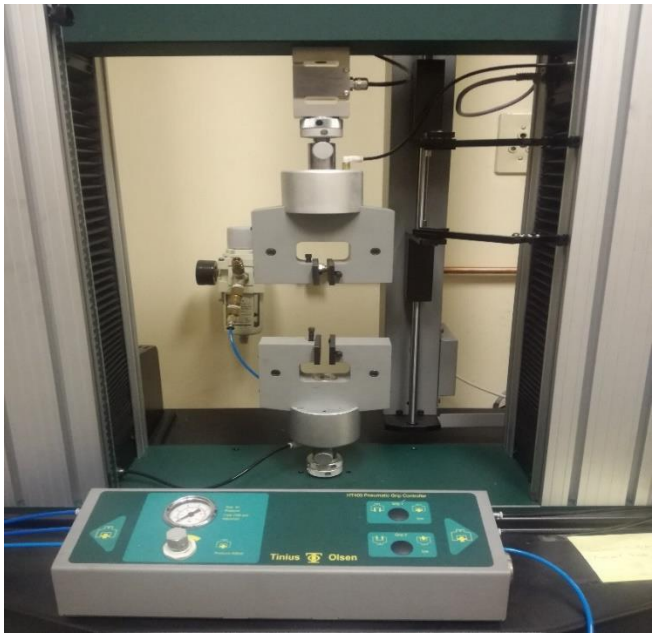

Figure 3.9: Hounsfield H10KT (Tinius Olsen Ltd) tensile tester

3.3.7 Dynamic mechanical analysis (DMA)

DMA is a technique that is used to determine the low-strain mechanical properties of the materials as a function of time, temperature, or frequency. It is used to calculate the storage modulus (E'), loss modulus (E") and mechanical loss factor tan δ (damping). The dynamic modulus response of the samples is divided into two parts, namely storage modulus and loss modulus. Storage modulus describes the energy recovered per cycle while the loss modulus is the net energy dissipated per cycle in the form of heat. The loss tangent is expressed as tan δ = E"/E'. The glass transition temperature (T_g) is normally determined from the loss modulus and tangent curves [4,9,10]. In the current study the dynamic mechanical analysis of all the materials were investigated using the Perkin-Elmer DMA 8000 (**Figure 3.10**). The samples analyses were done from -100 to 100 ^oC in bending mode with a heating rate of 3 ^oC/min and the frequency of 1 Hz.

Figure 3.10: DMA instrument that was employed for analysing the thermomechanical properties of the blends and composites

3.3.8 Impact testing

The impact properties of polymer blends and composites have attracted a lot attention recently due to the demand of these materials in the industrial sectors. Generally, impact is a collision of two or more objects, by interaction between the fluid, plastics and elasticity or synergy of any of the two interactions. According to the literature, there are four types of impact velocity which include ballistic, high velocity, low velocity as well as hypervelocity [11]. Both Charpy and Izod impact belongs to the low velocity impact. Impact test takes place by delivering an impact blow to a sample by pendulum-type hammer, whereby the impact value is recorded as the energy required to break the sample. The CEAST RESIL impactor junior (see **Figure 3.11**) was used to measure the impact properties of the samples at room temperature. The samples were rectangular shaped with a length of 83 mm, with of 4 mm and a thickness of 10 mm, with the samples tested at room temperature of 23 ℃. Three samples of each composition investigated were tested, with the average and standard deviation values reported.

Figure 3.11: The CEAST RESIL impactor junior machine

3.4 References

[1] Mochane, M.J. **2011**. Polymer encapsulated paraffin wax to be used as phase change material for energy storage. *MSc Thesis*, University of the Free State, Qwaqwa, South Africa.

[2] Sefadi, J.S. **2010**. The morphology and properties of EVA/Malaysian empty fruit bunch composites. *MSc Thesis*, University of the Free State, Qwaqwa, South Africa.

[3] Mngomezulu, M.E. **2009**. Phase change material based on polyethylene, paraffin wax and wood flour. *MSc Thesis*, University of the Free State, Qwaqwa, South Africa.

[4] Mofokeng, J.P. **2010.** Comparison of injection moulded, natural fibre reinforced composites with PP and PLA as matrices. *MSc Thesis,* University of the Free State, Qwaqwa, South Africa.

[5] Brown, M.E. Introduction to thermal analysis: Techniques and Applications, 1st Edition. Chapman & Hall, London, **1988.**

[6] Young, R.J., & Lovell, P.A. Introduction to polymers, 3rd Edition. **1981** p.435.

[7] Hato, M.J. **2009**. Polyhedral oligomeric silsesquioxanes (POSS) based polymer nanocomposites. *MSc Thesis,* University of the Free State, Qwaqwa, South Africa.

[8] Aldred, N., Wills, T., Williams, D.N., & Clare, A.S. **2007.** Tensile and dynamic mechanical analysis of the distal portion of mussel (Mytilus edulis) byssal threads. *Journal of the Royal Society Interface,* 4: 1159-1167. https://doi.org/10.1098/rsif.2007.1026

[9] Molaba, M.P. **2014**. Influence of the presence and amount of metal nanoparticles on the thermal and mechanical properties of iPP/soft paraffin wax phase change materials for thermal energy storage. *MSc Thesis*, University of the Free State, Qwaqwa, South Africa.

[10] Nhlapo, L.P. **2010**. Thermal and mechanical properties of LDPE/Sisal fibre composites compatibilized with paraffin waxes. *MSc Thesis*, University of the Free State, Qwaqwa, South Africa.

[11] Mochane, M.J., & Luyt, A.S. **2015**. The effect of expanded graphite on the flammability and thermal conductivity properties of phase change material based on PP/wax blends. *Polymer Bulletin,* 72: 2263-2283.

https://doi.org/10.1007/s00289-015-1401-9

Chapter 4: Results and discussion

4.1 Scanning electron microscopy (SEM)

Figure 4.1 shows SEM images of the fractured surfaces of extracted and non-extracted samples of the LLDPE/PW blend with 70/30 wt.% content (i.e., LLDPE contained 70 wt.%, while PW contained 30 wt.%). Image **(a)** depicts a phase separation for this blend, which suggests immiscibility between the linear-low density polyethylene (LLDPE) and paraffin wax (PW). This may be ascribed to the low molecular weight and low viscosity of the paraffin wax which made it easy to separate from the blend and form a phase separated blend. This behaviour was also confirmed by the DSC melt endotherms **(section 4.3)** of the LLDPE/PW blend which showed three melting peaks and TGA **(section 4.4)** showing two-step degradation. Luyt *et al.* [1] reported a phase separation between Wax S (it had low molecular weight and low viscosity) and LDPE, while there was a homogenous surface between LDPE and Wax FT due to a higher viscosity which made it difficult for Wax FT to diffuse out of the system. In this study there was no paraffin wax remaining in the blend after 28 hours of extraction using chloroform, as can be observed in image (**b**).

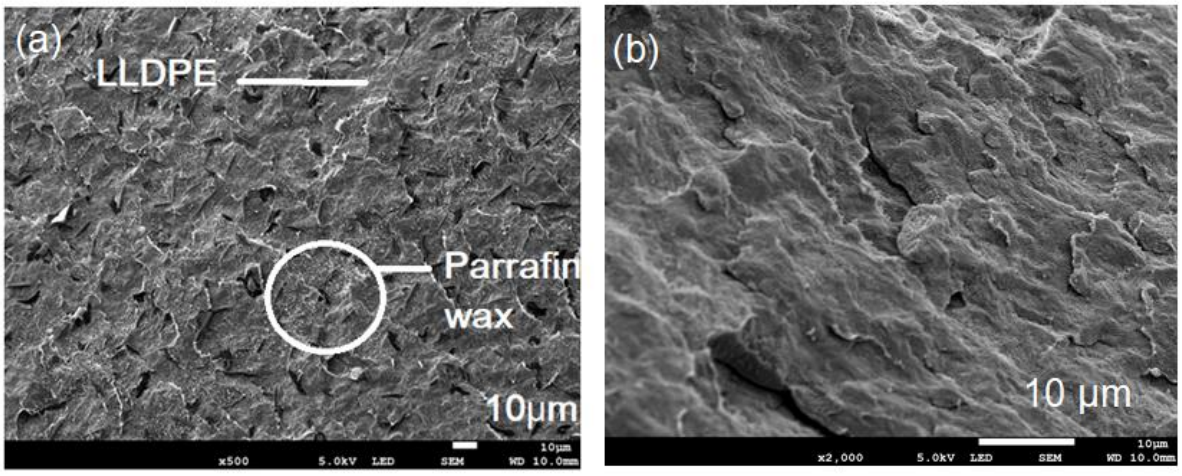

Figure 4.1: SEM images of: (a) Non extracted 70/30 w/w LLDPE/PW blend (b) Extracted 70/30 w/w LLDPE/wax blend with chloroform (scale bar of (a) and (b) is 10µm).

The SEM image of the LLDPE/BN composites with 2 wt.% of BN content are presented in **Figure 4.2**. It can be observed that there was a distribution of BN particles into LLDPE matrix with obvious agglomerates indicated by symbol E. There was thus, a poor interfacial interaction

between the LLDPE matrix and the BN particles. The same behaviour was observed for non-modified single-walled carbon nanotubes, as there seemed to be an agglomeration of carbon nanotubes as indicated by symbol F in **Figure 4.2 (b)**, even though there seemed to be some SWCNT embedded into the LLPDE matrix. Similar result was reported by Zhang *et al.* [2], who found that the non-functionalized 10 wt.% boron nitride showed agglomeration of the particles while both the functionalized BN and the incorporation of polyethylene-g-maleic anhydride resulted in a uniform dispersion and less agglomerates. Furthermore, Wang *et al* [3] indicated a phase separated system between BN and epoxy, with the presence of voids and defects with 5 and 20 wt.% content of h-boron nitride as well as c-boron nitride.

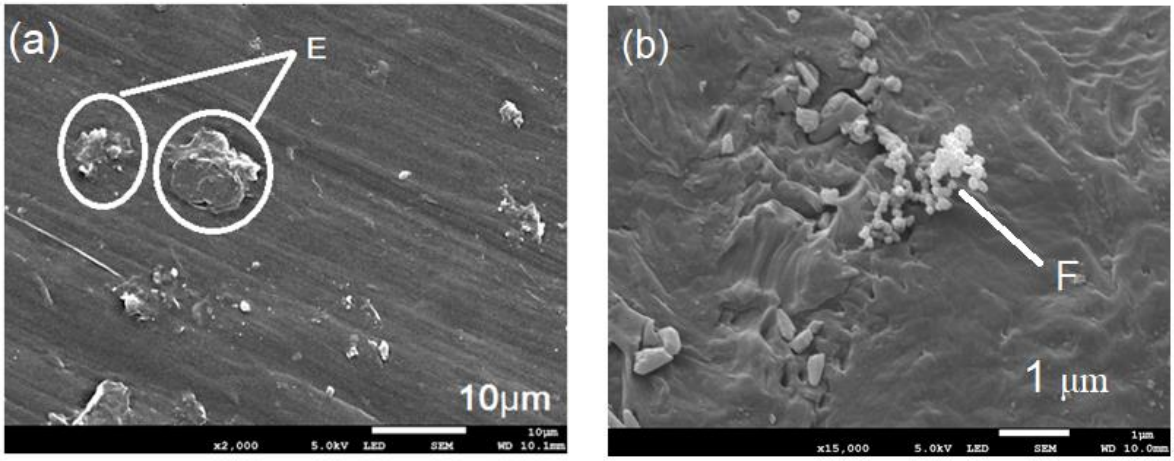

Figure 4.2: SEM image of: (a) 98/2 w/w LLDPE/BN; and (b) LLDPE/SWCNT composites (scale bar of (a) is 10µm and (b) is 1µm).

In **Figure 4.3** the 68.6/29.4/2 w/w content of LLDPE/PW/BN blend composites show an obvious debonding between the paraffin wax and boron nitride (symbol A, B, and C). Such system is unfavourable for a reduction of interfacial resistance between the filler and matrix. Furthermore, this behaviour showed that there was less affinity between paraffin wax and boron nitride. Similarly, as in case of the LLDPE/paraffin wax blend, 28-hour extraction by chloroform in the LLDPE/PW/BN composite showed the removal of paraffin wax **(Figure 4.3(b)**), with only LLDPE and BN remaining in the system. However, in the presence of carbon nanotubes, there seemed to be a better dispersion between conductive fillers (viz BN and SWCNT) and the LLDPE/paraffin wax blend matrix **(Figure 4.4(a))**. This behaviour may be attributed to a better affinity between the SWCNTs and paraffin wax, which might have resulted in a better dispersion of both fillers in the blend matrix. The low molecular weight and low viscosity paraffin wax enabled it to penetrate between the SWCNT chains, which resulted

in a good dispersion in the blend matrix. It is well-known that paraffin wax has high affinity for carbon-based conductive fillers compared with ceramics-based fillers [4]. Furthermore, due to a high surface to volume ratio of carbon nanotubes, the interaction between SWCNTs and paraffin was better than in the boron nitride-based system. Furthermore, the utilization of chloroform helped to remove the paraffin wax from the LLDPE/PW/ (BN+SWCNT) blend composite, leaving only boron nitride and single walled carbon nanotubes (SWCNT) in the blend composites (**see Figure 4.4(b)**), as was the case for LLDPE/paraffin wax blend and LLDPE/paraffin wax/BN.

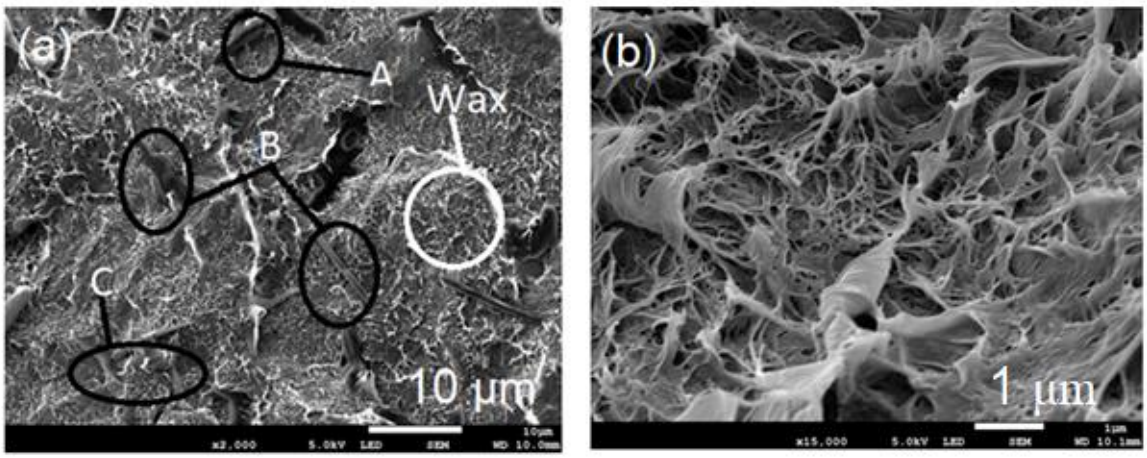

Figure 4.3: SEM image of: (a) Non-extracted 68.6/29.4/2 LLDPE/PW/BN blend composites and (b) Extracted 68.6/29.4/2 LLDPE/PW/BN blend composites with chloroform (scale bar of (a) is 10µm and (b) is 1µm).

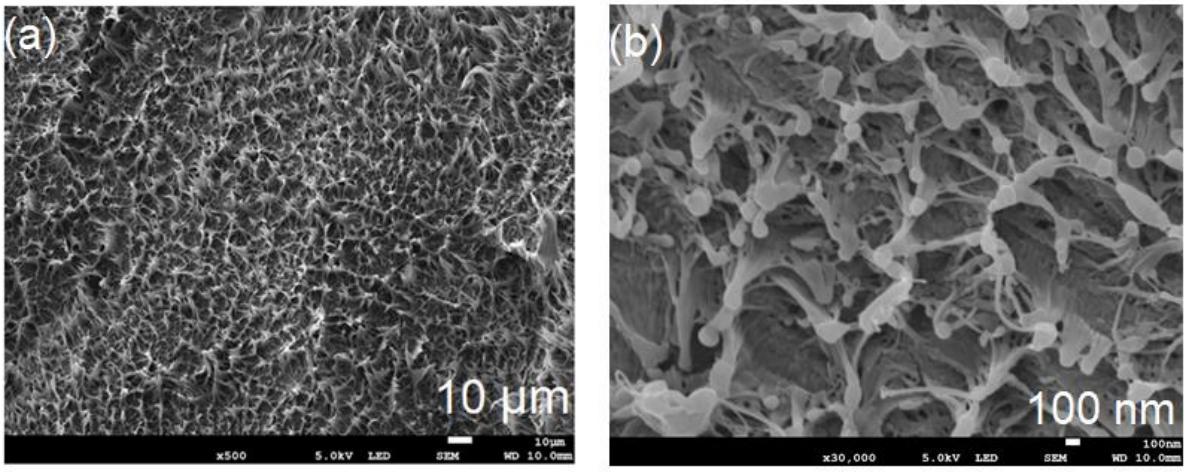

Figure 4.4: SEM image of: (a) Non extracted LLDPE/PW/(BN+SWCNT) and (b) Extracted LLDPE/PW/ (BN+SWCNT) blend composites (scale bar of (a) is 10µm and (b) is 100µm).

4.2 Melt flow Index (MFI)

Figure 4.5 depicts the melt flow index (MFI) of neat LLDPE, LLDPE/paraffin wax (PW) blend, LLDPE/PW/BN, LLDPE/PW/SWCNT and LLDPE/PW/SWCNT/BN composites. Melt flow index (MFI) was found to be one of the factors that influenced the dispersion of the filler and the quality of the resultant composite. The flow index of polymers is the foundation for quality control of the reactant's material i.e., raw material. A decrease in MFI is an indication of an increase in the viscosity of the material. **Figure 4.5** indicates that the LLDPE had a melt flow index (MFI) value of 3.20, and with the addition of the paraffin wax to the LLDPE matrix, the melt flow index was increased by 394%. The enhancement in MFI with the addition paraffin wax was ascribed to a low viscous paraffin wax molecule that penetrated the LLDPE chains, thus lowering the viscosity of the blend and increasing the melt flow index. The addition of inorganic fillers decreased the melt flow index of the paraffin wax blend, as the addition of 2 wt.% boron nitride decreased the MFI of the LLDPE/paraffin wax blend by 0.95%. Moreover, the addition of both inorganic fillers (viz boron nitride and single walled carbon nanotubes at 2 wt.%) further decreased the MFI of the blend by a 54.3% decline. This could be attributed to the stiffness of the inorganic fillers within the blend, as a result immobilizing the polymer chains, thus increasing the viscosity, and decreasing the MFI values of the blend composites. Similar results were obtained by Saini *et al.* [5] who observed a decrease in the MFI values of the LLDPE composites with the incorporation of the wastepaper powder (WPP). The latter authors attributed this observation to the rigidity of the fibers that affected the flowability of the polymer matrix. Similar to the latter study, Carvalho *et al.* [6] reported that the MFI values of all the HDPE composites tested in their study were reduced when wood particles were added. This reduction was due to restricted movement of the chains that was caused by the presence of WPs in the LLDPE composites as they reduced the flowability of the HDPE matrix.

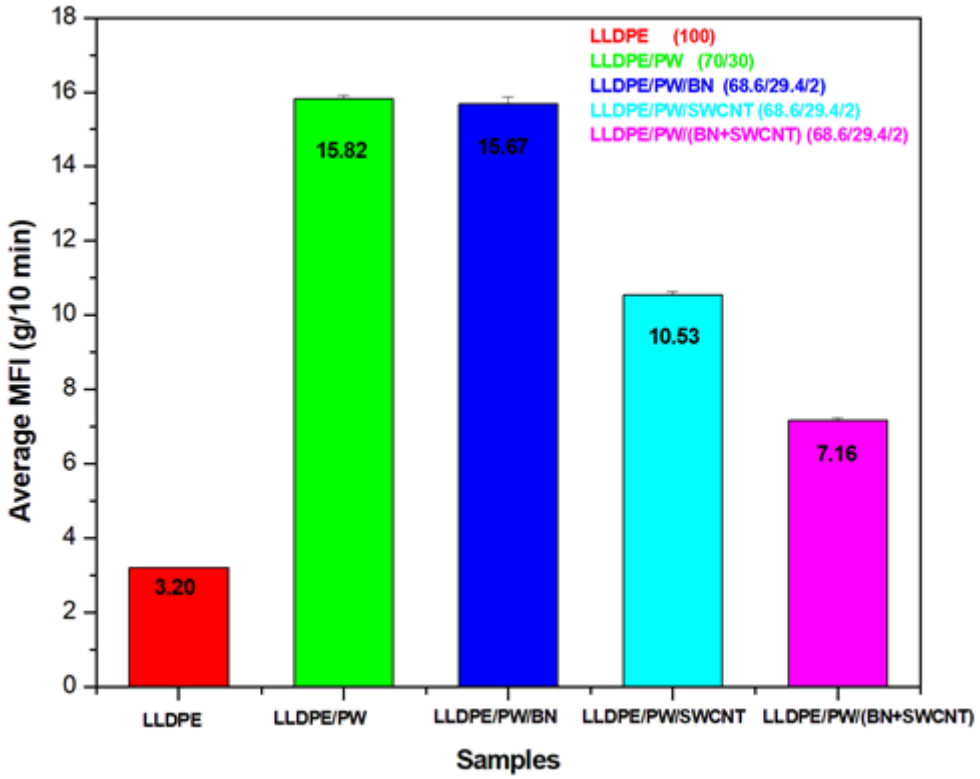

Figure 4.5: Melt flow index of the neat LLDPE, LLDPE/paraffin wax (PW) blend, LLDPE/PW/BN, LLDPE/PW/SWCNT and LLDPE/PW/(BN+SWCNT) composites

4.3 Differential scanning calorimetry (DSC)

The thermal properties of the neat LLDPE, pure PW, LLDPE/conductive fillers, LLDPE/PW blend, LLDPE/PW/conductive fillers composites were investigated by differential scanning calorimetry (DSC). The DSC curves were taken from the second heating rate because the first heating rate is generally associated with the removal of thermal history. **Figure 4.6** and **4.7** present the heating and cooling curves for pure LLDPE, pure PW and LLDPE/PW blend. On close examination of the curves, LLDPE showed one endothermic peak with a melting temperature of 127 ^{o}C and a melting enthalpy of 141 J/g, while PW showed two endothermic peaks (i.e., a shoulder and major peak). The shoulder peak was recorded at 31.3 ^{o}C and the major melting peak at 52.2 ^{o}C, whereas the melting enthalpies were 33.1 J/g and 134 J/g, respectively. The two peaks of PW were ascribed to the melting of different molecular weight fractions of the wax i.e., solid-solid transition and the melting of the crystallites, respectively. Similar results were reported by Molefi *et al.* [7], who compared LDPE, LLDPE, and HDPE

as matrices for phase change materials based on a soft Fischer-Tropsch paraffin wax. Zhou *et al.* [8] also investigated the thermal properties of paraffin/HDPE phase change blends. Both studies observed that PW showed two endothermic peaks which the authors attributed to the melting of solid-solid phase transition and the melting of crystallites, as was explained earlier.

Figure 4.7 shows the cooling curves of the neat LLDPE, PW and the LLDPE/PW blend. LLDPE was observed to have a crystallization temperature of 115 ℃ and the crystallization enthalpy of 131 J/g. On the other hand, PW crystallized at 28.3 ℃ and 50.2 ℃, with a crystallization enthalpy of 12.1 J/g and 144 J/g, respectively. The calculated degree of crystallinity value of pure LLDPE was 48.0 %. Note that PW curve was stopped at 100 ℃ due to its melting temperature that is around 50-60 ℃. There was no reason to further continue heating it to 160 ℃ like the other materials because its mechanical properties would have been destroyed and too high temperature may have resulted in decomposition of PW. The degree of crystallinity was calculated using the melting enthalpy values of pure LLDPE, LLDPE blends, LLDPE composites and blend composites. The crystallinity of all the samples were determined by equation 4.1 and 4.2. Equation 4.1 was used to determine the crystallinity of neat LLDPE and equation 4.2 was utilized to obtain the crystallinity of the composites and blend composites. The values for the calculated degree of crystallization are depicted in **Table 4.1**. The calculations were done as follows:

$$X_c(\%) = \frac{\Delta H_m}{\Delta H_m^\circ} \times 100\% \qquad \textbf{4.1}$$

$$X_c(\%) = \frac{\Delta H_m}{\Delta H_m^\circ} \times \frac{100\%}{wt.\%} \qquad \textbf{4.2}$$

Where ΔH_m is the experimental melting enthalpy, ΔH_m° is the melting enthalpy of completely crystalline LLDPE (293 J/g), and lastly wt.% is the weight fraction of the polymer in the blend and/or blend composites.

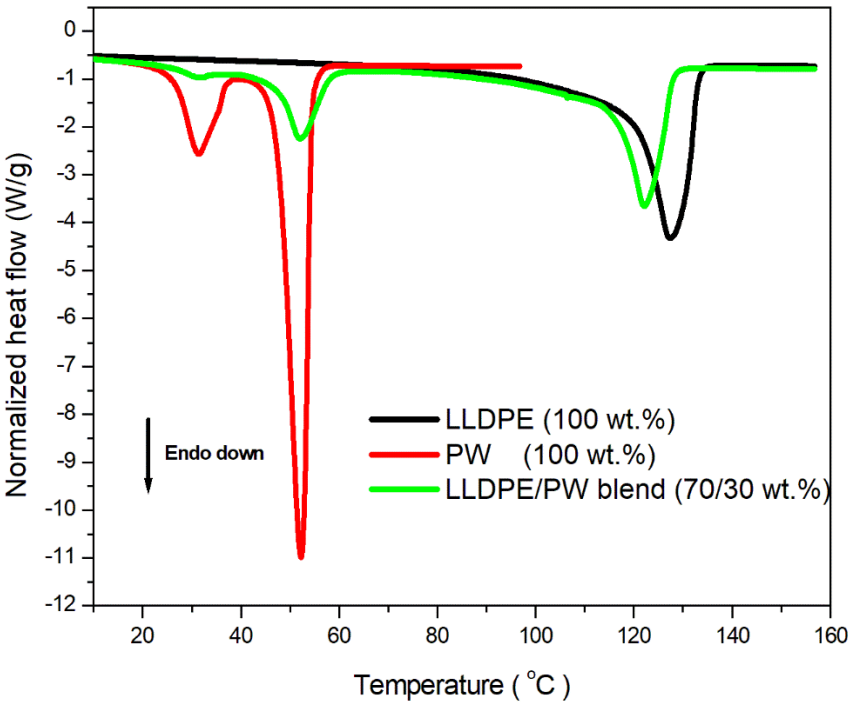

Figure 4.6: Heating curve of pure LLDPE, PW and the LLDPE/PW blend

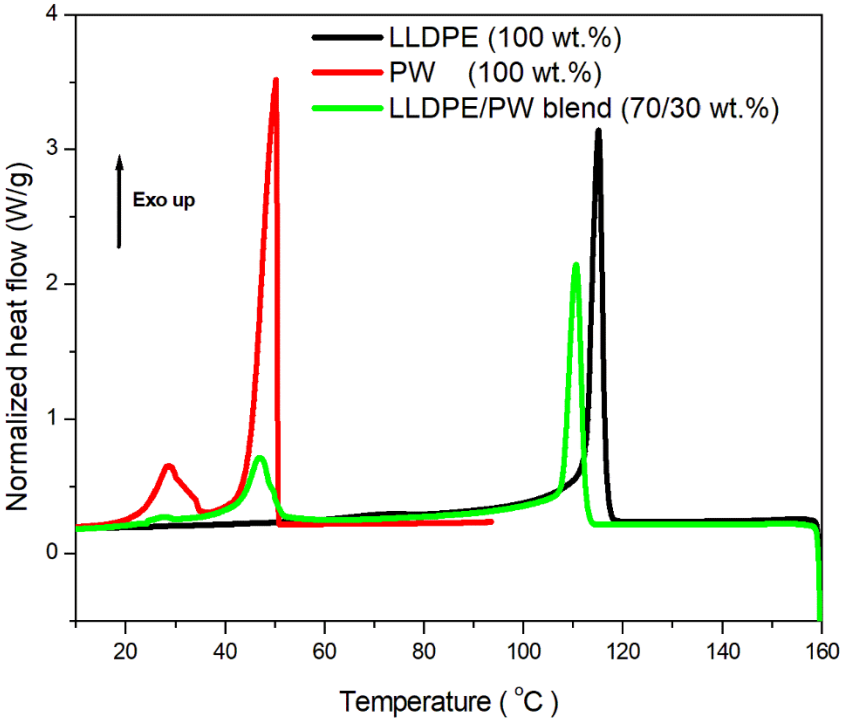

Figure 4.7: Cooling curves of pure LLDPE, PW and the LLDPE/PW blend.

Figure 4.6 shows that the LLDPE/PW blend had three endothermic peaks. This behaviour indicated that both LLDPE and PW are immiscible. The first melting peak temperature was

recorded at 29.7 ^{o}C and the second peak temperature at 52.0 ^{o}C. As was explained earlier in this document, such peaks may be associated with the melting temperature of the paraffin wax and the solid-solid phase transition. The third peak was recorded at around 122 ^{o}C which was ascribed to the melting peak of the LLDPE matrix. The incorporation of PW into LLDPE (**Figure 4.6**) reduced the melting temperature of LLDPE in the blends. This was attributed to the plasticizing effect of wax on the LLDPE matrix which enhanced the free volume in the system and, as a result, the melting temperature was reduced. Similar behaviour was observed by Krupa and Luyt [9], who observed three endothermic peaks with 30% and more of wax content. One peak was attributed to the LLDPE matrix while two endothermic peaks correlated with that of the paraffin wax.

Table 4.1: Thermal properties of pure LLDPE, pure paraffin wax, LLDPE/paraffin wax blends and the composites.

Samples	Melting process		Crystalline process		
	T_m (ºC)	ΔH_m (J/g)	T_c (ºC)	ΔH_c (J/g)	Xc (%)
LLDPE (100%)	127	141	115	131	48.0
PW (100%)	52.2[a]	134[a]	50.2[a]	144[a]	---
	31.3[b]	33.1[b]	28.3[b]	12.1[b]	---
LLDPE/BN					
99/1	130	148	117	125	50.8
98/2	132	151	117	121	52.4
97/3	128	151	118	133	53.0
LLDPE/SWCNT					
99/1	131	158	120	129	54.4
98/2	130	154	121	137	53.5
97/3	130	153	121	133	53.8

Cont…

Samples	Melting process		Crystalline process		
	T_m (°C)	ΔH_m (J/g)	T_c (°C)	ΔH_c (J/g)	Xc (%)
LLDPE/(BN+SWCNT)					
98/2	131	143	120	125	49.7
LLDPE/PW					
70/30	122[a]	105[a]	111[a]	94.2[a]	51.0[a]
	52.0[b]	29.1[b]	46.8[b]	34.5[b]	---
	29.7[c]	10.0[c]	20.4[c]	8.22[c]	---
LLDPE/PW/BN					
69.3/29.7/1	122[a]	88.2[a]	113[a]	80.1[a]	43.4[a]
	51.4[b]	34.3[b]	47.4[b]	39.6[b]	---
	29.6[c]	14.5[c]	23.2[c]	11.4[c]	---
68.6/29.4/2	123.[a]	89.4[a]	114[a]	92.0[a]	44.5[a]
	52.4[b]	27.5[b]	47.3[b]	43.0[b]	---
	28.6[c]	14.3[c]	22.0[c]	11.2[c]	---

Cont…

Samples	Melting process		Crystalline process		
	T_m (ºC)	ΔH_m (J/g)	T_c (ºC)	ΔH_c (J/g)	Xc (%)
67.9/29.1/3	124[a]	104[a]	114[a]	84.1[a]	52.2[a]
	52.7[b]	19.7[b]	46.4[b]	27.7[b]	---
	28.5[c]	15.4[c]	23.7[c]	11.8[c]	---
LLDPE/PW/SWCNT					
69.3/29.7/1	126[a]	111[a]	115[a]	89.5[a]	58.9[a]
	52.6[b]	26.6[b]	46.3[b]	28.7[b]	---
	28.3[c]	16.2[c]	27.2[c]	11.0[c]	---
68.6/29.4/2	124[a]	106[a]	116[a]	92.4[a]	52.5[a]
	51.5[b]	25.1[b]	46.8[b]	26.0[b]	---
	28.0[c]	14.1[c]	28.3[c]	10.1[c]	---

Cont…

Samples	Melting process		Crystalline process		
	T_m (ºC)	**ΔH_m (J/g)**	**T_c (ºC)**	**ΔH_c (J/g)**	**Xc (%)**
67.9/29.1/3	125[a]	108[a]	115[a]	90.0[a]	54.4[a]
	51.4[b]	25.5[b]	45.7[b]	27.0[b]	---
	28.7[c]	14.4[c]	29.7[c]	11.2[c]	---
LLDPE/PW/(BN+SWCNT)					
68.6/29.4/2	126[a]	111[b]	115[a]	102[a]	55.1[a]
	52.6[b]	24.2[b]	46.3[b]	27.2[b]	---
	29.2[c]	15.3[c]	29.8[c]	10.4[c]	---

T_m is the melting temperature, T_c is the crystalline temperature, ΔH_m is the melting latent heat, ΔH_c is the crystalline latent heat, and X_c is the degree of crystallinity.

Figure 4.8 to 4.10 represents the heating curves of LLDPE/BN, LLDPE/SWCNT and LLDPE/(BN+SWCNT) composites. It was observed that the melting temperature of the LLDPE (**Figure 4.8 and Table 4.1**) increased with the addition of conductive fillers (*viz* BN, SWCNT and BN+SWCNT). This behaviour showed that conductive fillers acted as a nucleating agent, thus increasing the melting temperature of the LLDPE composites [10,11]. **Figure 4.8** depict(s) the heating curve of LLDPE/BN composites. It can be observed that the LLDPE/BN composites with 2 wt.% BN was more effective in increasing the melting temperature of LLDPE i.e.,132 ℃, when compared with 1 wt.% BN (130 ^{o}C) and 2 wt.% BN content (128 ^{o}C), respectively. This may be ascribed to an effective nucleation of the BN filler at 2 wt.% content which enhanced crystallinity and, as a result, increased the melting temperature. **Table 4.1** shows that the addition of 1 wt.% SWCNT into the LLDPE matrix resulted in a slight increase in the melting temperature (131℃) compared with 2 wt.% (130 ℃) and 3 wt.% content (130 ℃). The heating curves clearly indicated that 1 wt.% of SWCNT and 2 wt.% of BN fillers were more effective in improving the melting temperature of LLDPE which showed that both fillers (*viz* BN and SWCNT) acted as a nucleation agent for LLDPE. As the result, the polymer crystals probably nucleated and became larger and thus higher melting temperatures of LLDPE were attained. The incorporation of 2 wt.% boron nitride alone enhanced the melting temperature of LLDPE more than what 2wt.% SWCNT and BN+SWCNT achieved, as is depicted in **Figure 4.10** and **Table 4.1**. It seemed as if boron nitride at this content acted as a better nucleating agent for LLDPE as it shifted the melting temperature of LLDPE to higher temperatures. Conversely, it was reported in the literature [12] that the melting temperature of the UHWMPE decreased with the addition of single (BN) filler and hybrid fillers (MWCNT+BN). Interestingly, Russo *et al.* [11] observed different behaviour when investigating polypropylene (PP)/multi walled carbon nanotubes (MWCNT) mixed with different fillers namely BN, $CaCO_3$, Talc, ZnO. The latter authors observed that the melting temperature of the PP was increased with the addition of MWCNT and hybrid fillers (*viz* MWCNT/BN, MWCNT/$CaCO_3$, MWCNT/Talc, and MWCNT/ZnO).

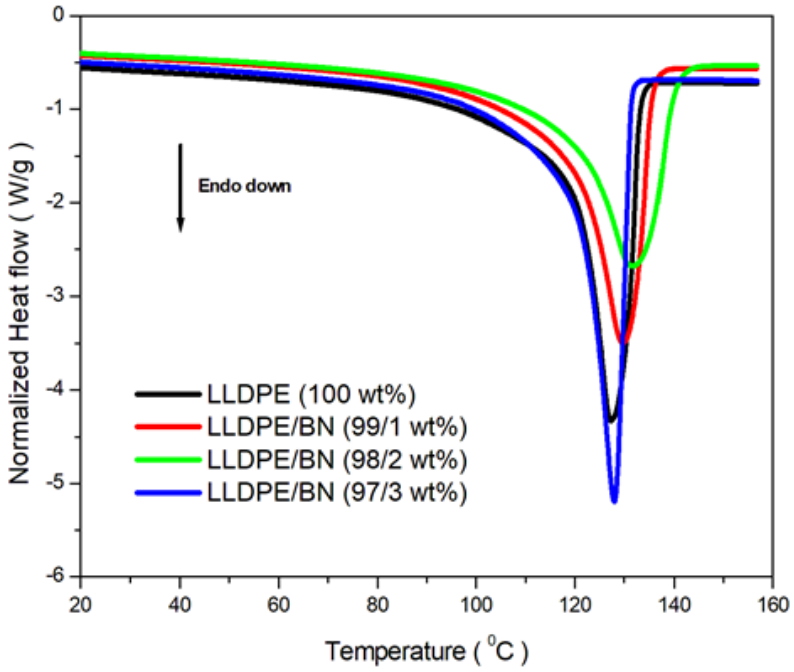

Figure 4.8: Heating curve of LLDPE/BN composites with 1, 2 and 3 wt.% BN content

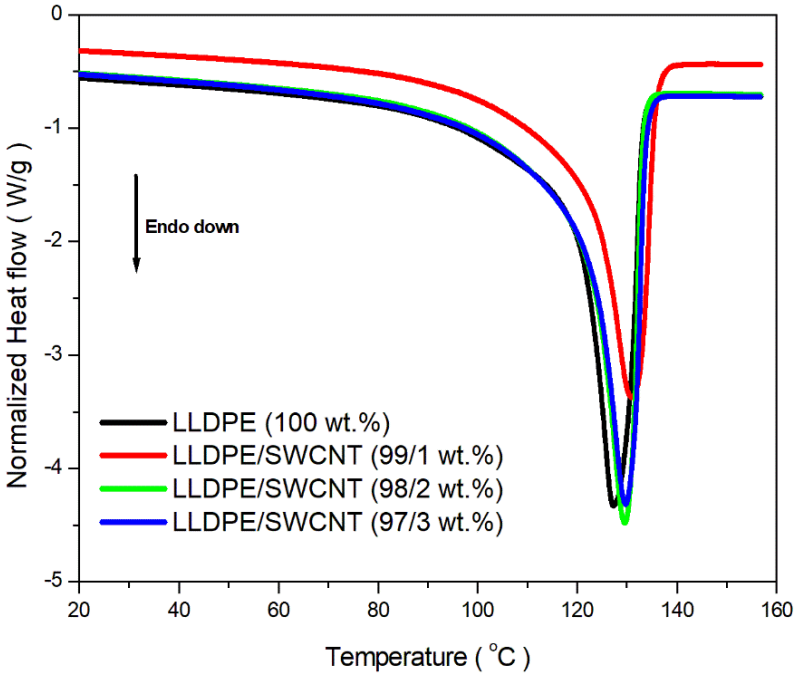

Figure 4.9: Heating curve of LLDPE/SWCNT composites with 1, 2 and 3 wt.% SWCNT

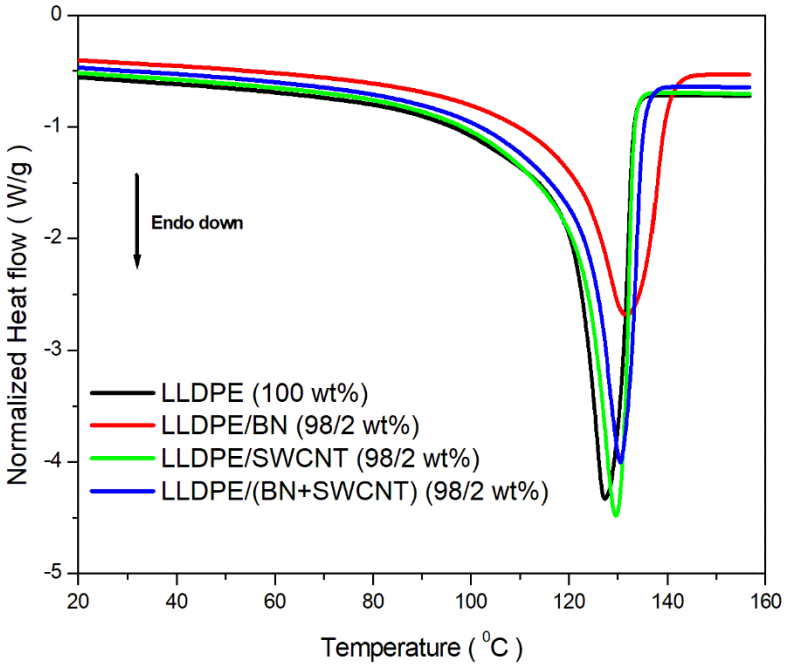

Figure 4.10: Heating curve of LLDPE/BN, LLDPE/SWCNT and LLDPE/(BN+SWCNT) hybrid composites all at 2 wt.% content

Figure 4.11 to **4.13** depicts the cooling curves of the LLDPE/BN, LLDPE/SWCNT and LLDPE/(BN+SWCNT) hybrid composites. It is well documented in the literature that inorganic fillers affect the polymer chains' mobility which is normally reflected by either an increase or a decrease in crystallization temperature (T_c) and degree of crystallinity (X_c) [13]. The crystallization temperature and degree of crystallinity (as seen from **Table 4.1**) of the LLDPE/BN, LLDPE/SWCNT and LLDPE/(BN+SWCNT) hybrid composites increased with the addition of conductive fillers and their hybrid fillers. This behaviour showed that BN, SWCNT and BN+SWCNT hybrid fillers probably acted as heterogeneous nucleating agents for the LLDPE matrix in the absence of paraffin wax. A similar observation was reported by Zhong *et al.* [14] who studied isotactic polypropylene (iPP)/hexagonal boron nitride (h-BN) composites mixed with multi walled carbon nanotubes (MWCNTs) and graphene nanoplatelets (GNPs). The authors observed that the addition of h-BN, h-BN/MWCNTs and h-BN/GNPs particles improved the crystallization temperature and degree of crystallinity of iPP matrix which they attributed to the nucleating effect of the two conductive fillers into the iPP matrix. It is clear from **Table 4.1** and **Figure 4.11** that at 3 wt.% BN content, the LLDPE/BN

composites showed slightly higher crystallization temperature (*viz* 118 ℃) and degree of crystallinity i.e., 53.5% when compared with 1 and 2 wt.% of boron nitrides. As for carbon nanotubes composites, it became very clear that the 1 wt.% SWCNT content in the LLDPE/SWCNT composites exhibited higher degree of crystallinity (**Table 4.1**) at a value of 54.4% compared with 2, and 3 wt.% of SWCNT. There was thus a 6.4 % enhancement in the degree of crystallinity for 1 wt.% of SWCNT in the LLDPE composites in comparison with neat LLDPE. It thus seems that the SWCNT filler is an effective nucleating agent at lower content. Interestingly, it can be seen from **Table 4.1** that the single fillers showed higher degree of crystallinity when compared with hybrid fillers (BN+SWCNT). This behavior was surprising as one would have expected that a combination of both fillers would better improve the melting temperature of the LLDPE matrix than the single fillers due to a combined property of the synergistic fillers.

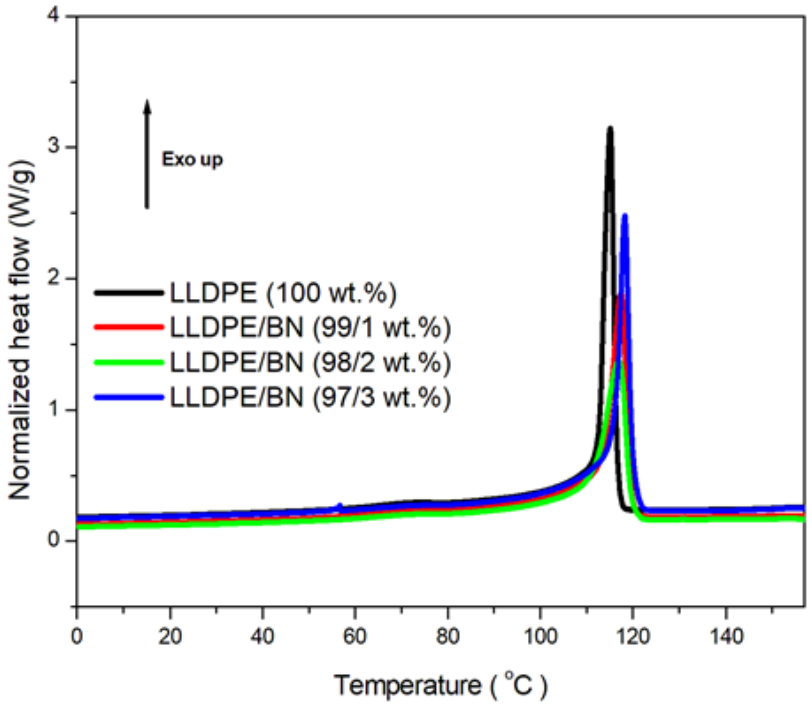

Figure 4.11: Cooling curve of the LLDPE/BN composites with 1, 2 and 3 wt.% BN content.

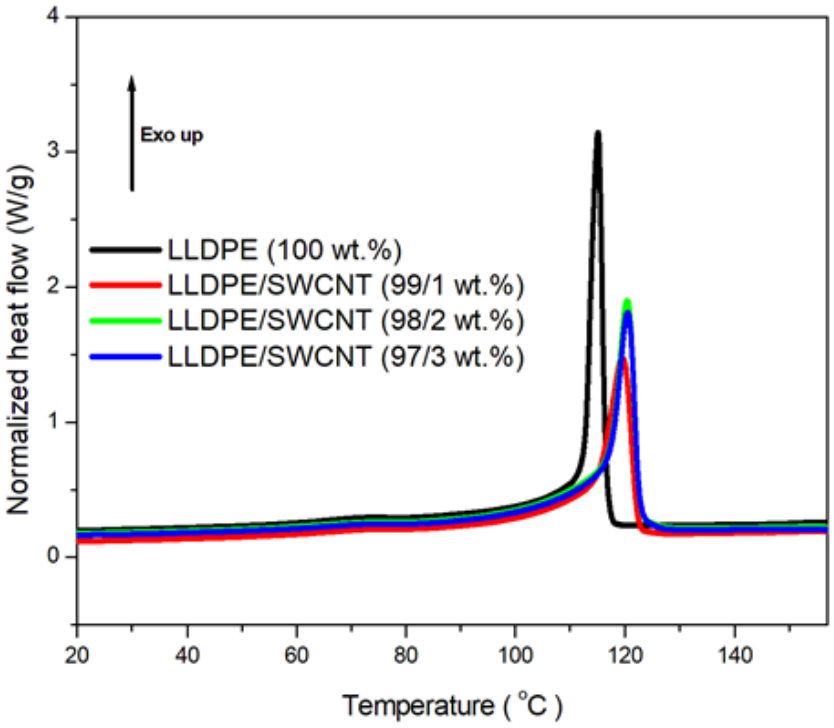

Figure 4.12: Cooling curve of LLDPE/SWCNT composites at different SWCNT content (1, 2 and 3 wt.%)

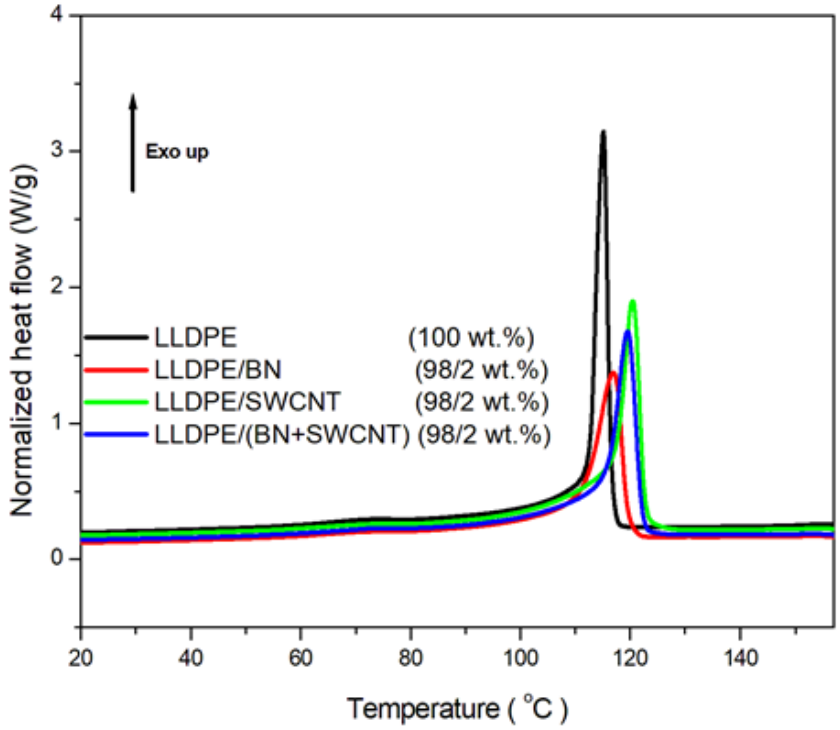

Figure 4.13: Cooling curve of LLDPE, LLDPE/BN, LLDPE/SWCNT and LLDPE/(BN+SWCNT) hybrid composites at 2 wt.% contents

Figure 4.14 to 4.16 depicts the heating curves of LLDPE/PW/BN, LLDPE/PW/SWCNT, and LLDPE/PW/(BN+SWCNT) hybrid composites. These Figures indicate that all the LLDPE/PW/BN, LLDPE/PW/SWCNT and LLDPE/PW/(BN+SWCNT) samples showed three endothermic peak temperatures. The first melting temperature that occurred at 28.6 ℃ was attributed to the solid-solid transition of the wax, while the second melting peak at 51.4 ℃ was attributed to the melting of the wax crystallites, and the third melting temperature that was observed at 123 ℃ was attributed to the melting temperature of the LLDPE matrix, as explained earlier in this document. Interestingly, the paraffin wax hybrid composites containing 2 wt.% BN+SWCNT showed a higher degree of crystallinity compared with 2 wt.% BN and 2 wt.% SWCNT incorporated into the LLDPE/paraffin wax blend. It seemed that the low molecular weight paraffin chains were able to penetrate between the two conductive fillers and thus improve the interaction between the conductive fillers and LLDPE, with the two conductive fillers better enhancing the crystallization of the LLDPE more compared with the single fillers. However, it is generally observed that the LLDPE/PW/SWCNT blend composites with 1 wt.% of carbon nanotubes (SWCNTs) had the highest degree of crystallinity when compared with both wax containing and non-wax containing samples. The presence of wax at this content of carbon nanotubes was able to penetrate between the SWCNTs chains, thereby enhancing its interaction with LLDPE. This resulted in the SWCNT enhancing the degree of crystallinity of the blend composites.

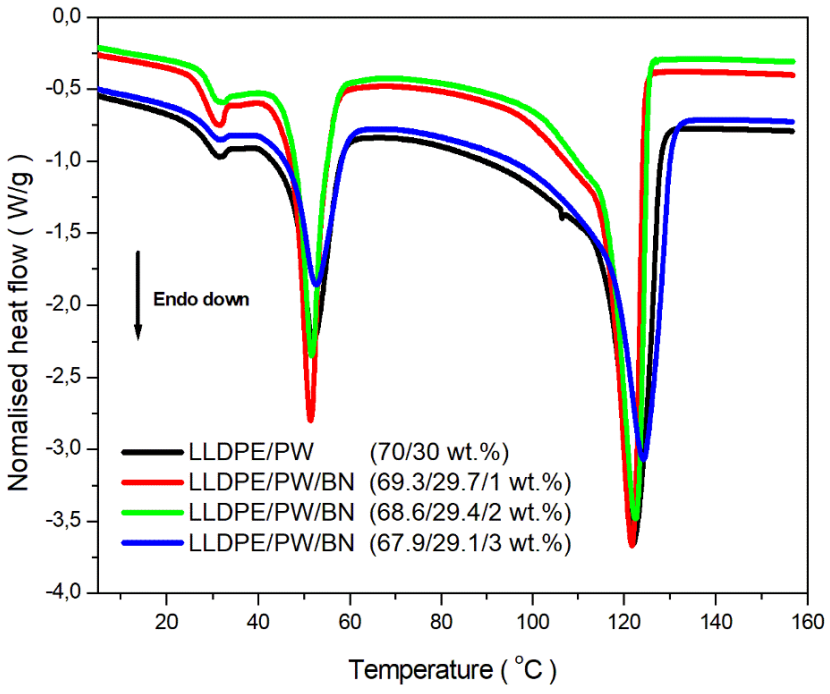

Figure 4.14: Heating curve of the LLDPE/PW blend and LLDPE/PW/BN composites with 1, 2, and 3 wt.% BN content

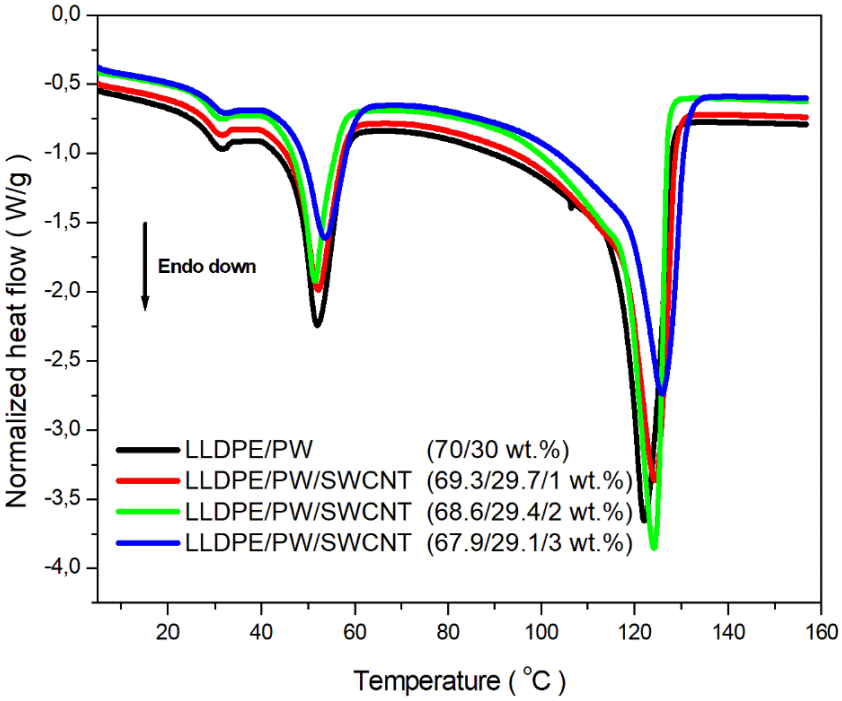

Figure 4.15: Heating curve of the LLDPE/PW blend and LLDPE/PW/SWCNT composites with 1, 2, and 3 wt.% SWCNT content

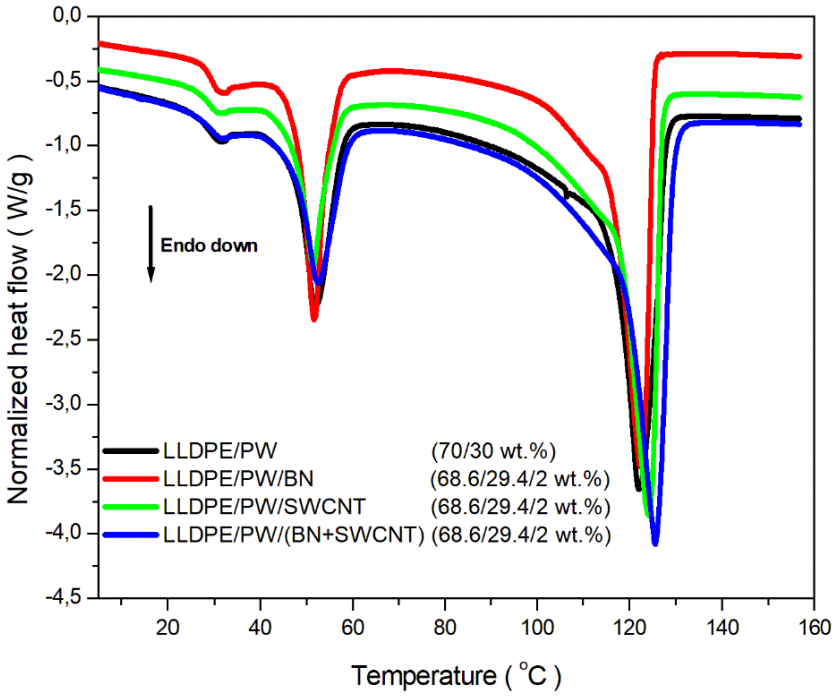

Figure 4.16: Heating curve of the LLDPE/PW blend, LLDPE/PW/BN, LLDPE/PW/SWCNT and LLDPE/PW/(BN+SWCNT) composites with 2 wt.% BN, SWCNT and BN+SWCNT content.

Figure 4.17 to 4.19 depicts the crystallization behaviour of the LLDPE/PW/BN, LLDPE/PW/SWCNT, and LLDPE/PW/(BN+SWCNT) hybrid composites. All investigated cooling curves samples of the LLDPE/PW/BN and LLDPE/PW/(BN+SWCNT) composites showed an increase in crystallization temperature with the incorporation of single fillers and hybrid fillers. The first crystallization temperature was recorded at 22.0 ℃ and the second crystallization temperature was recorded at 47.3 ℃, with both peaks belonging to the crystallization of paraffin wax. The third crystallization temperature that is observed at 114 ℃ was attributed to the crystallization of LLDPE. These Figures indicated that the presence of conductive fillers (*viz* BN and SWCNT) on the LLDPE/PW blend shifted the crystallization temperatures towards higher temperatures. This improvement was probably due to fillers acting as a nucleating agents on the LLDPE matrix. **Table 4.1** and **Figure 4.17** reveals that the composites with 3 wt.% BN content crystallized at higher crystallization temperatures than the other BN blend composites. This indicated that BN filler was more effective at higher content and this behaviour can also be seen by higher degree of crystallinity value of 52.2% at 3 wt.% BN content. On the other hand, SWCNT blend composites curves (see **Figure 4.18** and **Table 4.1**) showed that the SWCNT filler was more effective at lower content due to a high degree of crystallization value of 58.9 % attained when compared with other content(s) of SWCNT in the blend composites. Furthermore, the hybrid fillers (BN+SWCNT) also showed high degree of crystallinity value of 55.1 % which was higher than that of the BN blend composites, but lower than the SWCNT blend composites. One can deduce that the SWCNT at lower content(s) i.e., 1 and 2 wt.% was more effective than BN alone and its synergy with BN in terms of improving the thermal properties of the LLDPE.

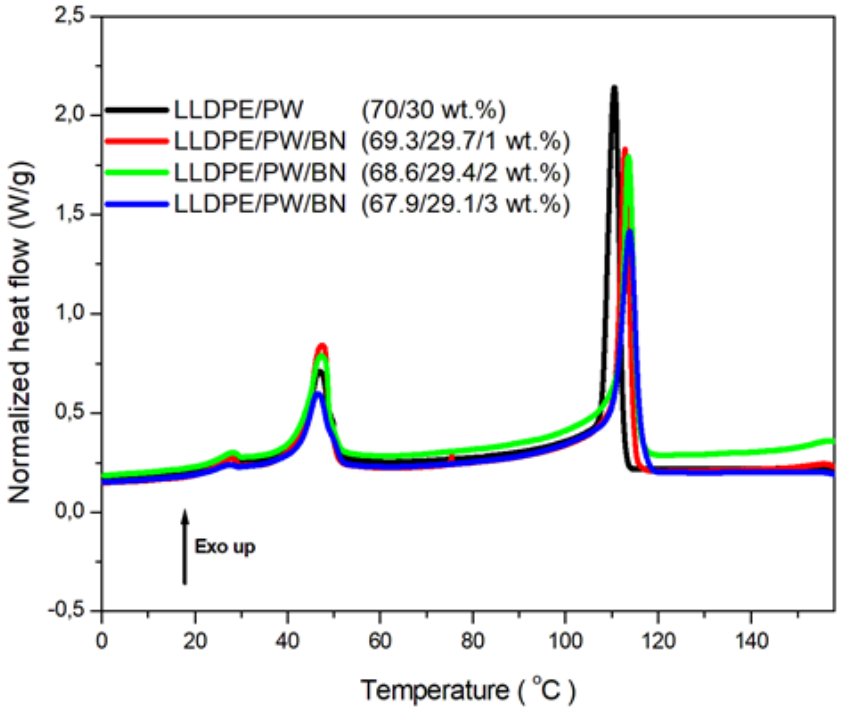

Figure 4.17: Cooling curve of the LLDPE/PW blend and LLDPE/PW/BN composites with 1, 2, and 3 wt.% BN content

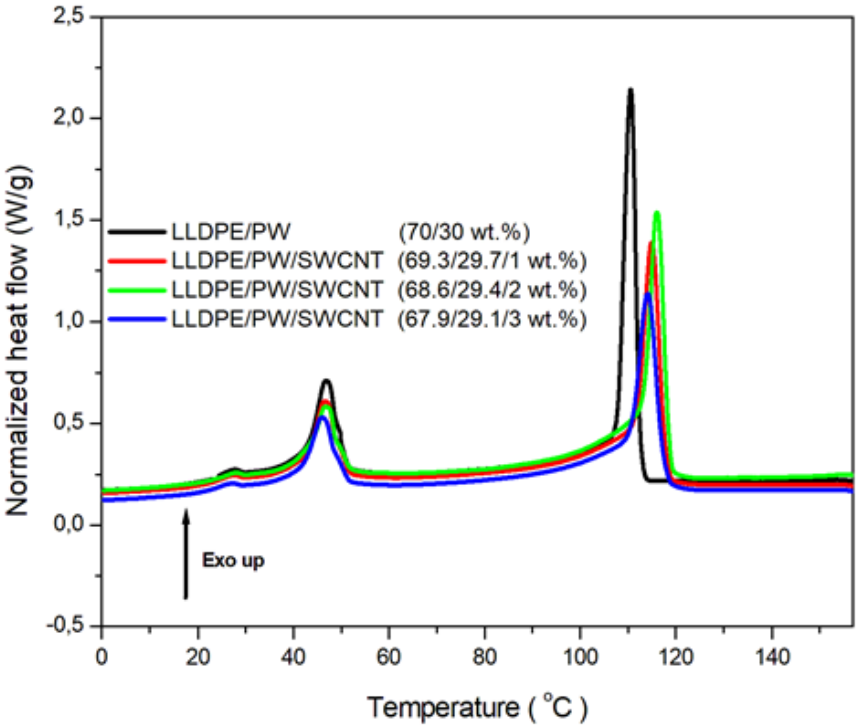

Figure 4.18: Cooling curve of the LLDPE/PW blend and LLDPE/PW/SWCNT composites with 1, 2, and 3 wt.% SWCNT content

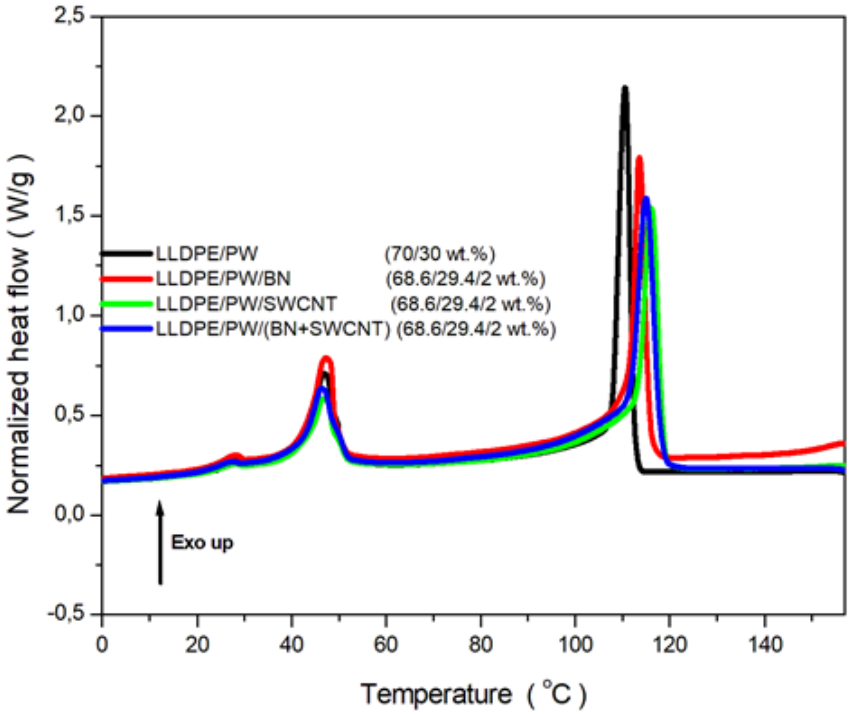

Figure 4.19: Cooling curve of the LLDPE/PW blend, LLDPE/PW/BN, LLDPE/PW/SWCNT and LLDPE/PW/(BN+SWCNT) composites with 2 wt.% BN, SWCNT and BN+SWCNT content.

4.4 Thermogravimetric analysis (TGA)

The thermal stability of the pure LLDPE, PW, LLDPE/PW blend, LLDPE/conductive fillers, LLDPE/hybrid conductive fillers, LLDPE/PW/conductive fillers and LLDPE/PW/hybrid conductive filler blend composites were examined using thermogravimetric analysis (TGA). The TGA results are tabulated in **Table 4.2.** The char residue for all the samples at 600 °C were also reported table. The $T_{20\%}$ and $T_{60\%}$ represent the weight loss temperatures of mass% taken at 20% and 60%, respectively. **Figure 4.20** depicts the thermal stability of the pure LLDPE, and PW. It was evident that LLDPE and PW degraded in one-step degradation with PW degrading at lower temperatures than the LLDPE polymer. This may be attributed to the short chain structures of the paraffin wax which happen to degrade at lower temperatures. The TGA curves of the LLDPE/BN, LLDPE/SWCNT composites and as well as LLDPE/(BN+SWCNT) hybrid composites are shown in **Figure 4.21, 4.22 and 4.23,** respectively. The results show that the thermal stability of LLDPE increased with the addition of BN, SWCNT fillers and BN+SWCNT hybrid fillers. This behaviour indicated that the fillers delayed the degradation

temperatures of the LLDPE matrix to higher temperatures. This may be ascribed to the fillers acting as a thermal heat barrier to protect LLDPE matrix from decomposing at lower temperatures. It is well-known that the inorganic fillers have a tendency to form char layers, that act as a thermal heat barrier and protect the polymer underneath against heat. Furthermore, it is well documented that the fabricated char layer has the ability to reduce pyrolysis of the polymer and, as a result, ensuring that the burning of combustible materials is decreased. In the current study (**Figure 4.21)** the 3 wt.% of BN content in the LLDPE/BN composites had higher thermal stability compared with pure LLDPE matrix and LLDPE/BN composites with 1 and 2wt.% of BN content. This enhancement in thermal stability may have been due a better heat resistance of BN particles at higher content, which happen to form a better char residue. It was most probably that this residue was well able to protect the penetration of heat better. This behaviour was also detected at $T_{20\%}$ and $T_{60\%}$ for 3 wt.% BN content (see **Table 4.2**), which showed higher weight loss values in comparison to pure LLDPE and LLDPE/BN composites. For example, there was 4.4% enhancement in $T_{60\%}$ for 3wt.% boron nitride when compared with pure LLDPE having 2.5% increase in $T_{60\%}$ values and 1 wt.% of boron nitride based LLDPE composites. The incorporation of SWCNT and its synergy with BN into LLDPE matrix (see **Figure 4.22** and **4.23**) to form LLDPE-based composites, enhanced the thermal stability when compared with neat LLDPE. This was because both BN and SWCNT could prevent the evaporation as well as diffusion of LLDPE degradation products and, as a result, enhance the thermal stability of the matrix. Furthermore, it is well-known that both BN and SWCNT can form a three-dimensional network structure capable of blocking the penetration of heat into the substrate material, in this case LLDPE matrix that performed this function.

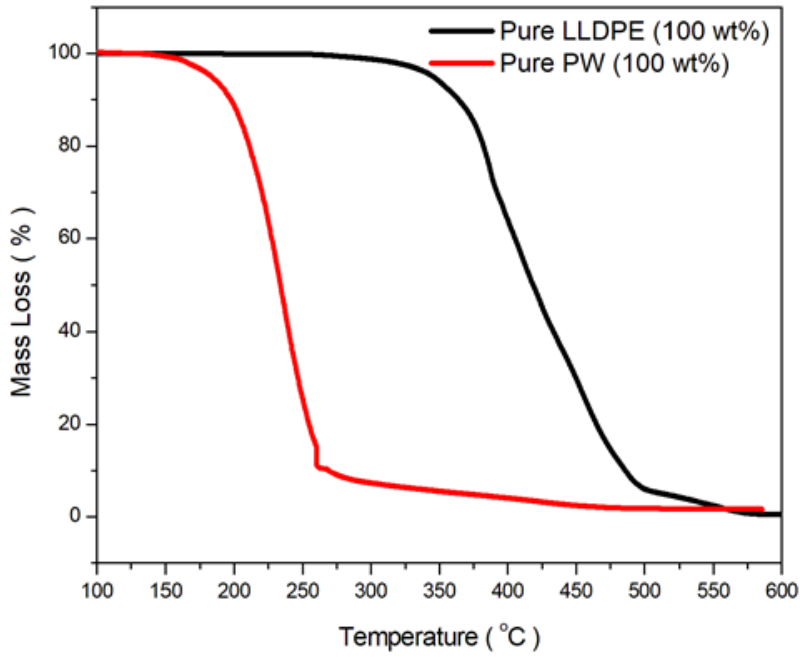

Figure 4.20: TGA curve of the neat LLDPE and PW.

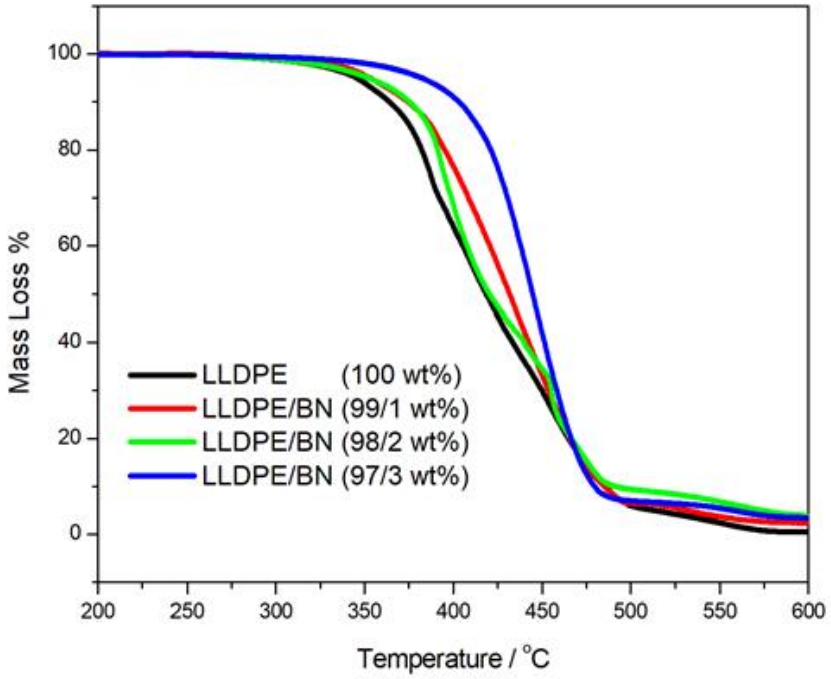

Figure 4.21: TGA curve of the neat LLDPE, and LLDPE/BN composites with 1, 2, ad 3 wt.% BN content.

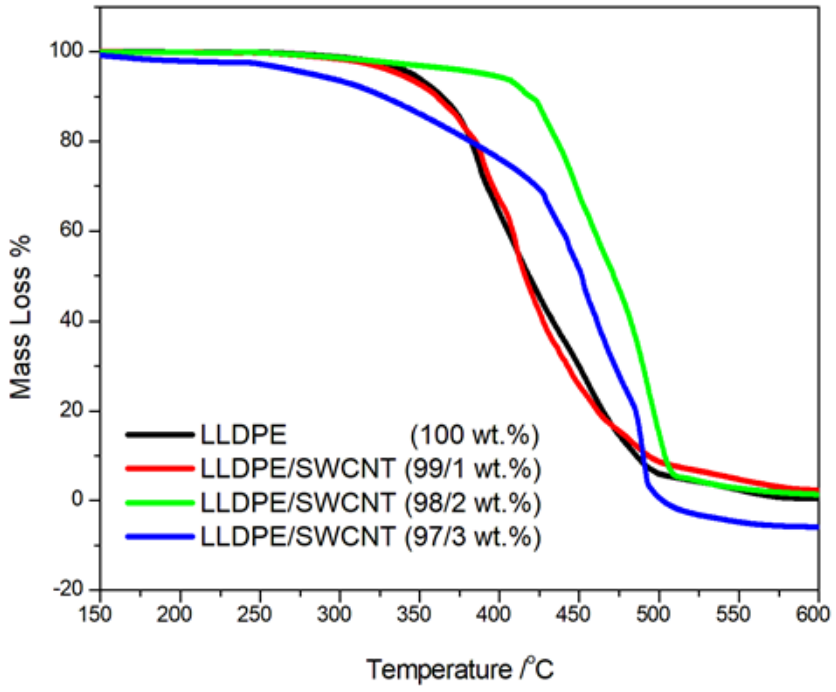

Figure 4.22: TGA curve of the neat LLDPE, and LLDPE/SWCNT composites with 1, 2, ad 3 wt.% SWCNT content.

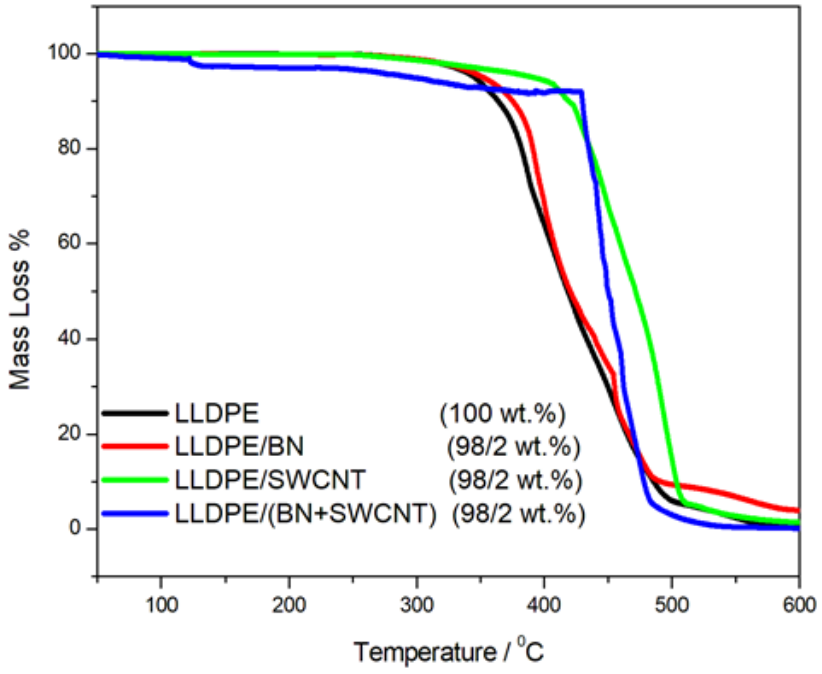

Figure 4.23: TGA curve of the neat LLDPE, LLDPE/BN, LLDPE/SWCNT and LLDPE/(BN+SWCNT) hybrid composites all at 2 wt.% BN, SWCNT and BN+SWCNT content.

Table 4.2: Summarized data of all the materials

Samples	Composition (wt.%)	$T_{20\%}$ [°C]	$T_{60\%}$ [°C]	Char residue at 600 °C
LLDPE	100	381	432	0.578
PW	100	209	239	0.174
LLDPE/PW	70/30	291	435	0.409
LLDPE/BN	99/1	394	440	2.46
	98/2	390	437	4.65
	97/3	421	451	3.34
LLDPE/SWCNT	99/1	383	426	2.70
	98/2	434	482	1.75
	97/3	378	460	---
LLDPE/(BN+SWCNT)	98/2	435	457	0.174
LLDPE/PW/BN	69.3/29.7/1	249	290	1.42
	68.6/29.4/2	287	431	---
	67.9/29.1/3	391	440	4.05

LLDPE/PW/SWCNT	69.3/29.7/1 68.6/29.4/2 67.9/29.1/3	298 303 304	471 458 444	1.95 1.31 2.46
LLDPE/PW/ (BN+SWCNT)	68.6/29.4/2	275	439	---

$T_{20\%}$ and $T_{60\%}$ represent the weight loss temperatures of mass taken at 20% and 60%, respectively

Figure 4.24 to 4.26 depicts the TGA curves of LLDPE/PW blend, LLDPE/PW/BN, LLDPE/PW/SWCNT composites and as well as LLDPE/PW/(BN+SWCNT) hybrid composites. The results indicated that the LLDPE/PW blend degraded in two-step degradation. The first-step degradation was ascribed to the degradation of PW, while the second-step degradation was attributed to the degradation of LLDPE. The mass loss at $T_{20\%}$ and $T_{60\%}$ were 291 ℃ and 435 ℃, respectively. The LLDPE/PW/BN blend composites degraded in two-step degradation as shown in **Figure 4.24,** with the first step obviously being ascribed to the paraffin wax and second step belonging to the LLDPE. It was also observed that the blend composites with 3 wt.% BN content had higher weight loss at $T_{20\%}$ (391 ℃) and $T_{60\%}$ (440 ℃), respectively when compared with 1wt.% and 2 wt.% of BN. This indicated that there was a delay in degradation temperature of LLDPE/PW blend which only reached higher temperatures with the addition of 3 wt.% BN content, as was reported earlier on this document. This may be ascribed to a possible interaction between the paraffin wax volatiles with BN resulting in a decreased rate of diffusion from the molten state of the sample [7]. **Figure 4.25** represents the TGA curves of LLDPE/PW/SWCNT blend composites. The results show that all the blend composites degraded in two-step degradation as was the case for LLDPE/PW/BN blend composites. The 2 wt.% SWCNT showed a better heat resistant in comparison to other LLDPE/PW/SWCNT blend composites and the synergy of BN and SWCNT. **Figure 4.26** shows the thermal stability of the LDPE/PW/BN and LLDPE/PW/SWCNT blend composites as well as that of the hybrid blend composites (LLDPE/PW/(BN+SWCNT) at 2 wt.% filler content. It was observed that the blend incorporated with SWCNT was more effective in increasing the thermal stability of the LLDPE/PW blend than the blend incorporated with BN and hybrid fillers (BN+SWCNT). It appeared as if the three-dimensional network structure formed by the synergy between the BN and SWCNT was not strong enough to protect the substrate against heat when compared with 2 wt.% SWCNT alone, as the latter was able to form compact char. This behaviour could also be attributed to a strong interaction between SWCNT with paraffin wax which might have contributed to enhanced thermal stability of the blend composites.

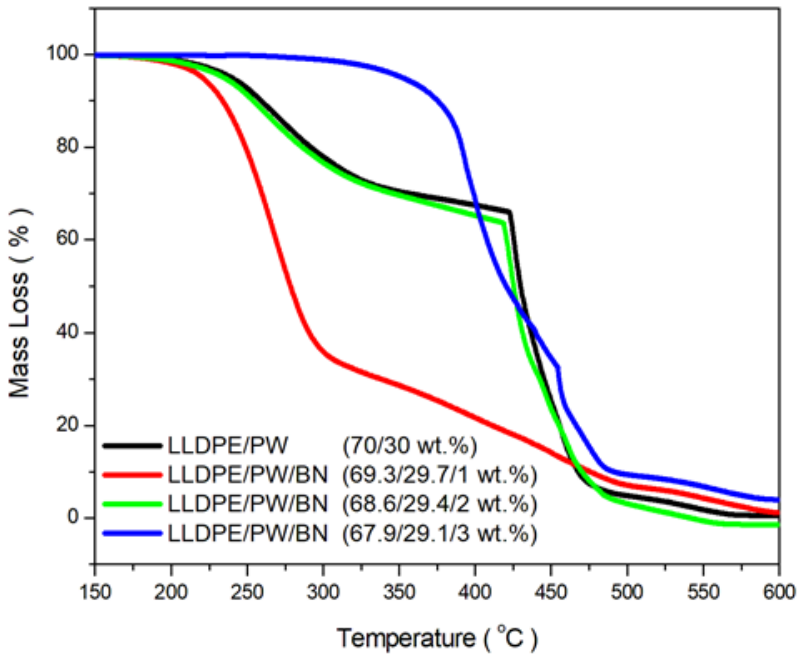

Figure 4.24: TGA curve of the LLDPE/PW blend and LLDPE/PW/BN composites with 1, 2, ad 3 wt.% BN content.

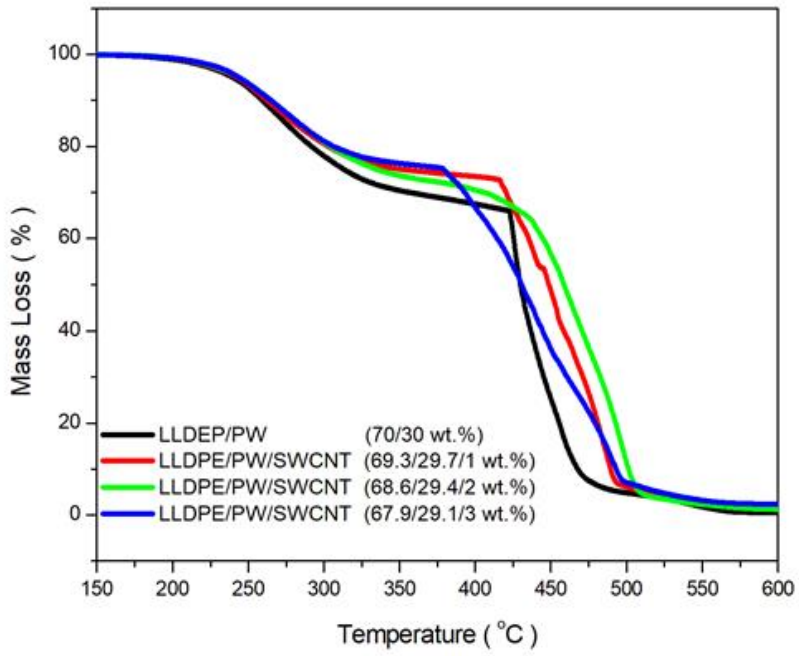

Figure 4.25: TGA curve of the LLDPE/PW blend, and LLDPE/PW/SWCNT composites with 1, 2, ad 3 wt.% SWCNT content.

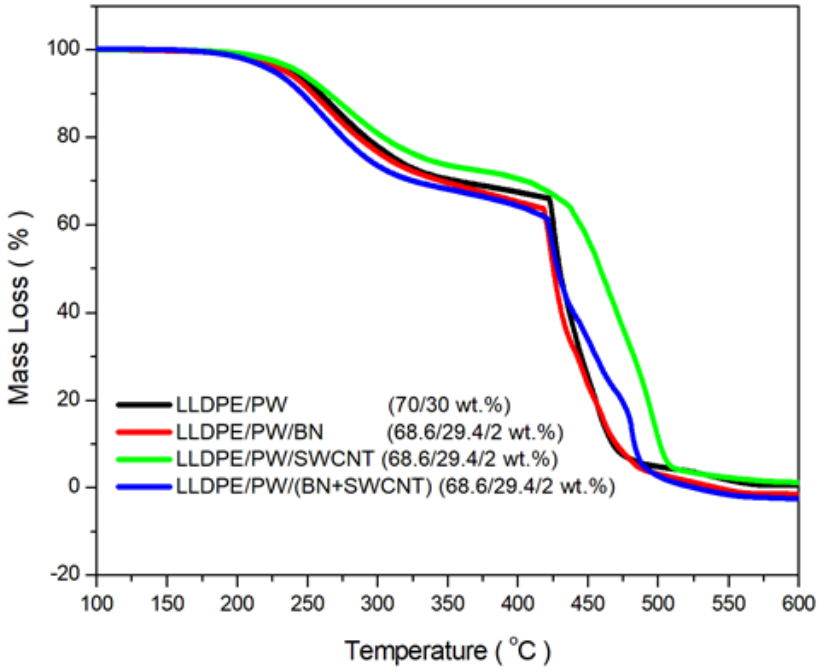

Figure 4.26: TGA curve of the LLDPE/PW blend, LLDPE/PW/BN, LLDPE/PW/SWCNT and LLDPE/PW/(BN+SWCNT) hybrid composites all at 2 wt.% BN, SWCNT and BN+SWCNT content.

4.5 Mechanical and thermomechanical properties

Figure 4.27 and **4.28** depicts the tensile stress and elongation at break rates of pure LLDPE, LLDPE composites, LLDPE/PW blend composites, and LLDPE/PW/SWCNT/BN hybrid composites. These results were obtained from the stress-strain curves as shown in **Appendix A**. **Table 4.3** summarizes the mechanical properties of the above-mentioned samples. The tensile strength of the LLDPE matrix was initially reduced from 18.0 MPa to 15.7 MPa at 2 wt.% BN content, while 3wt.% of both BN and SWCNT content(s) resulted in the increased tensile strength of the LLDPE matrix to 18.7 MPa and 22.0 MPa, respectively. The reduction in tensile strength at 2wt.% load of BN was associated with agglomeration of BN at this content (see **SEM section 4.1**), which may have acted as imperfections in the system thereby resulting in an early failure. However, the addition of a higher content of both ceramic and carbon-based fillers may have enhanced the tensile strength due to a high aspect ratio of this fillers. Generally, in the absence of paraffin, it is very clear that the carbon nanotubes-based composites showed higher tensile strength values at 3wt.% when compared with boron nitride-based composites

Figure 4.27 and **Table 4.3**. This behaviour may be ascribed to a higher crystallinity of the carbon-based composites compared with that of ceramic-based fillers. For an example, 3 wt.% of SWCNT had a crystallinity value of 53.8% compared with 53.1% of the 3wt.% boron nitride-based composites. This behaviour may be associated with the theory that the higher the crystallinity, the more the stiff or rigid polymer material becomes, resulting in improved tensile strength. This result was in line with the elongation at break, whereby the single walled carbon nanotubes (SWCNTs) composites showed lower elongation at break due to high crystallinity which restricted the molecular chain mobility of the polymer. Similar results were obtained by Kim and Kim [1] who investigated the mechanical properties of the boron nitride (BN)-multi walled carbon nanotubes (MWCNT)-polyphenylene sulfide (PPS) composites. The latter authors reported that the tensile strength of the PPS composites filled with uncoated MWCNT was higher than that of the uncoated BN-PPS composites. Basically, the authors observed a reduction in tensile strength with the addition of BN which may be ascribed to poor interaction between the filler and polymer matrix. The enhancement in tensile strength of the carbon nanotubes may be attribute to their stiffness and reinforcing ability, which ensures an easy load transfer from the polymer matrix to the CNTs, and results in enhanced tensile strength. Similarly, Wu *et al.* [2] investigated the mechanical properties of the high-density polyethylene (HDPE) filled with multi walled carbon nanotubes (MWCNTs). It was reported that the tensile strength of the HDPE was increased with the addition of and increase in content of the MWCNTs. However, Jin-hua *et al.* [3] observed a different behaviour when investigating the LLDPE/MWCNTs nanocomposites. There was a reduction in tensile strength at 3 wt.% content of MWCNTs, which they associated with the aggregation of the MWCNTs filler at higher content. In the current study **Figure 4.27** indicates that the addition of paraffin into the BN/LLDPE and SWCNT/LLDPE composites showed a reduction in the tensile strength even when compared with pure LLDPE. This might have been due to the presence of low molecular weight paraffin wax which could have deteriorated the tensile strength of the composites. It is well documented that paraffin wax has poor tensile properties, and furthermore, that the wax crystals may crystallize on the amorphous region of polymer, thereby acting as defect points for the initiation as well as propagation of stress cracking, thus reducing the tensile strength. Similar behaviour was reported by Krupa *et. al* [4], whereby the presence and increase in wax content in the LLDPE/wax/EG blend composites reduced the tensile strength which they had expected due to low molecular weight and low mechanical properties of wax than those of the LLDPE matrix. The latter authors also argued that wax acted as a plasticizer, thus reducing the tensile strength of the polymer matrix. In the current study the results recorded in **Figure 4.27**

and **Table 4.3** indicate that the carbon nanotubes/paraffin wax composites showed higher tensile strength when compared with boron nitride/paraffin wax-based composites. This behaviour may be ascribed to a better dispersion of the carbon-based fillers into the composites in the presence of paraffin wax, as it was clear that there was a high affinity of paraffin wax with carbon-based fillers when compared with ceramics fillers, and this generally enhanced the tensile strength.

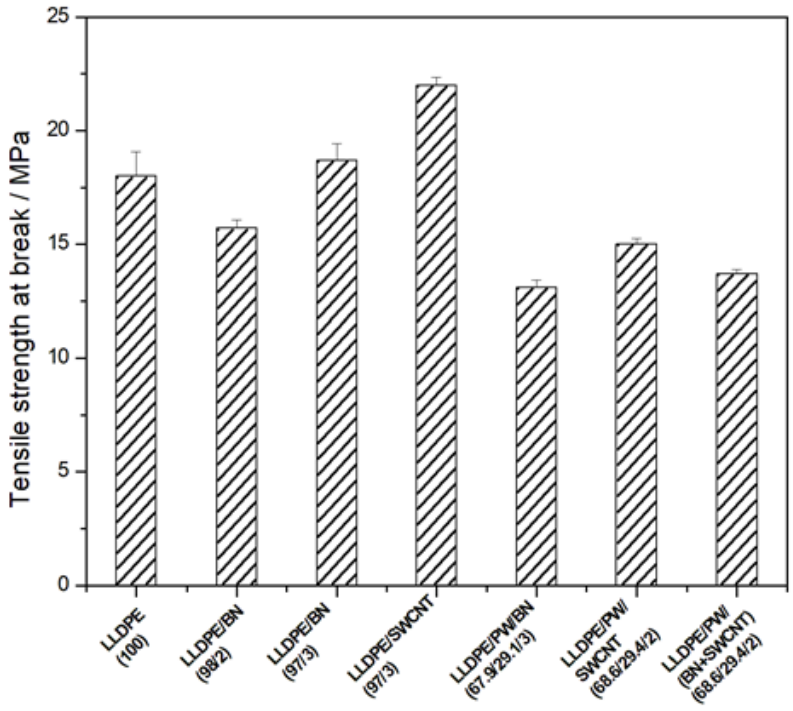

Figure 4.27: Tensile stress at break of neat LLDPE, LLDPE/BN, LLDPE/SWCNT composites and LLDPE/PW conductive fillers blend composites, and LLDPE/PW hybrid composites

Table 4.3 and **Figure 4.28** depict the elongation at break for pure LLDPE, LLDPE/BN, LLDPE/SWCNT composites and LLDPE/PW conductive fillers blend composites, and LLDPE/PW conductive fillers hybrid composites. Interestingly, the elongation at break of the composites filled with BN was found to be higher than that of the pure LLDPE matrix. There were 123% and 6% enhancement in elongation at break for the composites filled with 2 wt.% and 3 wt.% BN content, respectively. This was surprising because the incorporation of the inorganic fillers has a tendency of immobilize the chains of the polymer matrix, thereby increasing brittleness and as a result, reducing the elongation at break [5]. As was expected, the presence of SWCNTs reduced the elongation at break of the polymer matrix by 474.1% (at 3 wt.% SWCNT), 465.2% (for 2 wt.% SWCNT) in LLDPE/PW blend composites and by 469.9

% in the hybrid composites (LLDPE/PW/(BN+SWCNT), respectively. This behaviour was attributed to the effective restriction of the SWCNT into the molecular motion of the LLDPE matrix, which restricted the deformation of the LLDPE matrix. This confirmed the reinforcing behaviour of the SWCNT. Similar trend was observed by Jin-hua *et al*. [3], who reported that the incorporation of MWCNT into LLDPE decreased the elongation at break when compared with pure LLDPE.

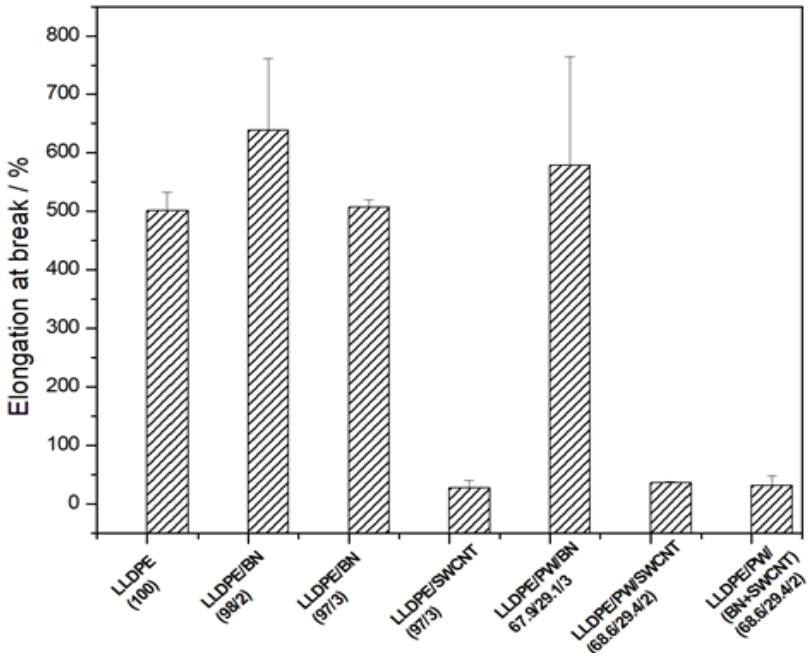

Figure 4.28: Tensile stress at break of neat LLDPE, LLDPE/BN, LLDPE/SWCNT and LLDPE/PW conductive fillers blend composites, and LLDPE/PW hybrid composites

Table 4.3: Mechanical properties of all the materials

Materials (wt.%)	$\sigma_b \pm S_{\sigma b}$/MPa	$\varepsilon_b \pm S_{\varepsilon b}$/ %
LLDPE (100)	18.0 ± 1.08	501 ± 31.6
LLDPE/BN		
(98/2)	15.7 ± 0.376	638 ± 123
(97/3)	18.7 ± 0.729	507 ± 12.7
LLDPE/SWCNT		
(97/3)	22.0 ± 0.336	26.9 ± 13.5
LLDPE/PW/BN		
(67.9/29.1/3)	13.1 ± 0.326	579 ± 185

LLDPE/PW/SWCNT (68.6/29.4/2)	15.0 ± 0.257	35.8 ± 2.14
LLDPE/PW(BN+SWCNT) (68.6/29.4/2)	13.7 ± 0.171	31.1 ± 16.3

$\sigma_b$is the tensile strength at break, ε_b is the elongation at break, $S_{\sigma b}$ *and* $S_{\varepsilon b}$ are their standard deviations, respectively.

The dynamic mechanical properties (thermomechanical properties) of the pure LLDPE, LLDPE/SWCNT (97/3) and LLDPE/BN (97/3) were investigated and the results are shown in **Figure 4.29**. The incorporation of 3 wt.% of SWCNTs seemed to improve the storage modulus in the investigated temperature range when compared with pure LLDPE and LLDPE/BN composites. This behaviour may be ascribed to the high crystallinity (53.8 %) of the LLDPE/SWCNT (97/3) composites when compared with the crystallinity of the LLDPE/BN (97/3) composites (53.0 %). It is well documented in the literature that the Modulus of semi-crystallinity polymers is directly proportionate to the crystallinity of semi-crystalline polymer materials [6,7,8.9].

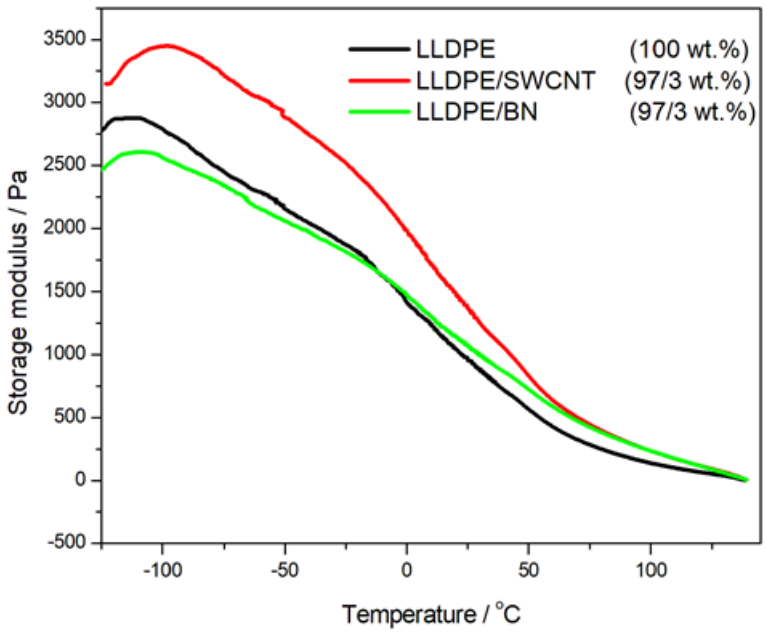

Figure 4.29: DMA curve of the LLDPE. LLDPE/BN and LLDPE/SWCNT composites

4.6 Impact strength

Impact strength is defined by the ability of the material to withstand an applied load and is expressed by energy. The samples for impact are normally measured by Izod impact strength test or Charpy impact test. Both types of impact strength tests are used to measure the impact energy required to fracture the sample. The impact strength of the pure LLDPE, LLDPE composites and LLDPE/PW blend composites, and as well as LLDPE/PW hybrid composites are depicted in **Figure 4.30**. The impact strength of the LLDPE matrix recorded at 103.22 KJ/m^2 and the value was reduced with the incorporation of BN into the LLDPE matrix. The main reason for such decrease was associated to the poor dispersion and aggregates of the boron nitride (**see SEM section 4.1**) into the LLDPE matrix. It is well documented that factors such as the filler particle size, and interaction between the filler and polymer matrix play a critical role in the impact strength of the composites. In case of agglomerated boron nitride composites it was highly possible that the BN particles acted as crack nucleation sites, and thus it is easy for cracks to form in the composites which in turn, reduced the overall impact strength. Qin *et al.* [1] reported that the impact strength of the PMMA was initially increased with the incorporation of BN filler up until 2 wt.%, but it decreased with increasing BN content. This observation was ascribed to the fact that BN filler particles got closer to one another due to agglomeration and, as the result, the materials cracked because of high stress concentration which showed that the impact energy was not absorbed by the materials. In the current study, the addition of wax into the system i.e., LLDPE/PW/SWCNT and LLDPE/PW/(BN+SWCNT) reduced the impact strength to a greater extent when compared with pure LLDPE. This behaviour may be associated with the low viscosity of paraffin wax which might have caused flaws within the matrix, thus acting as a catalyst for the initiation as well as propagation of stress cracking, which decreased the impact strength.

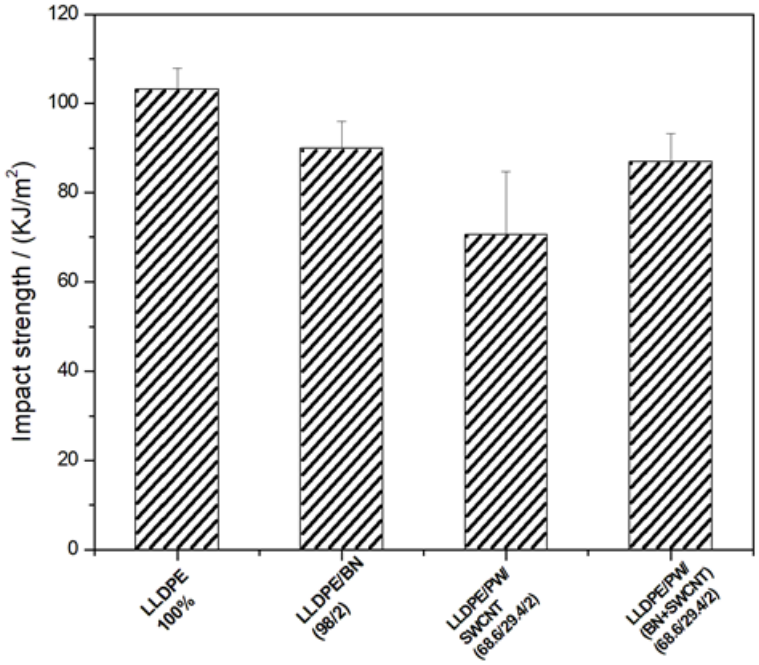

Figure 4.30: Impact strength of LLDPE, LLDPE/BN, LLDPE/PW/SWCNT and LLDPE/PW/(BN+SWCNT)

The incorporation of high contents of 3 wt.% SWCNTs improved the impact strength of the composites, except when wax was added in the composites **(Figure 4.31)**, whereas 3 wt.% BN seemed to have no impact on the toughness of the material. This behaviour at 3wt.% SWCNTs was noteworthy because one would have expected that a stiff material would reduce the toughness of the polymer matrix. However, in the current study it seemed as if there was still some free volume in the system at 3 wt.% SWCNTs, which might have allowed some movement of chains to some extent when the composite was subjected to impact force. Jin-hua et al [2] reported an improvement in impact strength of the LLDPE/MWCNTs at 1.0 wt.% content of the filler, which they attributed to a homogenous dispersion in the LLDPE matrix. However, the authors observed a reduction in impact strength with content above 1.0 wt.%, which they associated with agglomeration that acted as stress concentrator, thereby reducing impact strength.

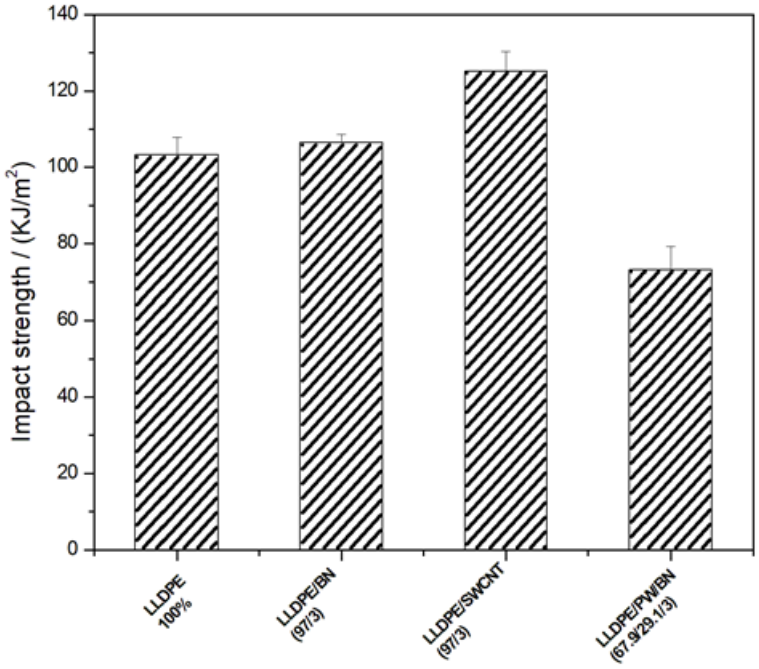

Figure 4.31: Impact strength of LLDPE, LLDPE/BN, LLDPE/PW/SWCNT and LLDPE/PW/(BN+SWCNT) hybrid composites

4.7 References

[1] Krupa, I., Mikova, G., & Luyt, A.S. **2007**. Phase change materials based on low-density polyethylene/paraffin wax blends. *European Polymer Journal*, 43: 4695-4705. https://doi.org/10.1016/j.eurpolymj.2007.08.022

[2] Zhang, X., Wu, H., & Guo, S. **2015**. Effect of interfacial interaction on morphology and properties of polyethylene/boron nitride thermally conductive composites. *Polymer-Plastics Technology and Engineering*, 54: 1097-1105. https://doi.org/10.1080/03602559.2014.974280

[3] Wang, L., Wang, H., Zhang, X., Liu, L., & Zhang, H. **2018**. Preparation and properties of boron nitride/epoxy composites with high thermal conductivity and electrical insulation. *Journal of Materials Science: Materials in Electronics*, 29: 14267-14276. https://doi.org/10.1007/s10854-018-9560-8

[4] Lionetto, F., Lopez-Munoz, R., Espinoza-Gonzalez, C., Mis-Fernandez, R., Rodriquez-Fernandez, O., & Maffezzoli, A. **2019**. A study on exfoliation of expanded graphite stacks in candelilla wax. *Materials*, 12: 2530. https://doi.org/10.3390/ma12162530

[5] Saini, A., Yadav, C., Bera, M., Gupta, P., & Maji, P.K. **2017**. Maleic anhydride grafted linear low density polyethylene/waste paper powder composites with superior mechanical behaviour. *Journal of Applied Polymer Science*, 134: 45167. https://doi.org/10.1002/app.45167

[6] Carvalho, M.S., Azevedo, J.B., & Barbosa, J.D.V. **2020**. Effect of the melt flow index of an HDPE matrix on the properties of composites with wood particles. *Polymer Testing*, 90: 106678. https://doi.org/10.1016/j.polymertesting.2020.106678

[7] Molefi, J.A., Luyt, A.S., & Krupa, I. **2010**. Comparison of LDPE, LLDPE, and HDPE as matrices for phase change materials based on a soft Fischer-Tropsch paraffin wax. *Thermochimica Acta*, 500: 88-92. https://doi.org/10.1016/j.tca.2010.01.002

[8] Zhou, T., Smith, M.K., Berenguer, J.P., Quill, T.J., Cola, B.A., Kalaitzidou, K., & Bougher, T.L. **2019**. The impact of polymer matrix blends on thermal and mechanical properties of boron nitride composites. *Journal of Applied Polymer Science*, 137: 48661. https://doi.org/10.1002/app.48661

[9] Krupa, I., & Luyt, A.S. **2001**. Thermal and mechanical properties of extruded LLDPE/wax blends. *Polymer Degradation and Stability*, 73: 157-161. PII: S0141-3910(01)00082-9

[10] Lomate, G.B., Dandi, B., & Mishra, S. **2018**. Development of antimicrobial LDPE/Cu nanocomposite food packaging film for extended shelf life of peda. *Food Packaging and Shelf Life*, 16: 211-219. https://doi.org/10.1016/j.fpsl.2018.04.001

[11] Russo, P., Patti, A., Petrarca, C., & Acierno, S. **2018**. Thermal conductivity and dielectric properties of polypropylene-based hybrid compounds containing multiwalled carbon nanotubes. *Journal of Applied Polymer Science*, 135: 46470. https://doi.org/10.1002/app.46470

[12] Ren, P.G., Si, X.H., Sun, Z.F., Ren, F., Pei, L., & Hou, S.Y. **2016**. Synergistic effect of BN and MWCNT hybrid fillers on thermal conductivity and thermal stability of

ultra-high-molecular-weight polyethylene composites with a segregated structure. *Journal of Polymer Research*, 23: 21.

https://doi.org/10.1007/s10965-015-0908-y

[13] Zhong, S., Zhou, Z., Zhang, K., Shi, Y., Chen, Y., Chen, X., Zeng, J., & Wang, M. **2016**. Formation of thermally conductive networks in isotactic polypropylene/hexagonal boron nitride composites via "Bridge Effect" of multi walled carbon nanotubes and graphene nanoplatelets. *RSC Advances*, 6: 98571-98580.

https://doi.org/10.1039/C6RA24046A

[14] Kim, K., & Kim, J. **2016**. BN-MWCNT-PPS core-shell structured composite for high thermal conductivity with electrical insulating via particle coating. *Polymer*, 101: 168-175.

https://doi.org/10.1016/j.polymer.2016.08.062

[15] Wu, Y., Dong, C., Yuan, C., Bai, X., Zhang, L., & Tian, Y. **2021**. MWCNTs filled high-density polyethylene composites to improve tribological performance. *Wear*, 2021: 203776.

https://doi.org/10.1016/j.wear.2021.203776

[16] Jin-Hua, T., Guo-qin, L., Huang, C., & Lin-Jian, S. **2012.** Mechanical properties and thermal behaviour of LLDPE/MWCNTs nanocomposites. *Materials Research*, 15: 1050-1056.

https://doi.org/10.1590/S1516-14392012005000122

[17] Krupa, I., Nogellova, Z., Spitalsky, Z., Malikova, M., Sobolciak, P., Abdelrazeq, H., Ouederni, M., Karkri, M., Janigova, I., & Al-Maadeed, M.A.S. **2015**. Positive influence of expanded graphite on the physical behaviour of phase change materials based on linear low-density polyethylene and paraffin wax. *Thermochimica Acta*, 614: 218-225.

https://doi.org/10.1016/j.tca.2015.06.028

[18] Unal, H., & Mimaroglu, A. **2004**. Influence of filler addition on the mechanical properties of nylon-6 polymer. *Journal of Reinforced Plastics and Composites*. 23: 461-469.

https://doi.org/10.1177/0731684404031977

[19] Huang, R., Xu, X., Lee, S., Zhang, Y., Kim, B., & Wu, Q. **2013**. High density polyethylene composites reinforced with hybrid inorganic fillers: Morphology, mechanical and thermal expansion performance, *Materials*, 6: 4122-4138.

https://doi.org/10.3390/ma6094122

[20] Li, J., Qiao, Y., Li, D., Zhang, S., & Liu, P. **2019.** Improving interfacial and mechanical properties of glass fabric/polyphenylene sulfide composites via grafting multi-walled carbon nanotubes. *RSC Advances*, 9: 32634-32643. https://doi.org/10.1039/c9ra05805b

[21] Song, W., & Li, Q.C., Lin, L., & Chen, Y. **2013**. Research on the mechanical and thermal properties of MWCNTs/CF reinforced epoxy resin matrix composite patch. *Physics Procedia*, 50: 405-409. https://doi.org/10.1016/j.phpro.2013.11.062

[22] Kim, K., Yoo, M., Ahn, K., & Kim, J. **2015**. Thermal and mechanical properties of AIN/BN-filled PDVF composite for solar cell backsheet application. *Ceramics International*, 41: 179-187. https://doi.org/10.1016/j.ceramint.2014.08.056

[23] Qin, L., Li, G., Hou, J., Yu, X., Ding, H., Zhang, Q., Wang, N., & Qu, X. **2015**. Preparation, characterization, and thermal properties of poly (methyl methacrylate)/boron nitride composites by bulk polymerization. *Polymer composites*, 36: 1675-1684. https://doi.org/10.1002/pc.23078

Chapter 5: Conclusion and Recommendations for Future Research

The aim of this study was to investigate the effect of two conductive fillers (*viz* boron nitride and single walled carbon nanotubes) and their synergy on the properties of LLDPE matrix and LLDPE/paraffin wax blend (ratio of 70/30). Boron nitride and single walled carbon nanotubes were incorporated into the LLDPE matrix and LLDPE/paraffin wax blend using Rheomix Haake PolyLab 600. Different content of the filler loading was used i.e. 1, 2, and 3 wt.%. It was observed that, in the absence of paraffin wax, BN particles were distributed in the LLDPE matrix with obvious agglomeration, thus indicating poor interaction between the LLDPE matrix and the BN filler. However, the opposite was observed for LLDPE/wax/BN/SWCNT composites, which showed a better dispersion of fillers in these composites. This better dispersion in the presence of SWCNT/paraffin wax composites was associated with a high affinity of the paraffin wax with the carbon-based fillers. There was a clear immiscibility between the paraffin wax and LLDPE, which was confirmed by DSC and TGA results. DSC revealed two separate melting peaks between paraffin wax and LLDPE, whereas TGA by two degradation steps. Moreover, Boron nitride and single walled carbon nanotubes were found to be effective in enhancing the thermal properties the LLDPE/conductive composites. Generally, there was also enhancement in the degree of crystallization of the LLDPE with the addition of the boron nitride (BN) and single walled carbon nanotubes (SWCNT), with 1 wt.% of carbon nanotubes (SWCNTs) showing the highest degree of crystallinity when compared with both wax containing and non-wax containing samples. The presence of wax at this content of carbon nanotubes was able to penetrate between the SWCNTs chains, thereby enhancing its interaction with LLDPE. This resulted in SWCNT enhancing the degree of crystallinity of the blend composites.

It can be concluded that the incorporation of both ceramic and carbon-based fillers enhanced thermal stability of the LLDPE matrix in the absence of paraffin wax, which was attributed to a shielding against heat by both fillers. The blend composites incorporated with SWCNT was more effective in increasing the thermal stability and it showed a better heat resistance in comparison with the blend composites incorporated with BN and BN+SWCNT synergy. It was thus also concluded that the incorporation of paraffin wax into the BN/LLDPE and

SWCNT/LLDPE composites resulted in a reduction in the tensile strength even when compared with pure LLDPE. This might have been due to the presence of low molecular weight paraffin wax, which could have deteriorated the tensile strength of the composites.

The best result that this study achieved with the ratio of LLDPE/paraffin wax was 70/30, and Future studies thus need to increase the content of paraffin wax incorporated into polymer matrix. It is well-known that the amount of paraffin is directly proportional to the energy that is being stored, however above 30% of wax we realized that there was wax leakage in the polymer matrix. This phenomenon should thus be further investigated.

For future studies there is a need for methods such as encapsulation of paraffin wax before being incorporated into polymer matrix, with the aim of enhancing the amount energy being stored. The encapsulation of paraffin wax will also broaden its application in the field of energy storage in such a way that advanced methods such interfacial polymerization, emulsion and suspension polymerization can be utilized effectively. The fabrication of polymer/paraffin wax blends has been done by using petroleum-based polymers, but these pose a serious greenhouse threat as they emit gases such as methane and carbon dioxide that contribute to the serious issue of global warming. There is thus a need for utilization of environmentally friendly polymer matrices (biopolymers) for fabrication of paraffin wax/biopolymer blends in the near future.

Appendix A

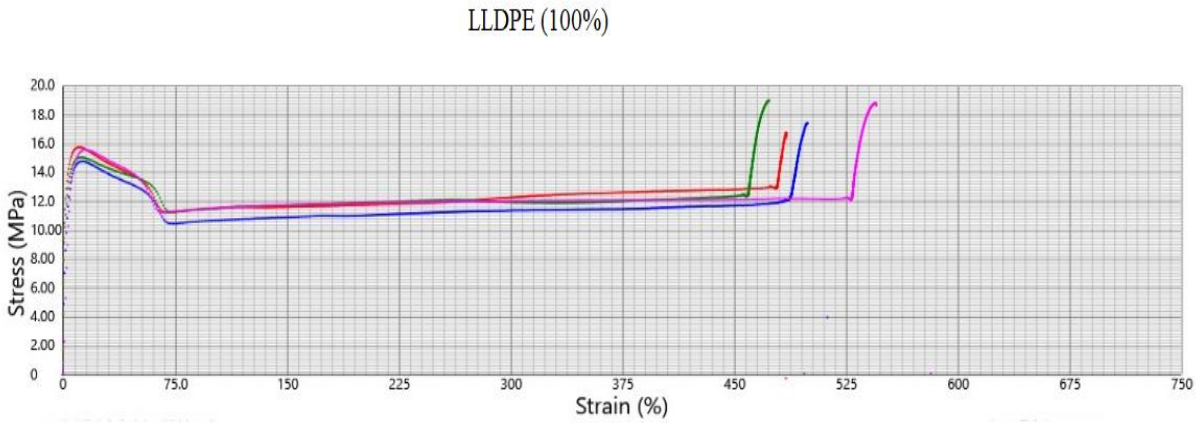

A1 Pure LLDPE

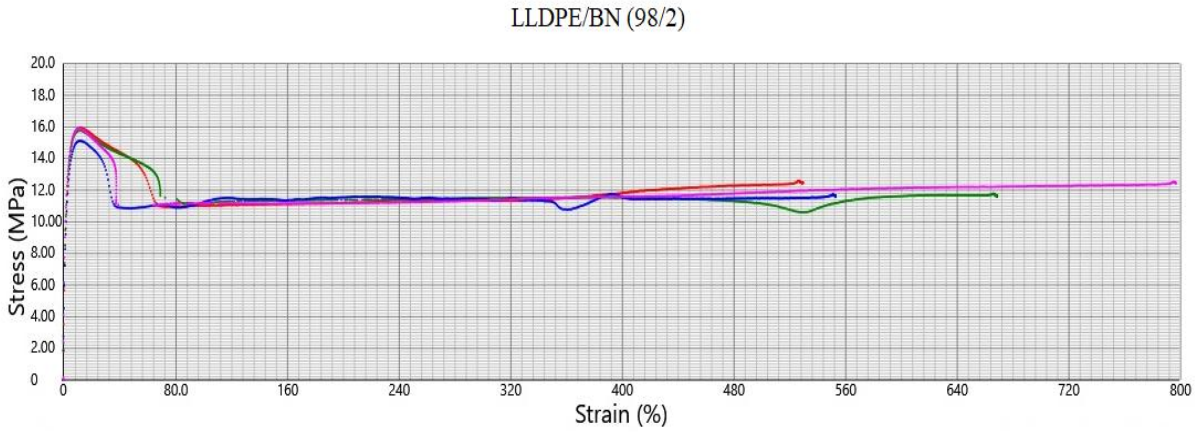

A2 LLDPE/BN composites with 2 wt.% BN content

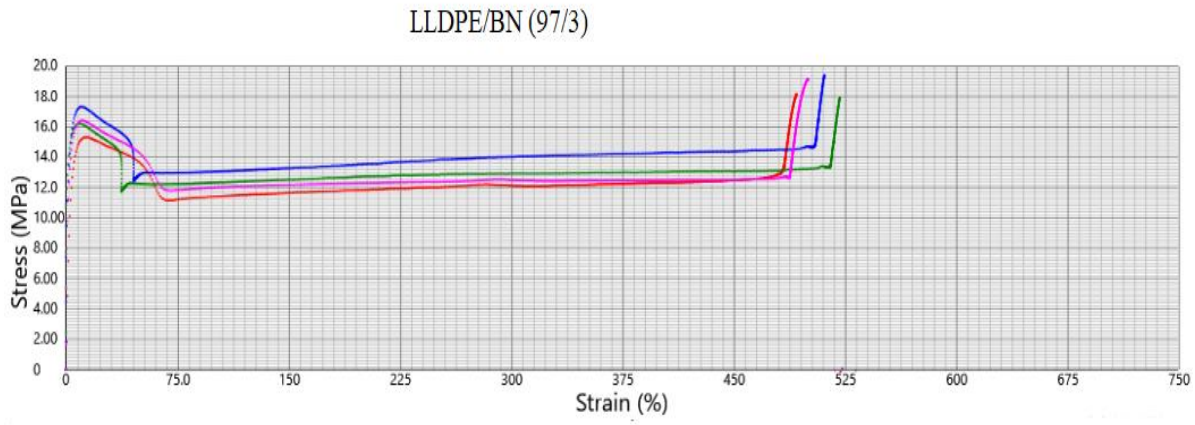

A3 LLDPE/BN composites with 3 wt.% BN content

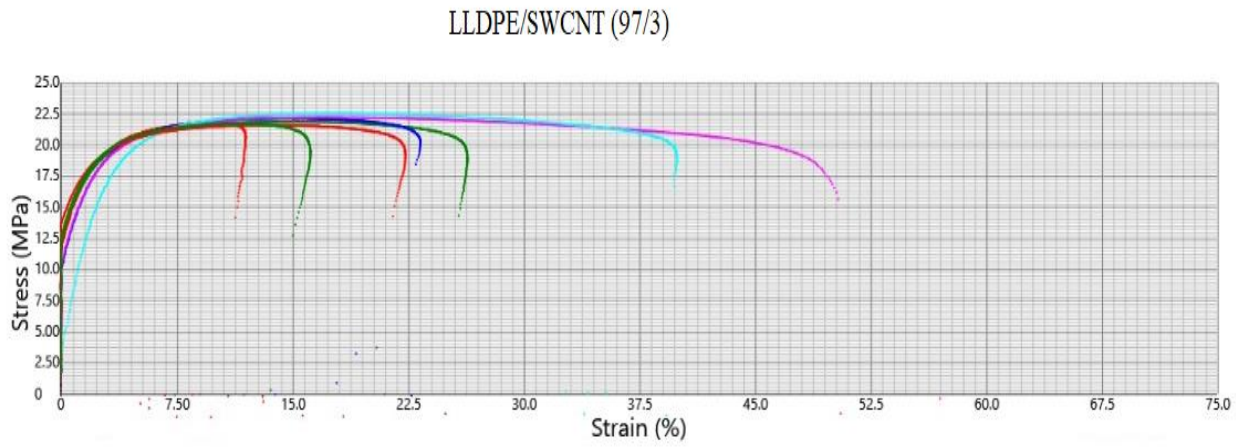

A4 LLDPE/SWCNT composites with 3 wt.% SWCNT content

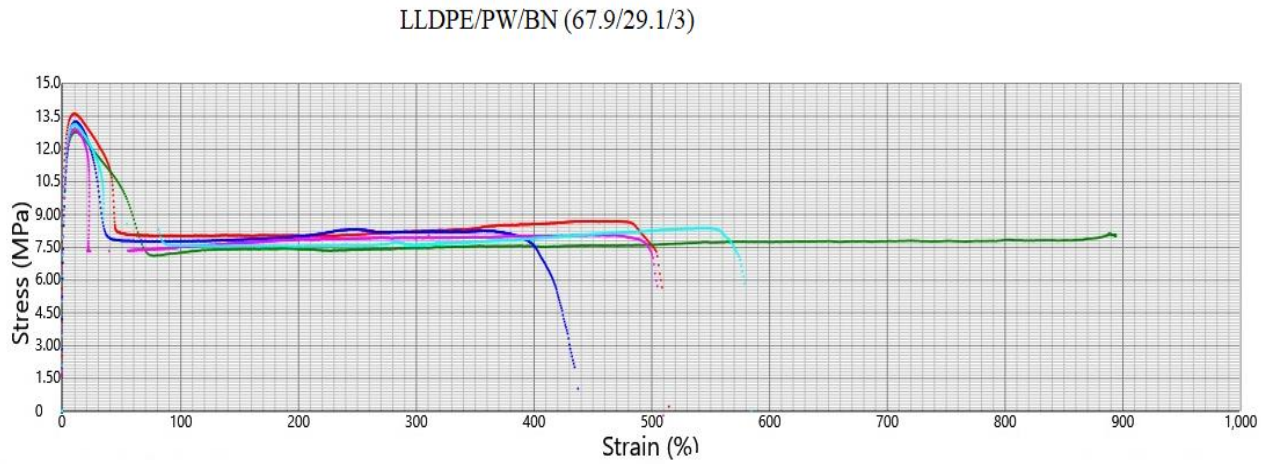

A5 LLDPE/PW/BN blend composites

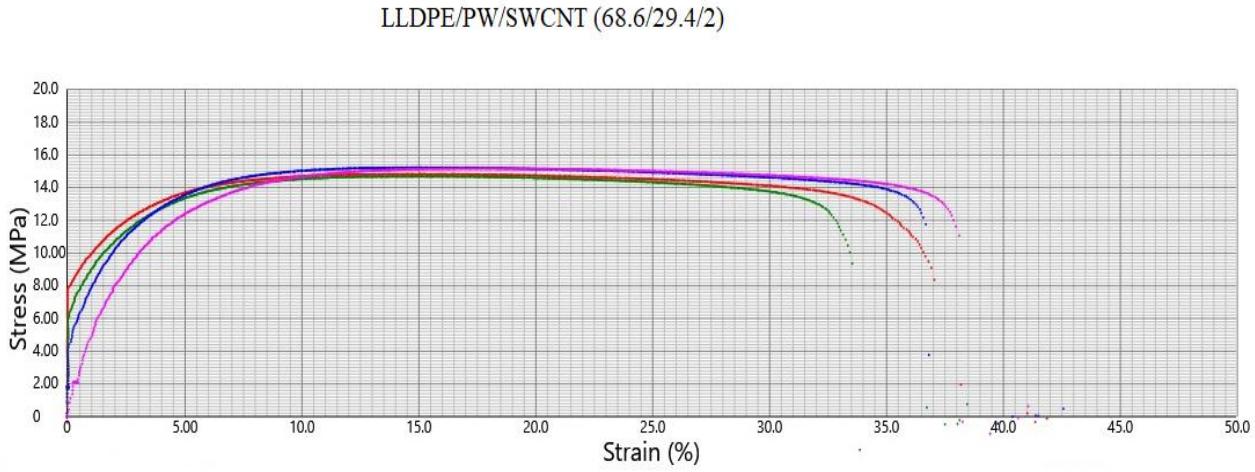

A6 LLDPE/PW/SWCNT blend composites

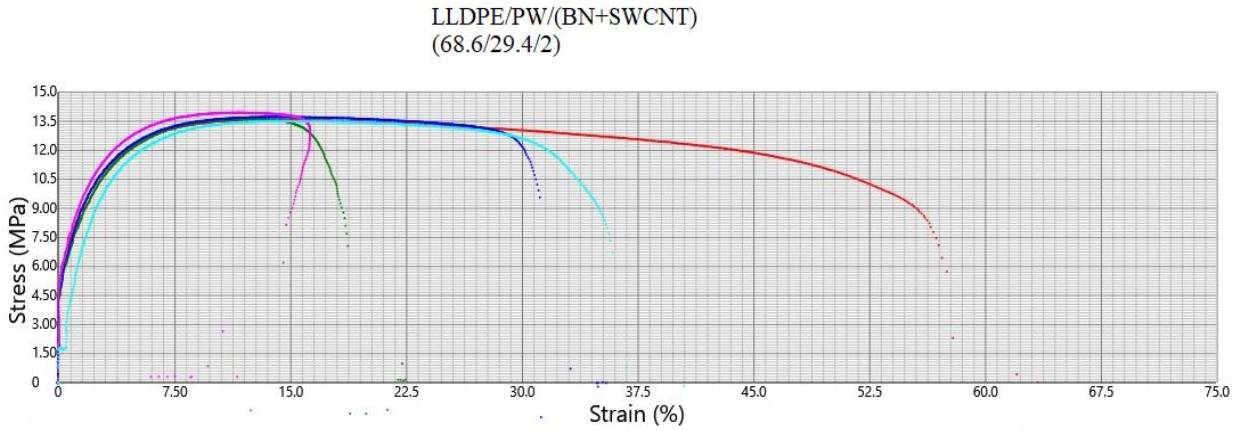

A7 LLDPE/PW/(BN+SWCNT) blend hybrid composites